ISSN 1112-3745

Bulletin des Sciences Géographiques

N° 24

2ème Semestre 2009 • 12ème année • Prix 40 DA • Etranger 15 € • ISSN 1112-3745

Edité et publié par:
l'Institut National de Cartographie et de Télédétection

I N C T
BULLETIN DES SCIENCES GÉOGRAPHIQUES

N° 24
2ème Semestre 2009

Publication semestrielle de l'Institut National de Cartographie et de Télédétection (INCT), Algérie.

Fondé en Octobre 1997
N°24 - 2ème Semestre 2009
ISSN 1112-3745

Responsable de la revue : INCT

Éditeur : Centre de la Documentation et de la Conservation de l'Information Géographique, INCT, Alger.

Adresse : Bulletin des Sciences Géographiques, INCT, 123, rue de Tripoli Hussein Dey 16040, BP 430, Alger, Algérie.
Tél: (021) 47 09 20
(021) 47 00 30
Fax: (021) 23 43 81
(021) 47 00 29
E-mail : inct99@wissal.dz

Tirage :

150 Exemplaires

Sommaire **Pages**

Satellite Laser Ranging Mobile Station : Presentation and Geodetic Applications

B. Gourine, S. Kahlouche, B. Ghezali & H. Taibi
Centre des Techniques Spatiales – Division de Géodésie Spatiale
BP n°13, 31200 Arzew – ALGERIE, Fax : (213) 041 47 36 65
bachirgourine@yahoo.com

ملخّص : يقدّم المقال محطة قياس البعد الليزري الفائقة التحرّك (FTLRS) وتجاربها في المواقع الجغرافية بكورسيكا (فرنسا). عمل موّقع في إطار التعاون في مجال الجيوديزيا الفضائية بين مركز التقنيات الفضائية (CTS ، الجزائر) و مرصد ساحل أزور Côte d'Azur (GEMINI / OCA ، فرنسا). يعّد الموقع الجيوديزي لأجاسيو بكورسيكا من أهم مواقع المعايرة بالنسبة لقياس إرتفاع القمر الصناعي في منطقة البحر الأبيض المتوسط . تقدّم في مهام قياس الإرتفاع مثل (2001) et Envisat (2002) TOPEX/Poseidon (T/P, 1992), Jason-1 عُرض هناك FTLRS خلال الحملتين الليزريتين ، في 2002 و 2005 . نقدّم حساب مجموعتي الإحدثيات المركزية الأرضية من معطيات FTLRS المحصّل عليها من الحملتين خصوصاً في الأقمار الصناعية الجيوديزية الأرضية المنخفضة : Starlette و Stella (ارتفاع يقدّر بـــ 800 كلم). يلخّص المقال المراحل المختلفة لمعالجة المعطيات الليزرية . يقدّر معدّل الأقواس RMS تقريبا بـــ 2-1 سم بالنسبة للأقمار الصناعية Lageos-1, Lageos-2 Starlette و Stella ؛ تبيّن بأنّ أحسن نتائج مدار القمر الصناعي و المواقع المركزية الأرضية قد تمّ الحصول عليها من نموذج الجاذبية Eigen- Grace03s . يكون فرق المواقع 3D المطلق ، بين 2002 و 2005 ، تقريبا بـــ 7.7 ملم (i.e., 2.6 mm / yr) أقل من الأخطاء الباقية لسرعة ITRF2005 (تقريبا بـــ 4.3 ملم/ yr). أخيراً ، تمّ قبول بعض الإقتراحات للإستعمال FTLRS في الجزائر في التطبيقات الجيوديزية.

الكلمات الأساسية : محطة قياس البعد الليزري الفائقة التحرّك المواقع ، إستقرار ، قياس البعد الليزري للقمر صناعي ، نموذج حقل الجاذبية الأرضية.

Résumé : Le présent travail est souscrit dans le cadre de coopération dans le domaine de la géodésie spatiale entre le Centre des Techniques Spatiales (CTS, Algérie) et l'Observatoire de la Côte d'Azur (GEMINI / OCA, France). L'article présente la station de Télémétrie laser ultra mobile (FTLRS) et ses expériences de positionnement géographique en Corse (France). Le site géodésique d'Ajaccio en Corse est le site principal du calibrage d'altimètres du satellite dans la région méditerranéenne. Il a été développé pour les missions altimétriques tel que TOPEX / Poseidon (T/P, 1992), Jason-1 (2001) et Envisat (2002). Le FTLRS a été déployé là pendant deux campagnes laser, en 2002 et 2005. Ici, nous présentons le calcul des deux ensembles de coordonnées géocentriques des données FTLRS acquises principalement dans les deux campagnes sur les satellites géodésiques Terrestres basses: Starlette et Stella (altitude de 800 km).

L'article résume les différentes étapes du traitement des données laser. La moyenne des arcs RMS obtenu est environ de 1-2 centimètre pour les satellites Lageos-1, Lageos-2, Starlette et Stella; il est indiqué que les meilleurs résultats des orbitographies du satellite et de positionnement géocentrique sont obtenus avec le modèle de gravité Eigen-Grace03s. La différence du positionnement 3D absolu du FTLRS, entre 2002 et 2005, d'environ 7.7 mm (i.e., 2.6 mm / yr) est moins que les erreurs résiduelles de vélocité ITRF2005 (d'environ 4.3 mm/yr). Finalement, quelques suggestions de l'usage de FTLRS en Algérie pour les applications géodésiques sont faites.

Mots-clés : station de Télémétrie laser ultra mobile (FTLRS), Positionnement, Stabilité, télémétrie Laser du Satellite, modèle du champ de gravité terrestre.

Abstract : The present work is subscribed in the framework of cooperation in space geodesy domain between the Centre des Techniques Spatiales (CTS, Algeria) and the observatory of the Azure coast (GEMINI/OCA, France). The paper deals with the presentation of the French Transportable Laser Ranging Station (FTLRS) and its experiences of geographic positioning at Corsica (France). The geodetic site of Ajaccio in Corsica is the main calibration site of satellite altimeters in the Mediterranean area. It has been developed for altimetric missions such as TOPEX/Poseidon (T/P, 1992), Jason-1 (2001) and Envisat (2002). The FTLRS was deployed there during two laser campaigns, at 2002 and 2005. Here, we present the computation of the two sets of geocentric coordinates from the FTLRS range data acquired in the two campaigns mainly on the low Earth geodetic satellites: Starlette and Stella (altitude of 800 km).

The paper summarizes the different steps of the laser data processing. The average arcs RMS (Root Mean Square) obtained are about 1-2 cm for Lageos-1, Lageos-2, Starlette and Stella satellites; it is showed that best results of satellite orbits determination and geocentric positioning are obtained with Eigen-Grace03s gravity model.

The difference of FTLRS absolute 3D positioning, between 2002 and 2005, of about 7.7 mm (i.e., 2.6 mm/yr) is less than residual errors of ITRF2005 velocities (of about 4.3 mm/yr). Finally, some suggestions of the use of FTLRS in Algeria for geodetic applications are made.

Key words : French Transportable Laser Ranging Station (FTLRS), Positioning, Stability, Satellite Laser Ranging (SLR), Earth gravity field model.

1. Introduction

The Satellite Laser Ranging (SLR) plays a key role both in the determination of the orbit of oceanographic satellites (in particular for the calibration passes) and of the geocentric positioning of the site [2]. In issue of collaboration between CNES, IGN, INSU and OCA, the French Transportable Laser Ranging System (FTLRS) has been developed specifically for realizing geodetic campaigns. This highly mobile system, with a weight of 300 kg and a telescope of 13 cm diameter, is the smallest operational SLR station in the world [3]. If its great mobility is its main advantage that confers it campaigns on dedicated sites, its indispensable miniaturization could constitute a disadvantage. In particular, its small telescope makes difficult the reception of laser pulse echoes from high orbiting satellites (as LAGEOS geodynamical satellites at an altitude of 6000 km) particularly at elevations lower than 40 degrees [1].

Therefore, to compute highly accurate geocentric coordinates the difficulty lies in using range data of low Earth orbiting geodetic satellites (like Starlette and Stella, at an altitude of 800 km). As a consequence of their lower altitude, the accuracy of their orbit determination is more sensitive to remaining uncertainties in the dynamical models. The error budget of the geocentric positioning then is affected notably by introducing correlations between the satellite geocentric altitude and the adjusted terrestrial coordinates [2].

Operational since 1996, the FTLRS has participated to several absolute calibration campaigns in the framework of the T/P and Jason-1 CNES and NASA missions: in Ajaccio in 2002 [2], in Crete (at Chania University) in 2003 [6], and for the second time in Ajaccio in 2005.

The present article deals with the description of FTLRS experiences carried out in Ajaccio (Corsica), during SLR tracking campaigns made in 2002 (from January to September) and in 2005 (from May to October).

2. Satellite Laser Ranging (SLR) Technique

The SLR technique is based on ultra precise timing (approximately 30 Pico seconds) of round trip of flight of ultra short pulses of light from a station on the ground (Telescope) to a satellite equipped with retro-reflectors (made up of cube corners). This provides instantaneous range measurements of millimeter level precision, which can be accumulated to provide accurate measurement of orbits and a host of important scientific data.

The telescopes laser are equipped with motorized tracking systems, precise and fast so as to be able to track the satellites of which speed can reach 7 km/s. The only information collected by these instruments is the distance telescope satellite and the precise moment of the measurement, fig.1.(a) [3].

However, the technique is tributary of the methodology and of the need of technicians specialized for its implementation. The contribution of the SLR measurements, gathered these last years, on the geodetic satellites, see fig.(1.b) : Starlette, Stella, Ajisai, Etalon, Lageos, etc, was important in the improvement of the terrestrial gravity field model (first model coefficients and their variations), for orbitography, positioning and space oceanography.

Among the space geodesy techniques, SLR technique does not seem to be the most precise one with the best temporal resolution. However, it is most exact on long term, which confers to it a unique place for observation of slowly variable phenomena (e.g. postglacial rebound), and for the realization of a stable geocentric terrestrial reference frame. By providing an absolute scale factor via the determination of the gravitational constant (GM), and its contribution in the calibration of the radar altimeters of the French organisations CNES, IGN, and OCA have developed a new concept of satellite laser ranging (SLR) system called the French Transportable Laser Ranging Station (FTLRS), fig. (2).

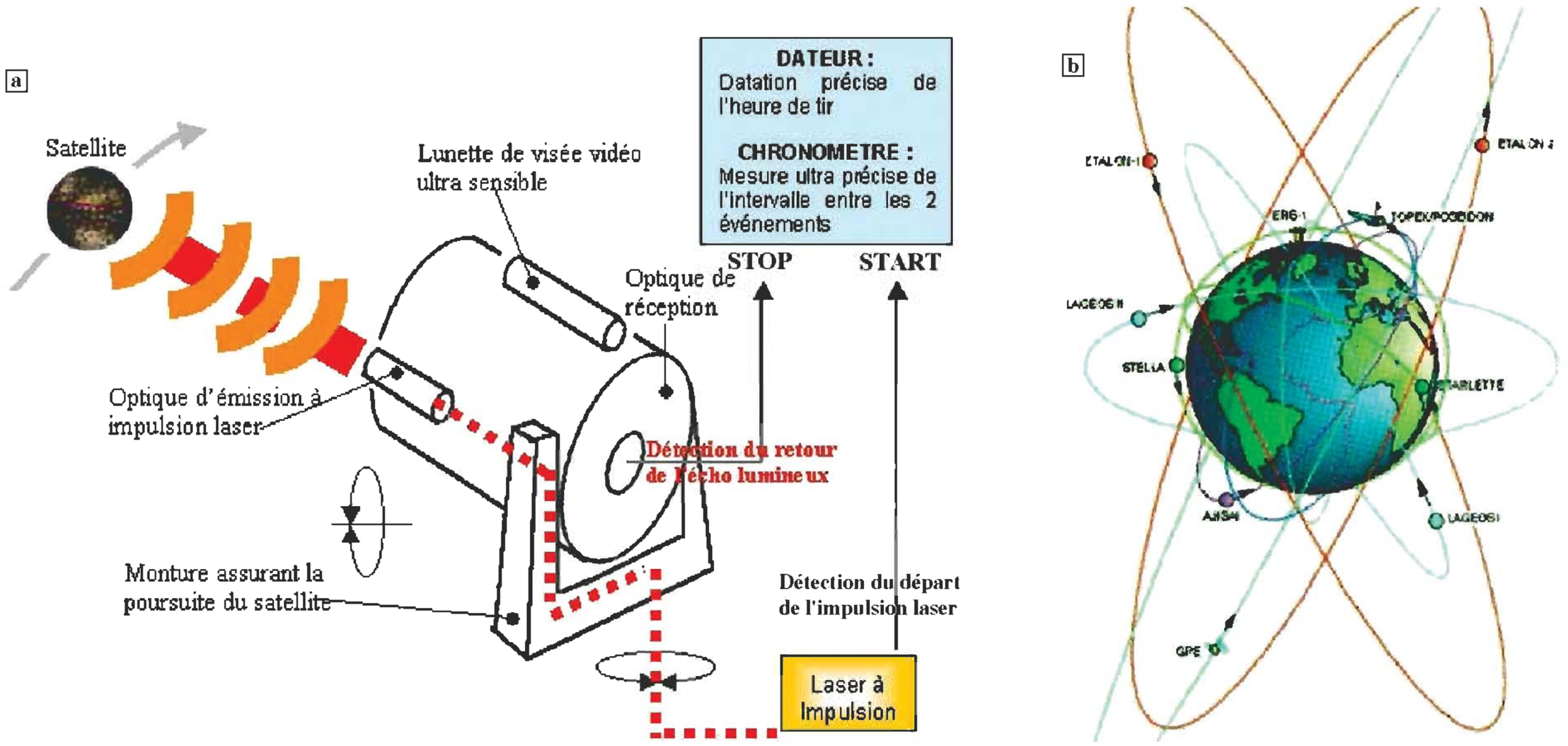

Fig. 1 Satellite Laser Ranging (SLR). **(a)** Principle of the SLR measurement [3] **(b)** Orbits of principle SLR satellites.

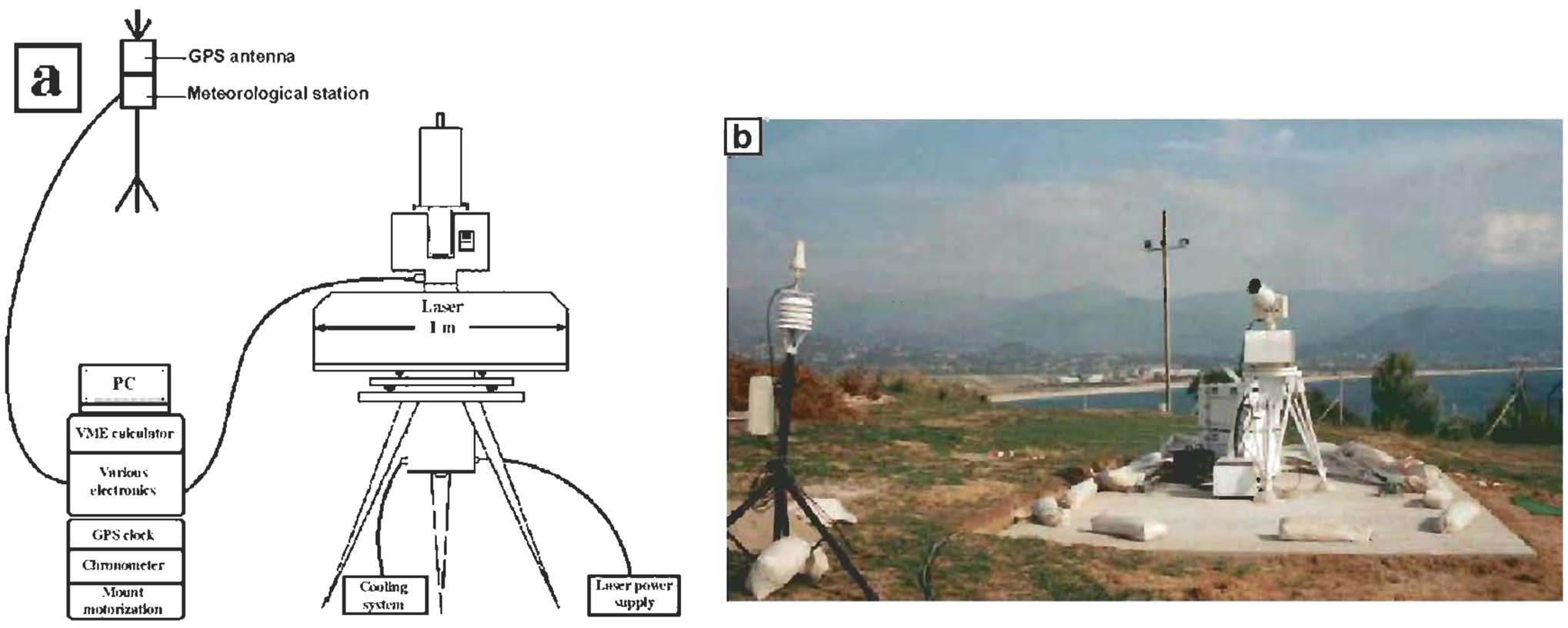

Fig. 2 French Transportable Laser Ranging Station. **(a)** Main components of FTLRS **(b)** Photo of FTLRS during the Corsica campaign (on left, the meteorological station and GPS antenna).

The idea was to realise a very small SLR station (telescope of 13 cm diameter, weight 300 kg), that is easily transportable, for example to make measurements in oceanic zones such as islands or offshore platforms. The technical description of the instrument is described in the table 1.

Table 1. Summary of FTLRS characteristics [3].

Total weight :	300 kg (8 containers <55kg)
Laser :	Nd:YAG doubled in frequency, λ=532 nm (green), 50 mJ by impulse, 10Hz, impulse width of 35 ps
Detector :	Photodiode with avalanche in Geiger mode
Telescope :	13 cm diameter , 2 kg
Climatic Conditions of use :	0 to +35°C, until 95% of humidity
Calibration :	External target, target on the outlet side of the telescope
Error of pointing :	≤10" rms
System of chronometer :	Standford SR620, Rubidium controlled on GPS

The main objectives are to participate in space oceanography, centimetric calibration of radar altimeters, precise positioning and geodynamics. To reach this performance, many major improvements have been carried out on the FTLRS. According to Pierron et al. [7] and Nicolas [3], they mainly concern :
Topex/Poseidon, Jason-1, ERS, etc., this technique occupies an essential and complementary place for other space techniques.

3. FTLRS Description

- Laser configuration (wavelength, pulse width, cooling, stability, reliability in hard environments);
- Detection package with new optical configuration and C-SPAD (Compensated Single Photon Avalanche Diode) detector;
- Start detection with permanent laser monitoring;
- New GPS steered rubidium clock;
- Software improvement.

The success of all these upgrades has been confirmed at the level of few millimetres by the analysis of a collocation experiment performed at the Grasse observatory between the three laser instruments (autumn 2001) and the evaluation of data set from the 2002 Corsica campaign [4].

4. FTLRS Experiences in Corsica

The geographic configuration of the Corsica area is shown in Fig.3. Effectively, the TOPEX/Poseidon and Jason-1 ground tracks pass over the Senetosa Cape which is the dedicated site for altimeter calibration where in situ instruments (tide gauges, GPS, and a meteorological station) have been installed permanently. The naval base at Aspretto (Ajaccio) is used since 1996 as a semi-permanent site where the FTLRS can be deployed for several month campaigns assuring security and local facilities.

During the two campaigns, the laser tracking has been done both on oceanographic and geodetic satellites. The LAGEOS-1 & -2, due to their high altitude, are difficult to reach as it is shown by the low number of normal points collected on these satellites (Table 2). The only measurements available on these two satellites are not enough to perform a 3D geocentric positioning at the level of less than 1 cm. On the other hand, the data acquired on low Earth satellites, mainly Starlette and Stella (see Table 2), form the great part of the basis of our computation.

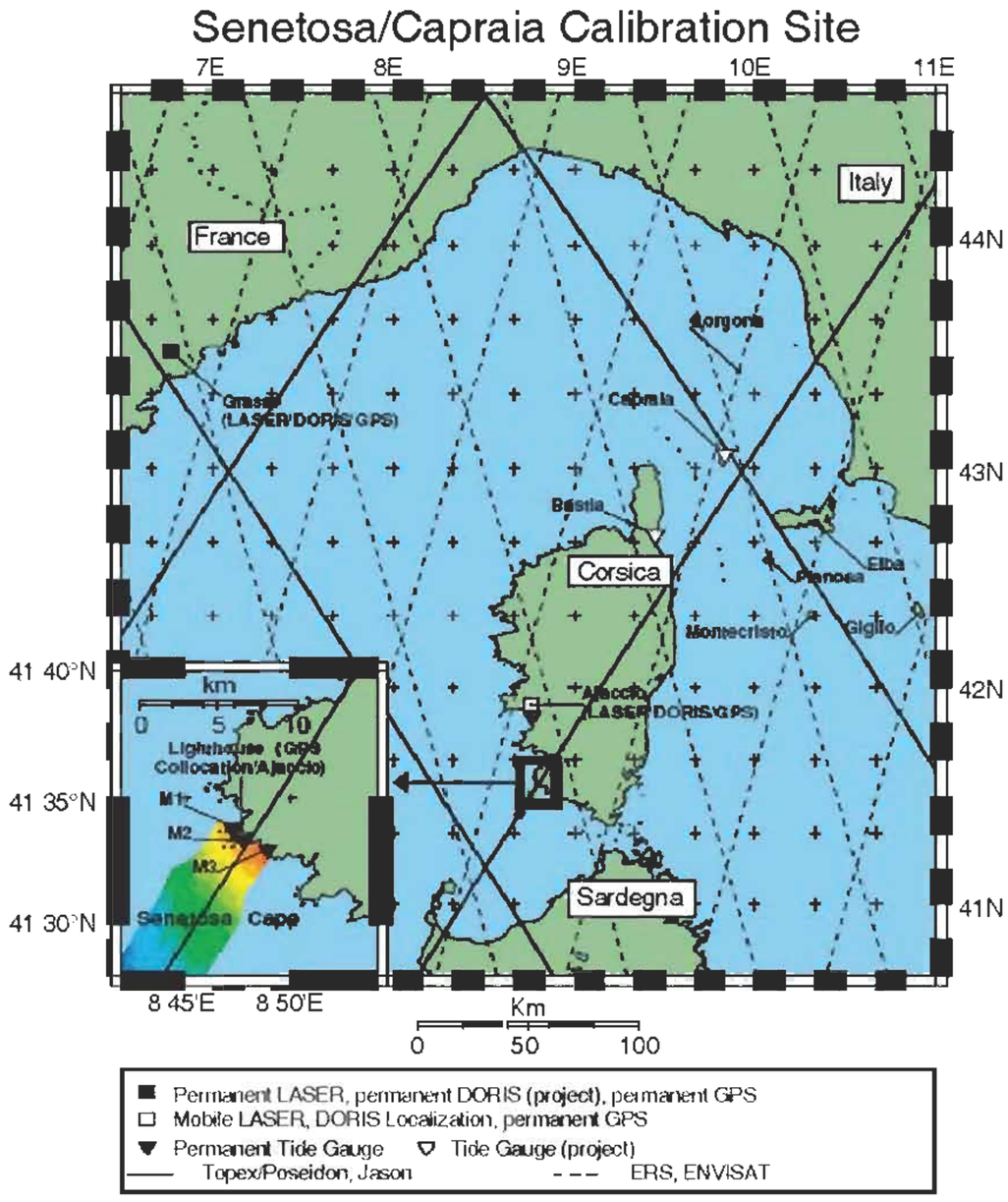

Fig. 3 Ajaccio Site in Corsica.

Table 2. Number of normal points collected by FTLRS during 2002 and 2005 campaigns.

Satellite	2002 Campaign	2005 Campaign
LAGEOS-1	301	377
LAGEOS-2	323	235
Starlette	3413	5294
Stella	1731	2069
Total	5768	7975

The adopted methodology to determinate the FTLRS geographic position, at Ajaccio site, is based on a multi-satellite semi-dynamical approach [2]. First, orbits are computed as precisely as possible (especially for the lower altitude satellites) without the FTLRS tracking data. Then, the normal matrices are established and the FTLRS parameters (coordinate updates and range biases) are solved through a weighted least-squares adjustment.
The precise orbit determination is performed by GINS *(Géodésie par Intégration Numérique; Geodesy by Simultaneous Numerical Integration,* in English) software (GRGS, Toulouse) assuming the following dynamical models and reference frame listed bellow (see Table 3). A subset of SLR fixed stations from the International Laser Ranging Service (ILRS) network, which are well distributed on the Earth, is used as the reference frame for the orbitography. Of course, the FTLRS range data are not included in the orbit computation.

Table 3. Some dynamical models used for the orbit computation.

Model	Designation
Gravity field model	GRIM5-C1 or EIGEN-GRACE03S
Atmospheric pressure	ECMWF
Solar activity	ACSOL2
Atmospheric density	DTM-94
Ocean tides	FES-2002
Planets	DE403
Terrestrial reference frame	ITRF2000
Earth Orientation Parameters	EOPC04

The orbit quality is given by the rms of orbit residuals after fit. Table 4 gives these rms for the four used satellites: all arcs of 2002 and 2005 periods for the two considered solutions. As expected, the orbits of the Lageos-1 and Lageos-2 are more precise (2 times) than those of Starlette and Stella, and they are also less affected by the change of the gravity field model. Based on these tests and other recent results concerning the assimilation of GRACE data into Earth models, we have adopted the EIGEN-GRACE03S gravity model for the 2002 and 2005 positioning.

Table 4. Average weighted rms (in mm) of the range residuals after orbit fits of the satellites used for the FTLRS positioning.

	2002 campaign		2005 campaign	
Satellite	**GRIM**	**EIGEN**	**GRIM**	**EIGEN**
LAGEOS-1	13	-	11	11
LAGEOS-2	10	-	10	09
Starlette	23	18	23	18
Stella	23	19	21	16

SLR technique is known as the most accurate technique for positioning, more especially in the vertical direction. However, SLR measurements present biases which are mainly due to satellite ignatures and to inaccurate internal calibration of tracking instruments. These biases pose problems because they are strongly correlated with the vertical component of the station position (correlation greater than 0.9).

However, this component is important for the geodynamical studies since it holds ⅔ amplitude of signals acting on the station motion [1]. To reach the intrinsic accuracy of SLR technique, the data processing strategy must gua-rantee a correct estimation of the biases. Exertier et al. [2] have developed a specific method, called *temporal decorrelation*, decreasing the correlation between biases and vertical coordinates at level of 0.5.

The estimation of station coordinates updates and of the FTLRS range bias is performed using the MATLO (*MAThématiques pour la Localisation et l'Orbitographie; MAThematics for Localization and Orbitography,* in English) software (OCA, Grasse) [1]. For both campaigns, the initial coordinates used in the adjustment are the published ones by Exertier et al. [2]. These later correspond to the 2002 epoch. The FTLRS coordinates of the first campaign were recalculated with respect to the published position, which was corrected from plate tectonics (ITRF2000 velocities) at Ajaccio.

Table 5 gives, for the two periods 2002 and 2005, the range bias per satellite and the geographic coordinate updates. Concerning the bias, one can note that the global mean (-5 mm) is very close to the value which had been determined previously (–7±2 mm, [2]). We know that this value did not change since the first technological tests made in 2001 [8]. The differences between the 2002 and the 2005 solutions, in terms of geographical coordinates, are very small and are at the level of residual errors of the ITRF2005 velocities. By consequence, differences between 2002 and 2005 coordinates are at level of the tectonic movement and show that the point is locally stable.

Table 5. Range bias per satellite and geographic coordinate updates (in **mm**) of the FTLRS, for the two campaigns 2002 and 2005.

	Mean Lageos	Starlette	Stella	Mean Starlette & Stella	Δφ	Δλ	Δh	3D
2002	-6	-13	-13	-13.0 ± 0.7	-0.8 ±0.7	+1.6±0.7	+0.2±0.8	+1.8±1.3
2005	+4	-6	-4	-5.0 ± 0.8	+4.1±0.4	-2.9± 0.4	+4.0±0.4	+6.4±0.7
2005–2002					+4.9	−4.5	+3.8	+7.7

The fig. 3 represents the coordinate update time series with their standard deviations, according to the two gravity field models during the two observation campaigns. Statistically, the estimates of coordinate updates with the Eigen-Grace03s model are better than those with the Grim5-c1 model. Indeed, we have reduced the weighted mean of the geographical position from about 7.7±1.3 mm to 1.8±1.3 mm (in 2002) and from about 16.8 ±1.0 mm to 6.4 ±0.7 mm (in 2005).

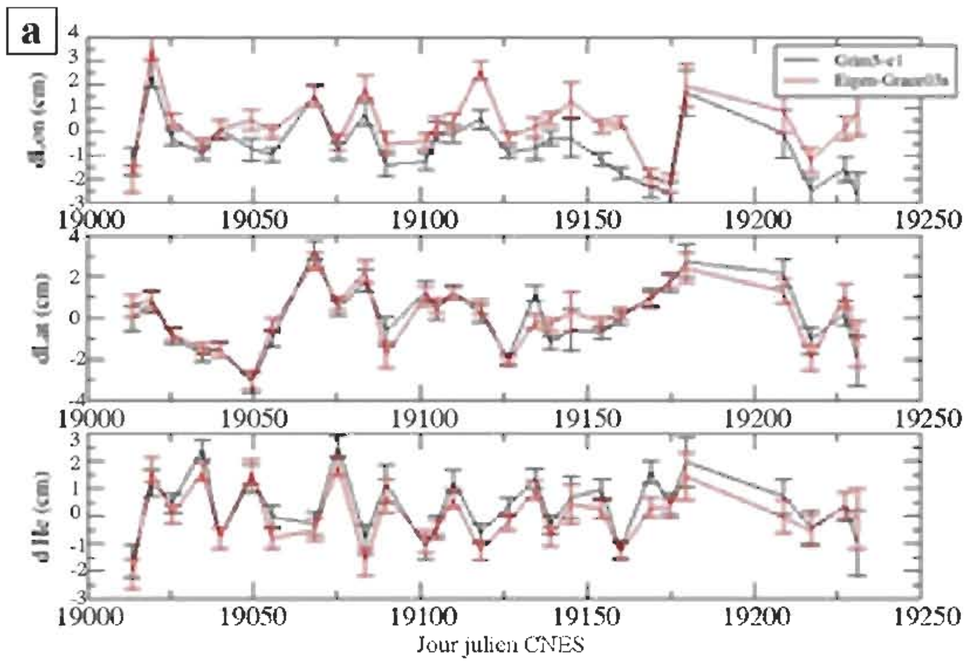

Fig. 3 Coordinate updates time series of the FTLRS (a) 2002 campaign (b) 2005 campaign.

5. Some suggestions of the use of the FTLRS in Algeria for geodetic applications

We propose some suggestions of the use of the FTLRS in Algeria, as following :
Until today, there is no point of ITRF network on the Algerian territory (and even on the North of Africa), where the interest of deploying the FTLRS in our country in view to :

a. Contribution to the International Terrestrial Reference Frame (ITRF) densification in North of Africa

- improve of the ITRF quality in term of configuration and also to allow to Algerian researchers to participate in ITRF observations programs.
- its extension to the national territory for the revaluation of the Algerian geodetic system (Nord Sahara 1959) in order to validate its quality and to facilitate the utilization of space techniques, notably the possibility of passage between the different systems used.

b. Study of geophysical and geodynamical phenomena

SLR technique, by measure for long periods of stations positions, contributes to observation and study of geophysical and geodynamical phenomenon (geological movements, notably the plates tectonic). It contributes also to the study of movements of Geocentre and terrestrial pole. In addition, considering insufficiencies of the national cartography relative to the seismic risks, the contribution of this space technique in deformation monitoring of the North of Algeria will have a positive impact on all works and projects relative to the study of seismic risk in Algeria.

c. Space oceanography

SLR allows precise tracking of oceanographic satellites. Thereby, it plays an important role in space altimetry missions (ERS-1, TOPEX/Poseidon, Jason-1, ...) dedicated to monitor the evolution of the mean level of Mediterranean sea, phenomenon that interest Algeria, in priority. This priority is justified by the important population density on coastal zones (as, in Algiers, Oran, Annaba,..). Another advantage of this system is its contribution in the determination of an absolute altimetric reference (geodetic fixing of SLR stations to the tide gauges) which constitutes capital information for representation of the third dimension of the National geodetic system.

d. ALSAT Tracking

Installation of Laser retro-reflectors on future Algerian satellites (ALSAT generations), permits to allow making measurements by FTLRS for the orbital monitoring.

6. Conclusion

The FTLRS system confirms its place, as a unique highly mobile SLR system designed to participate to tracking campaigns on dedicated sites. According to the results obtained from the Corsica experiences, the FTLRS has demonstrated successful performance in the absolute geographic positioning as well as in CAL/VAL missions. For future campaigns, and parallel to the technological progress of the FTLRS instrumentation (according to Nicolas et al., 2002), ideas were discussed between the OCA and the different French partners for planning the development of a new telescope of 25 cm diameter. This will permit to greatly improve the tracking particularly at mean and low elevations, as for high geodetic targets as for satellites equipped with small laser retro-reflectors. Thus, this will contribute to the importance of the role of SLR technique for altimeter calibration missions as for space geodesy and so in the realization of the ITRF. Finally, the idea to deploy this laser mobile station in Algeria is very interesting and fruitful for national geodetic applications as contribution of ITRF densification in North of Africa, geodynamics studies, space altimetry and ALSAT tracking.

Acknowledgements

The authors acknowledge the researchers of the GEMINI/OCA/France, particularly, Prof. Exertier P., Berio P., Bonnefond P., Deleflie F., Pierron F. and Feraudy D., for the scientific and technical assistance and for the access to the FTLRS data.

Bibliographical References

Coulot D., 2005, Télémétrie Laser sur Satellites et Combinaison de Techniques Géodésiques: Contributions aux systèmes de référence terrestres et applications. Thèse de Doctorat de l'Observatoire de Paris / OCA,Grasse–juillet2005.

Exertier P., J. Nicolas, P. Berio, D. Coulot, P. Bonnefond, O. Laurain, 2004, The role of Laser Ranging for calibrating Jason-1: The Corsica tracking campaign. *Marine Geodesy*, Vol. 26, No. 3-4, 333-340, 2004.

Nicolas J., 2000, La station Laser Ultra Mobile de l'obtention d'une exactitude centimétrique des mesures à des applications en océanographie et géodésie spatiales. Thèse de Doctorat de l'Observatoire de Paris, soutenue en décembre 2000.

Nicolas J., P. Bonnefond, O. Laurain, P. Bério, P. Exertier, and F. Barlier, 2002, Triple laser ranging collocation experiment at the Grasse observatory, France, Phys. and Chem. of the Earth, 2002.

Nicolas J., P. Bonnefond, P. Exertier, O. Laurain, F. Pierron, 2002, Presentation of the 2002 Corsica FTLRS campaign for the JASON-1 CAL/VAL experiment. Proceedings of the 13th International Laser Ranging Workshop, Washington - USA, Oct 7-11, 2002.

Pavlis, E. C., S. P. Mertikas and the GAVDOS Team, The GAVDOS Mean Sea Level and Altimeter Calibration Facility: Results for Jason-1, Marine Geodesy, Vol. 26, No. 3-4, 631-655, 2004.

Pierron F., E. Samain, J. Nicolas, J.-L. Hatat, M. Pierron, J.-F. Mangin, H. Viot, M. Laplanche, J. Paris, and E. Cuot, 2002, Improvements of the French Transportable Laser Ranging Station to high accuracy level, Proceedings of the 13th International Laser Ranging Workshop, Washington USA, October 7-11, 2002.

Pierron M., D. Feraudy, M. Furia, F. Pierron, 2004, FTLRS laser staff, Laboratory Tests and Calibration on Chronometry for the French Transportable Laser Ranging Station, 14th International Laser Ranging Workshop, San Fernando, Spain, June 7-11, 2004.

Reigber Ch., R. Schmidt, F. Flechtner, R. Konig, U. Meyer, 2005, An earth gravity field model complete to degree and order 150 from GRACE: Eigen-Grace02S. Journal of Geodynamics, Vol. 39, 1-10, 2005.

Determination and analysis of stations coordinates based on Starlette and Lageos-1 &-2 satellites laser ranging data

B. Gourine[1], S. Kahlouche[1] and M.F. Belbachir[2]
(1): Centre des Techniques Spatiales (CTS)–Division de Géodésie Spatiale, BP 13, 31200, Arzew – Algérie
(2): Université des Sciences et de la Technologie (USTO), Faculté du Génie Electrique,
Département d'Électronique, Oran - Algérie

ملخص : يعالج هذا العمل حساب شبكة المصلحة الدولية لقياس البعد الليزري (IRLS) القائمة ليس فقط على أرصاد القمرين الصناعيين LAGEOS لكن أيضاً على الأقمار الصناعية ذات مدار أرضي منخفظ (LEO) ، مثل Starlette . يكمن التحدي في الحصول على نوعية جيّدة من إحدثيات المحطات بدمج بين القمر الصناعي ذات معطيات عليا و منخفضة للأقمار الصناعية .
أنجزت إستعادة مدار الأقمار الصناعية المختلفة بالبرنامج GINS (GRGS, France) و معالجة المعطيات الليزرية بالبرنامج MATLO (فرنسا ، OCA & IGN)، لفترة طويلة نسبياً قدّرت بـــ 14 سنة (بين أكتوبر 1993 إلي فيفري 2007) . تمّ تقديم ومناقشة النتائج الأوّلية لتحليل دمج معطيات SLR لـــ 14 سنة من أجل دراسة معالم المرجع الأرضي (TRF) .

الكلمات الأساسية : إستعادة المدار ، دمج بين الأقمار الصناعية ، تقنية SLR ، تحليل طيفي ، دراسة التشويش .

Résumé : Le présent travail traite le calcul du réseau du Service International de Télémétrie Laser (ILRS) non seulement basé sur les observations des deux satellites LAGEOS mais aussi sur ceux des satellites d'Orbite terrestre basse (LEO), tel que Starlette. Le défi est d'obtenir une bonne qualité des coordonnées des stations par la combinaison inter satellite de Hautes et Basses données satellitaires.
La restitution d'orbite de différents satellites est effectuée avec le logiciel GINS (GRGS, France) et le traitement des données laser est réalisé avec le logiciel MATLO (OCA & IGN, France), pour une période relativement longue de 14 années (entre octobre 1993 et février 2007). Les résultats préliminaires de l'analyse de la combinaison de données SLR de 14 années, pour étudier les repères de Référence Terrestre (TRF) sont présentés et discutés.

Mots-clés : restitution d'Orbite, combinaison Inter satellite, technique SLR, analyse Spectrale, étude du Bruit.

Abstract : The present work deals with the calculation of International Laser Ranging Service (ILRS) network notonly based on observations of both LAGEOS satellites but also on those of Low Earth Orbit (LEO) satellites,such as Starlette. The challenge is to achieve good quality on stations coordinates by inter-satellite combination of High and Low satellites data. The orbit restitution of the different satellites is carried out by GINS software (GRGS, France) and the laser data processing is performed with MATLO software (OCA & IGN, France), for a relatively long period of 14 years (between October 1993 and February 2007). The preliminary results about the analysis of 14 years SLR data combination, in order to study the Terrestrial Reference Frames (TRF) are presented and discussed.

Key words: Orbit restitution, Inter-satellite combination, SLR technique, Spectral analysis, Noise study.

1. Introduction

Satellite Laser Ranging (SLR) is one of the main spacegeodesy techniques for the establishment and the maintenance of the International Terrestrial Reference Frame (ITRF), as Very Long Baseline Interferometry(VLBI), Global Positioning System (GPS) and Doppler Orbitography Radiopositioning Integrated by Satellite(DORIS). It contributes to the frame determination by providing time series of terrestrial stations positions, i.e.,Terrestrial Reference Frame (TRF), and Earth Orientation Parameters (EOPs). Generally, for such determination, only the measurements on high altitude satellites (LAGEOS-1 & LAGEOS-2, 6000 km) are used. However, computation of the laser ranging station's coordinates on the basis of data other than those from LAGEOS-1&-2 observations is desirable for the following reasons: (1) significantly increases the number of observations used for determination of the station's coordinates and EOPs, (2) permit verification of results obtained from the LAGEOS-1 &-2 data, (3) permit determination of coordinates of the stations that cannot observe LAGEOS satellites. The aim of the study is to check if the laser ranging observations of low altitude satellites such as Starlette (altitude of 800 km) can be used for a precise determination of the laser ranging stations' coordinates and to investigate the contribution of the Starlette data on the geodynamic study, during relatively a long period. Hence, the work concern the re-computation of the network of International Laser Ranging Service (ILRS) based on both LAGEOS satellites measurements with those of Starlette over 14 years period (from October 1993 to February 2007), according to three data combination solutions, namely LAGEOS-1 (LA-1), LAGEOS-1&-2 (LA-1&-2) and LAGEOS-1 & Starlette (LA-1 &STAR). The methodology adopted, in this paper, comprises three main steps:

a. The orbit restitution of different tracked satellites is performed by the GINS (Géodésie par Intégration Numérique Simultanée, Geodesy by Simultaneous Numerical Integration, in English) software (GRGS,France), based on purely dynamical approach, see section 2.
b. The estimation of stations coordinates updates and of Earth orientation parameters is performed using the MATLO (MAThématiques pour la Localisation et l'Orbitographie, MAThematics for Localization and Orbitography, in English) software (IGN, Grasse)[6], which can also determine orbit correction via simply kinematical assumptions, see sections 3 and 4. This estimation provides weekly time series of stations positions, in which their analysis permits tomake in evidence the geophy-sical phenomena effects on the station vertical coordinate (Up component).
c. Analysis of coordinate time series based on *(i)* frequency analysis by FAMOUS software *(Frequency Analysis Mapping On Unusual Sampling)* [9], and (ii) noise estimation (type and level noise) by Allan variance method.

Finally, the preliminary results of 14 years combined SLR data analysis of different satellites used, namely, LAGEOS-1 &-2 and Starlette, for the study the TRF are presented and discussed in section 4.

2. Determination of Orbital Arcs

The orbit restitution of different satellites used (LAGEOS-1, LAGEOS-2 and Starlette) is performed with the GINS software, from a subset of SLR fixed stations well distributed on the Earth as reference frame for the orbitography. For example, the dynamical models and the reference frame used are: *Fes-2004* ocean tides model, *Dtm-94* atmospheric density model, *Ecmwf* atmospheric pressure model, *EOPC04* conventional pole model etc. and *ITRF2005* solution [5].

We have used the Grim5-s1 for LAGEOS satellites and Eigen-Grace03s for Starlette, in order to reach more precision in the orbit estimation [7].

The satellites arcs were calculated using the laser ranging data from precise ILRS stations.

Great quantities of observations were collected during a period of 14 years (from 2nd October 1993 to 24th February 2007). The quality of the positioning is directly linked to the accuracy of the orbits used (in addition to the data accuracy it self). For this reason high altitude geodetic satellites (LAGEOS-1 and LAGEOS-2) are used primarily by geodesists to the SLR network computation (EOPs and stations coordinates). Indeed, these satellites have the advantage of being less sensitive to remaining uncertainties in the dynamical models than low attitude satellites like Starlette. It concerns gravitational and non gravitational effects. But since few years, global Earth gravity field models have greatly improved the accuracy of their coefficients notably thanks to the recent GRACE mission [10]. As a consequence, empirical coefficients can be estimated along the orbit with more consistency than before; their role is to compensate part of the unknown non gravitational forces (constant and periodic). In this fact, we have used Eigen-Grace03s gravity field model for Starlette [7].

The last ITRF realization has shown that a scale difference between SLR and VLBI exists and has revealed a bias in scale factor between both solutions of about 1.0 ppb (drift of 0.08 ppb/year) at epoch 2000.0. The ITRF2005 scale is defined by VLBI technique. Consequently, it was decided to make available to SLR users an SLR solution extracted from the ITRF2005 and re-scaled back by the aforementioned scale and scale rate [4]. So, this ITRF rescaled version is considered in our all computations.The figure (1) illustrates the ILRS network considered in the determination of the ITRF2005. The table (1) gives some statistics resulting from calculations of different satellites orbits. One can retain that the WRMS of orbit residuals are at the centimetre level but with more precision for LAGEOS satellites orbits, because they have low sensitivity to gravitational and non gravitational forces effects. However Starlette data are slightly dominating the measurements set and the average contribution of normal points per satellite is about 36.8 % of all data.

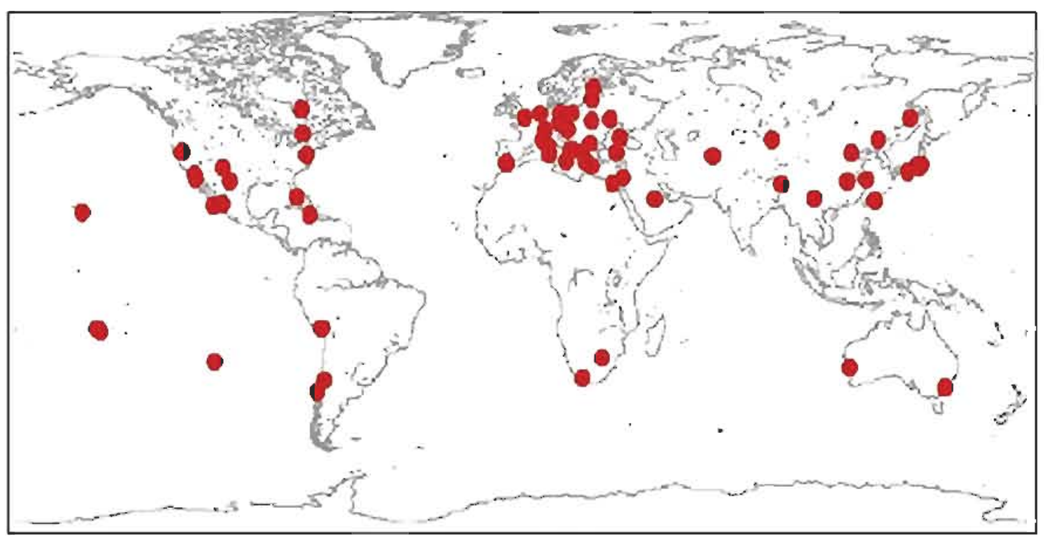

Fig. 1 ITRF2005: ILRS network, source: [3].

Table 1. Statistics of the orbit residuals (in mm). RMS: Root Mean Square of orbit residuals & WRMS: Weighted Root Mean Square of orbit residuals.

Satellite	Normal points Number & (%)	Mean residual RMS	Mean residual WRMS
LAGEOS-1	543969 (32.2%)	12.7	9.8
LAGEOS-2	521734 (30.9%)	12.2	8.5
Starlette	621408 (36.8)	18.3	13.9

3. Computation of SLR Stations Coordinates

The determination of SLR stations coordinates was carried out by MATLO software [6]. In this study, the computation comprises two principal phases. The first relates to the use of the *minimal constraints* for the resolution of the weekly normal equations systems of the network which are initially singulars due the rank defect corresponding to three rotations, in case of the laser ranging technique. In order to define the datum of the network in question, we have applied the following values of constraints: ±1mm (3.3 mas) for rotations (*Rx*, *Ry* and *Rz*) and ±1cm for range bias per station and per satellite.

The reference frame of the network was defined by the ILRS stations among the best ones as (7090, 7840, 7080, 7110, 7105, 7810, 7839, 7237).

The results obtained are in terms of time series of coordinate updates which are considered as individual solutions. Each solution generates its proper terrestrial reference frame.

However, the second phase consists in applying a seven parameters Helmert transformation (3 translations, 1 scale factor and 3 rotations), by choosing a set of stations of good quality, on weekly solutions of the stations coordinate updates. This transformation permits to project the individual solutions according to a combined and homogeneous terrestrial reference frame. The results of the processing carried out, illustrated hereafter, are expressed according to topocentric coordinate updates of laser tracking stations (North component: *N*, East component: *E* and Up component: *U*).

4. Results and Analysis

The station position time series are estimated with respect to the ITRF2005 mean position corrected from plate tectonics (ITRF2005 velocities), Earth solid tides, pole tide and oceanic loading effects. These time series must consequently evidence the atmospheric and hydrologic loading effects. The figure 2 gives examples of series of topocentric coordinate updates (*N, E, U*) for two stations 7080 and 7090, according to different combination solutions.

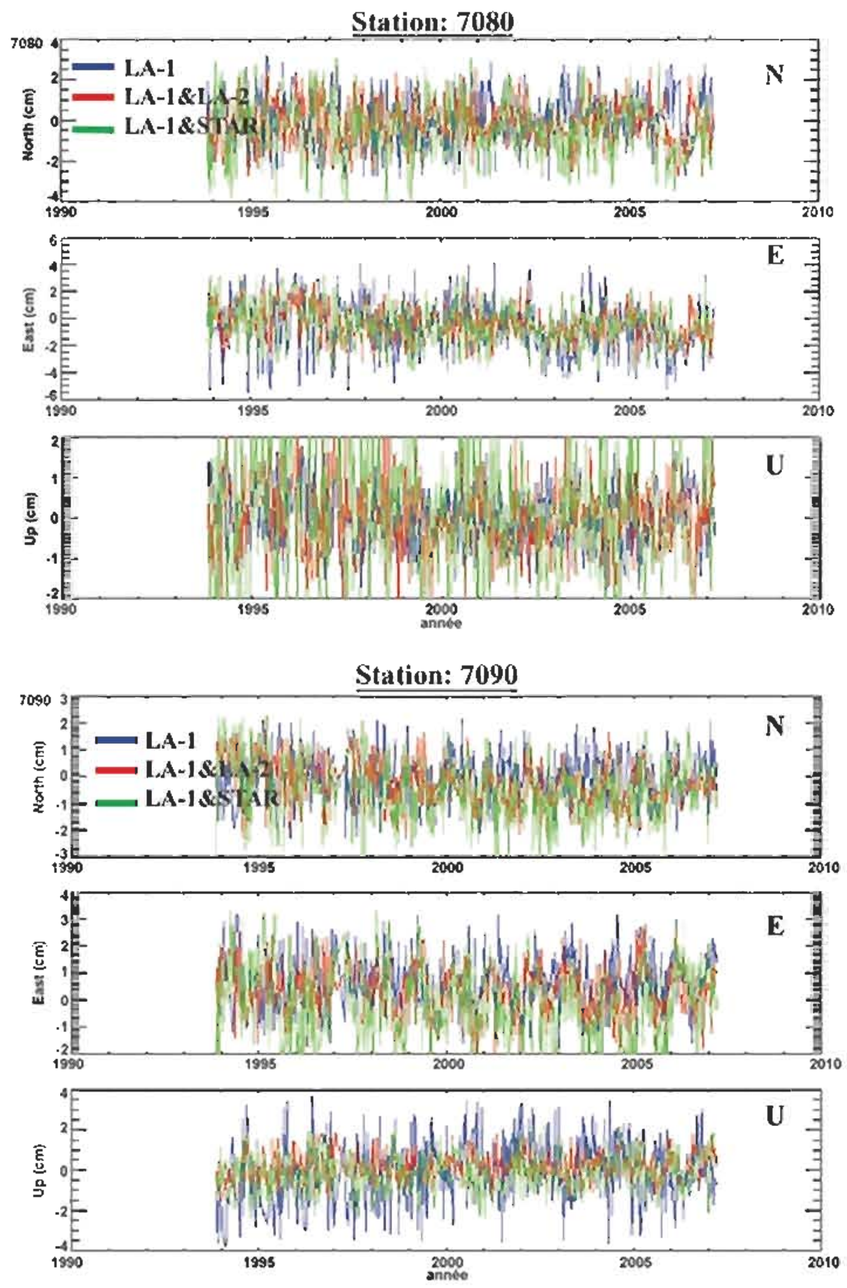

Fig. 2 Topocentric coordinate updates of SLR stations : 7080 and 7090. The series corresponding to the satellites combinations are in red for LA-1, in green for LA-1&-2, and in blue for LA-1 & STAR.

Table (2) exhibits the statistics of results obtained on coordinates updates of some ILRS stations. The contribution of the Starlette data on the determination of the estimated parameters of these stations is as follows:

- Increase of solutions number compared to those obtained from the LA-1 and LA-1&LA-2 solutions;
- Improvement, of some mm, the quality of few series; for example UP series of station 7090 and East series of station 7105; by adopting the solution LA-1&STAR compared to that of LA-1. However, we notice in general, a quite degradation of quality of coordinate updates series of about 3–5 mm which is mainly due to noise induced by low altitude orbit of Starlette;
- Statistically, the results obtained by the Starlette observations without and with weighting are slightly identical with a margin of some millimetres.

The interest of the time series of stations coordinates calculated in a homogeneous reference frame is to enable us to highlight residual signals compared to the a priori signals used in modelisation (geophysical signals). In this framework, one carried out a frequency analysis on vertical component series of some stations by FAMOUS software. We have focused on this component because it is important for the geodynamical studies since it holds amplitude ⅔ of signals acting on the station motion [6].

The results in terms of amplitude and phase of the signal in each UP series of station and according to combination solutions (LA-1, LA-1&LA-2 and LA-1&STAR) are given by table 3. One could detect annual and semi-annual signals, in vertical time series of stations (7080, 7840, 8834, 7110 and 7839), with amplitudes between 1 to 8 mm. Since, the effects of ocean loading were considered in the model a priori of restitution, the signals detected are probably related to residual loading effects as atmospheric and hydrologic loading effects, which typically have amplitudes of a few mm, (see figure 3).

Table 2. RMS and number solutions of the topocentric coordinates of some stations, according to different satellite combinations. The letters a and b correspond to non weighted observations and weighted observations of Starlette satellite, respectively.

Station	Combination	North (cm)		East (cm)		Up (cm)	
7090	LA-1	±0.90	527	±1.02	605	±1.52	594
	LA-1&LA-2	±0.84	590	±0.96	602	±0.69	580
	LA-1&STAR (a)	±1.14	599	±1.39	600	±0.96	587
	LA-1&STAR (b)	±1.22	613	±1.79	617	±1.06	600
7105	LA-1	±1.20	459	±1.88	489	±0.62	513
	LA-1&LA-2	±0.90	521	±0.99	531	±0.87	528
	LA-1&STAR (a)	±1.43	568	±1.49	556	±1.34	561
	LA-1&STAR (b)	±1.20	546	±1.39	557	±1.33	552
7403	LA-1	±2.68	230	±1.60	246	±2.22	261
	LA-1&LA-2	±1.41	304	±1.46	302	±1.81	290
	LA-1&STAR (a)	±3.00	368	±3.16	369	±2.81	341
	LA-1&STAR (b)	±2.48	361	±2.52	356	±2.57	341
8834	LA-1	±1.46	451	±1.57	461	±1.30	470
	LA-1&LA-2	±1.12	489	±0.87	468	±1.31	488
	LA-1&STAR (a)	±1.40	507	±1.36	510	±1.68	501
	LA-1&STAR (b)	±1.34	508	±1.26	498	±1.87	515
7840	LA-1	±1.15	549	±1.18	536	±0.90	576
	LA-1&LA-2	±0.76	556	±0.76	578	±0.94	578
	LA-1&STAR (a)	±1.16	596	±1.05	590	±1.30	585
	LA-1&STAR (b)	±1.12	596	±0.97	576	±1.21	591
7839	LA-1	±1.26	512	±1.17	497	±0.96	517
	LA-1&LA-2	±0.74	516	±0.78	555	±1.18	576
	LA-1&STAR (a)	±1.05	547	±1.04	549	±1.36	560
	LA-1&STAR (b)	±1.09	572	±0.98	563	±1.32	568

Table 3. Annual and semi-annual terms of vertical coordinate (Up component) of some stations, according to combinations (LA-1, LA-1&-2 and LA-1&STAR). Amplitude (A in mm) and Phase (φ in degrees).

		LA-1		LA-1&LA-2		LA-1&STAR	
Station	Period	$A \pm \sigma A$	$\varphi \pm \sigma\varphi$	$A \pm \sigma A$	$\varphi \pm \sigma\varphi$	$A \pm \sigma A$	$\varphi \pm \sigma\varphi$
7110	1 yr	1.2 ± 0.6	215.2 ± 30.7	3.7 ± 0.7	241.8 ± 12.5	4.1 ± 0.7	263.9 ± 18.8
7090	1 yr	6.6 ± 1.3	43.5 ± 11.4		-	2.1 ± 0.8	53.4 ±23.2
	½ yr		-	1.4 ± 0.4	177.3 ± 33.7		-
7080	1 yr		-	2.9 ± 0.9	220.9 ± 17.4	3.6 ± 1.3	235.4 ± 21.9
	½ yr	2.4 ± 0.7	139.9 ± 17.4		-		-
7105	1 yr		-	2.2 ± 0.8	56.8 ± 22.6	4.2 ± 0.7	88.1 ± 20.4
	½ yr	1.6 ± 0.6	220.8 ± 22.3		-		-
8834	1 yr		-	2.9 ± 0.9	350.5 ± 30.4	4.8 ± 1.1	98.9 ± 23.0
	½ yr		-		-	4.4 ± 1.5	59.0 ± 22.3

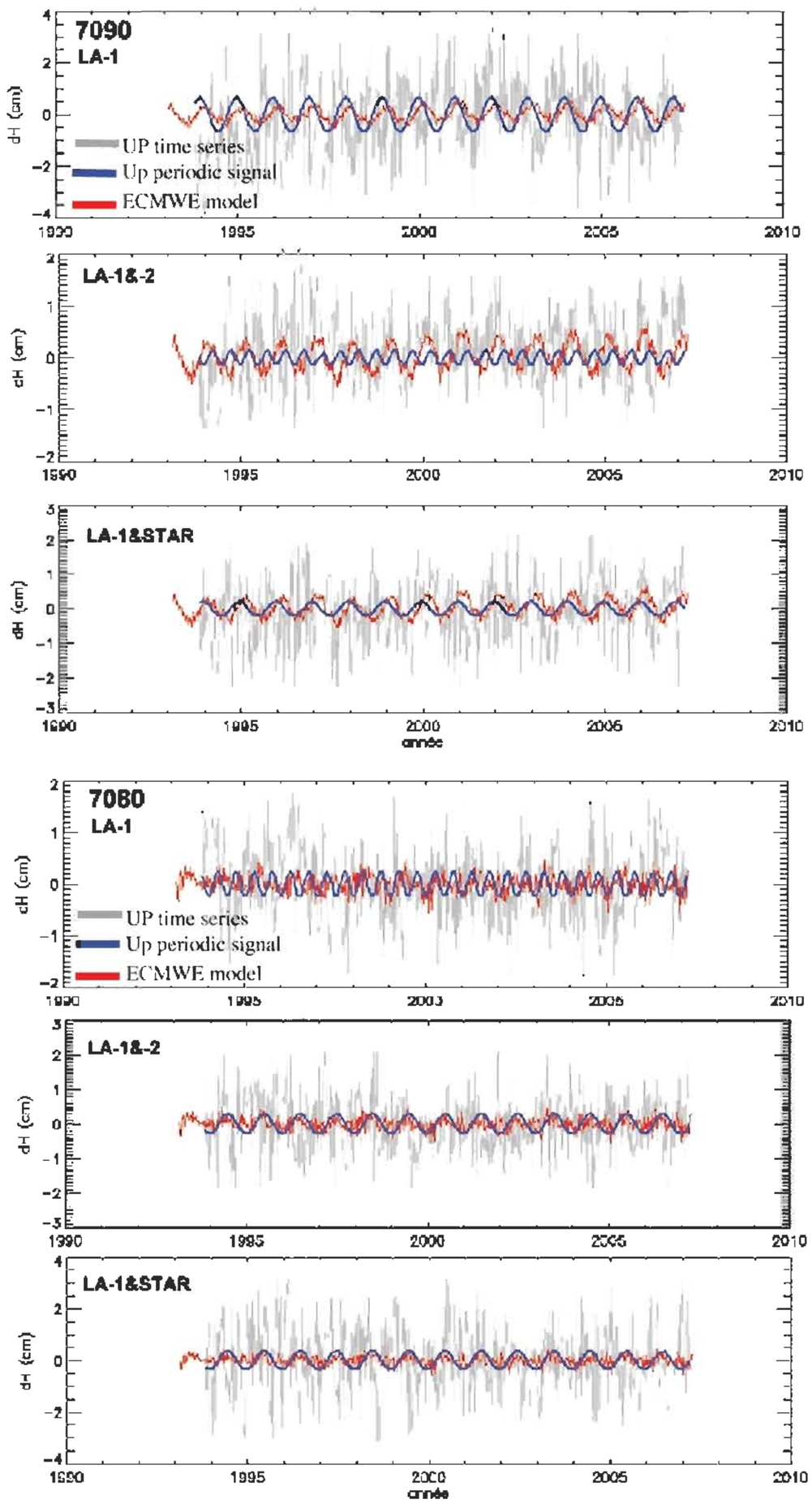

Fig. 3 Comparison between seasonal signals of the Up components and atmospheric loads model (ECMWF) for 7090 and 7080 stations.

The figure (3) gives an example of comparison between the UP periodic signals according to the different combinations and the atmospheric loads model (ECMWF series), for 7080 and 7090 laser stations. The correlation between the two signals is about 40-50%, in the case of the LA1&STAR combination, which explains that the UP variations of the two stations (7080 and 7090) are due to atmospheric loads. The remain variations are mainly come from noise.

It is interesting to exhibit which type of noise affecting the time series of coordinates in order to determine the possible sources of errors in the estimation of these parameters. In this stage, we have used the Allan variance [1],[2]. By definition the Allan variance of position residuals, for a given time interval, is computed by averaging position the residuals over that interval and computing the variance of differences between adjacent averaged values. The Allan variance analysis was developed and is widely used for estimating the frequency stability of atomic clocks. This tool was extended to geodetic data. It allows one to characterize the type of noise and, in particular, to identify white noise (spectral density S independent of frequency f), flicker noise (S proportional to $1/f$), and random walk noise (S proportional to $1/f^2$).

The dependence of the Allan variance of a time series on the sampling time τ can be interpreted in terms of its error spectrum by means of the Allan diagram, which gives Allan variances for increasing values of τ [8].

In logari-thmic scales, slopes –1,0 and +1 correspond to white noise, flicker noise and random noise, respectively.

In the context of this study, a white noise signature in the position residuals would point to random errors (Gaussian errors) affecting the measurements, while a flicker noise signature would point to perturbations that may have different origins, like local tectonics, instrument defects, analysis consistency, etc.

The noise type is measured by the slope of the Allan graph, which describes the log-log relationship of the Allan variance of the time series.

The noise level measured by the Allan deviation for a one-year sampling time of the non-linear, non-seasonal position time-series.

The table 4 provides the bias and slope of the Allan graph of some stations UP components. According to figure 4, and as first interpretation, we notice that the white noise is the dominant noise in these series according to the different solutions (LA-1, LA-1 &LA-2 and LA-1&STAR).

While a weak flicker noise combined with white noise is observed in the Up component of the different stations, according to the LA-1 and LA-1&LA-2 solutions. In addition, periodic signal was detected in UP series of 7835 station.

According to the table 4, the noise level is about of 3 – 7 mm.

Table 4. Slope and bias of noise affecting the Up component signals of some SLR stations, according to the LA-1, LA-1&-2 and LA-1&STAR solutions. These values are computed from Allan variance for each series. The noise type, (Wh.) or Flicker noise (Fl.) is listed when available. Ps. means periodic signal.

Station	Solution	Slope (cm/yr)	Noise level (cm)	Noise type
7080	LA-1	-0.6	0.3	Wh.+ *weak* Fl.
	LA-1&-2	-0.7	0.4	Wh.+ *weak* Fl.
	LA-1&STAR	-0.9	0.5	Wh.
7090	LA-1	-0.7	0.6	Wh.+ *weak* Fl.
	LA-1&-2	-0.6	0.3	Wh.+ *weak* Fl.
	LA-1&STAR	-0.9	0.4	Wh.
7835	LA-1	-0.4	0.6	Wh. +Fl.+ ps
	LA-1&-2	-0.5	0.6	Wh. +Fl.+ ps.
	LA-1&STAR	-0.7	0.7	Wh.+ ps.
7110	LA-1	-0.5	0.3	Wh. +Fl.
	LA-1&-2	-0.6	0.3	Wh. +Fl.
	LA-1&STAR	-0.9	0.4	Wh.

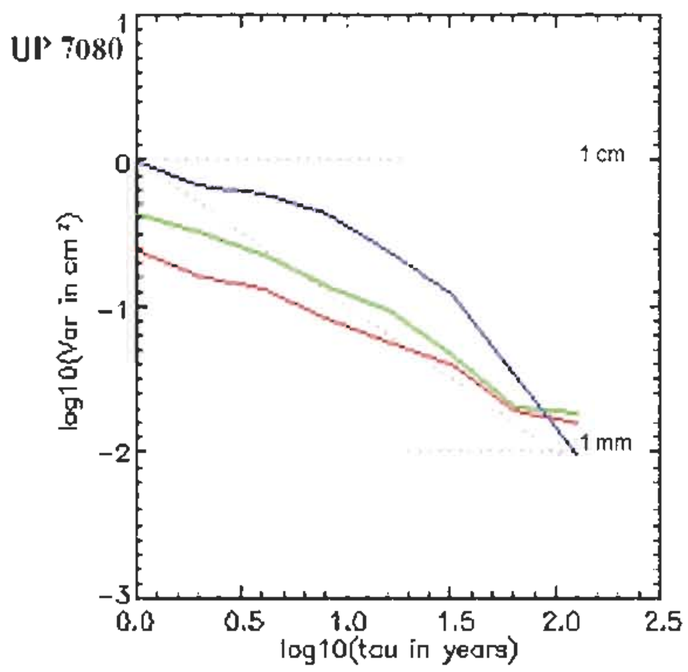

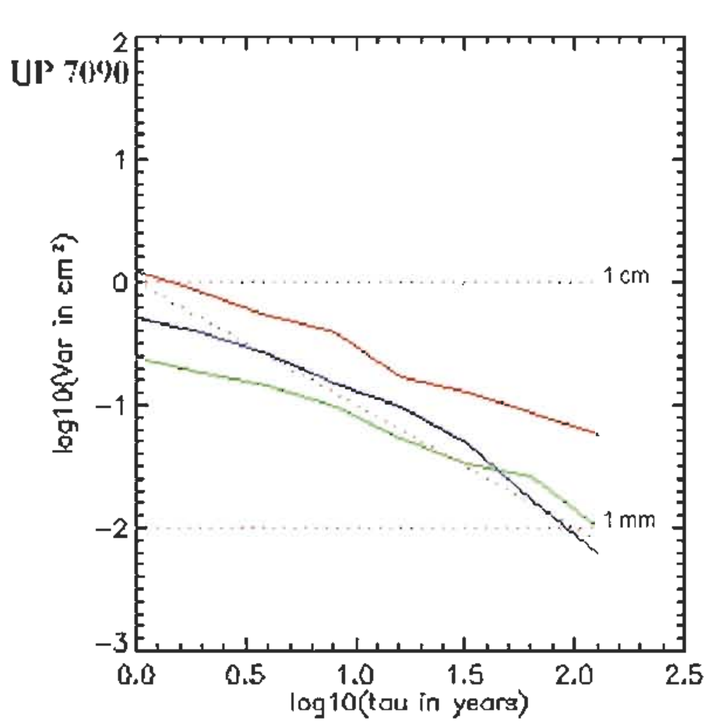

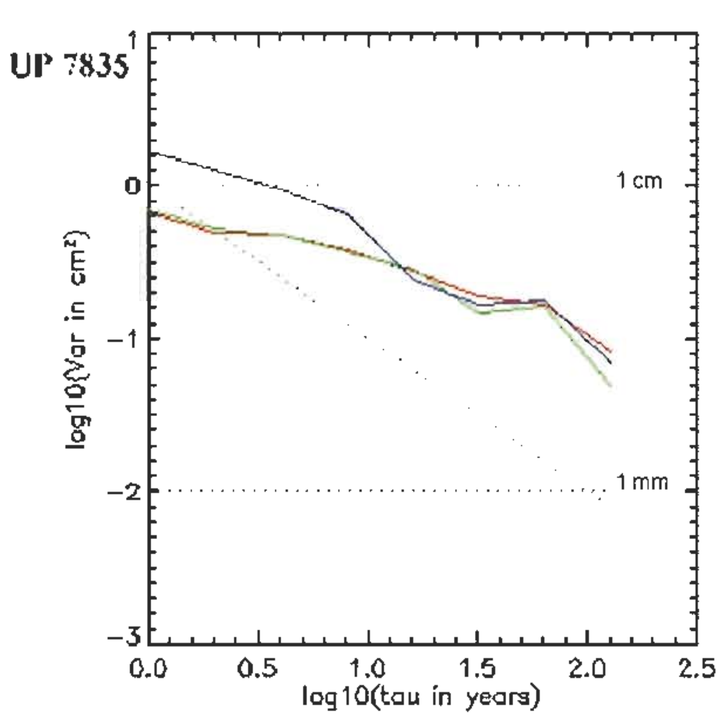

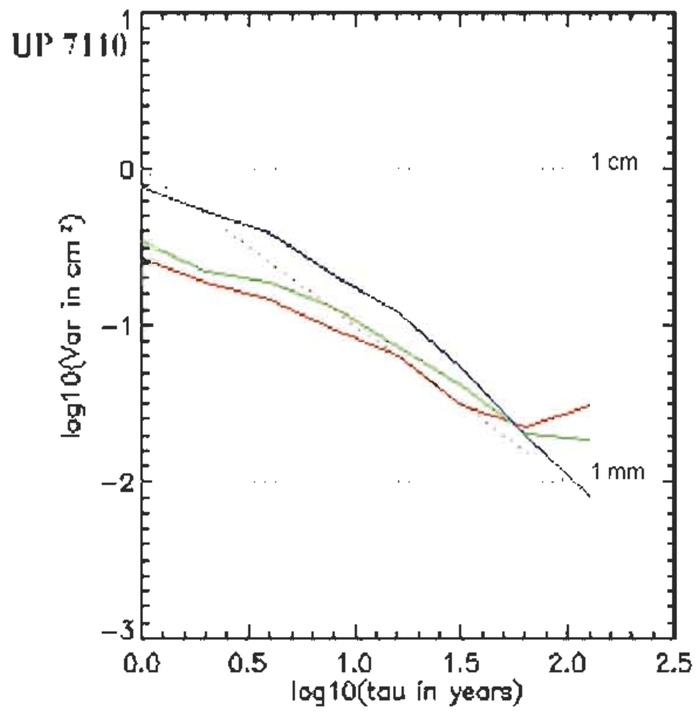

Fig. 4 Allan variance graph of Up component updates of stations 7080, 7090, 7835 and 7110. The series corresponding to the satellites combinations are in red for LA-1, in green for LA-1&-2, and in blue for LA-1 & STAR.

5. Conclusion

The results obtained revealed that the contribution of the Starlette data is acceptable, in general, to study the Terrestrial Reference Frame and to analyse the quality of the related parameters. In spite of the significant number of the normal points on this satellite and the recent dynamic models used, in particular the Eigen-Grace03s gravity field model, in the calculation of its orbit, the impact of Starlette remain not very important. Nevertheless, we demonstrate that the use of low orbit altitude such Starlette, in geodynamic field, is reliable in order to supply the study of behaviour of stations position motion.

In order to improve these results, it is necessary to develop and to investigate the following points:

- method of rigorous weighting of measurements SLR by satellite and station;
- comparison of the coordinate time series with geophysical signals.

As prospects, it will be interesting to generate and to study, for a long period (34 years: 1976 – 2009), the time series of TRF and Earth Orientation Parameters (EOPs), based on low satellites such Stella, Topex/Poseidon, Jason-1, in addition to Starlette and LAGEOS satellites.

Acknowledgments

Special thanks to GMC team (P. Exertier, Ph. Berio, D. Feraudy and D. Coulot, etc.) from Observatoire de la Côte d'Azur (OCA), Grasse – France, for their precious technical aid and scientific assistance to achieve this work.

Bibliographical References

Allan, D.W.: Statistics of Atomic Frequency Standards, Proc. IEEE, 54, 221-231, 1966.

Allan, D.W.: *Time and frequency characterisation, estimation, and prediction of precision clocks and oscillators.* IEEE Trans. UFCC, 34, 647-654, 1987.

Altamimi, Z. and X. Collilieux : *Time Series Analysis of ILRS SLR Weekly Solutions.* ILRS Workshop, Grasse, France , September, 2007.

Altamimi, Z. : Système de référence terrestres : *définition, réalisation, application à l'ITRF, état actuel et perspectives.* Dossier d'Habilitation à Diriger des Recherches, Université Pierre et Marie Curie (Paris 6), 2006.

Altamimi, Z., X. Collilieux, J. Legrand, B.Garayt, and C. Boucher: *ITRF2005: a new release of the International Terrestrial Reference Frame based on time series of stations positions and Earth Orientation Parameters.* Journal of Geophysical Research, Vol. 112, B09401, doi : 10.1029/2007 JB004949, 2007.

Coulot, D.: *Télémétrie laser sur satellites et combinaison de techniques géodésiques. Contributions aux systèmes de référence terrestres et applications.* PhD thesis, Observatoire de Paris, 2005.

Gourine, B., S. Kahlouche, P. Exertier, Ph. Berio, D. Coulot, and P. Bonnefond: *Positioning of the French Transportable Laser Ranging System (FTLRS) in Corsica over the 2002 and 2005 campaigns.* XXIII FIG Congress Proceedings, Munich, Germany, October 2006.

Le Bail, K.: *Etude statistique de la stabilité des stations de géodésie spatiale – Application à DORIS.* PhD thesis, Observatoire de Paris, 2004.

Mignard,: *Guide d'utilisation du logiciel FAMOUS.* Internal Report OCA- France, 2005.

Reigber Ch., R. Schmidt, F. Flechtner, R. Konig, U. Meyer: *An earth gravity field model complete to degree and order 150 from GRACE: Eigen-Grace02S.* Journal of Geodynamics, Vol. 39, 1-10, 2005.

Détermination du Geoïde Gravimétrique au nord de l'Algerie : Méthode de Stokes-Helmert

N. Zekkour & M. Aarizou
Centre des Techniques Spatiales. BP 13 Arzew-Oran
E-mail: zekkour.nesrine@gmail.com

ملخّص: يصاغ مشكل القيم الحدية الجيوديزية في نظرية Stokes وفق شروط توافقية للكمون المضطرب و في غياب الكتل الطبوغرافية خارج المساحة الحدية للجيود، لكن في الواقع هذه الشروط غير محققة وعليه نقوم بصياغة مبسطة للفرضيات على كثافة الكتل الطوبوغرافية وكذا تكامل Poisson لإيجاد الحل. الهدف من المقال هو استعمال طريقة Stokes-Helmert لصياغة مشكل القيم الحدية و للتعبير عن فرق الجاذبية في فضاء Helmert. وفي هذه الحالة نأخذ بعين الاعتبار التأثيرات الطبوغرافية المباشرة الجوية على كمون الجاذبية، تصحيحات اهليليجية وطريقة الاستمرارية نحو الأسفل لفروق الجاذبية. تركزالاختبارات التي أجريت على تحديد الجيود في شمال الجزائر من خلال طريقة Stokes - Helmert.

الكلمات الأساسية: التأثيرات الطبوغرافية، التأثيرات الجوية، الجيود، الكمون.

Résumé : Dans la théorie de Stokes, le problème de valeurs aux limites géodésiques de troisième espèce est formulé sous les conditions d'harmonicité du potentiel perturbateur et d'absence de masses topographiques à l'extérieur de la surface limite qui est le géoïde. Or, en pratique, ces conditions ne peuvent être satisfaites et, de ce fait, des hypothèses simplificatrices sur la densité des masses topographiques et sur l'analycité de l'intégrale de Poisson sont émises pour obtenir une solution du problème. La reformulation du problème de valeurs aux limites dans l'espace de «Helmert» permet une meilleure modélisation de la topographie et mène ainsi à une estimation plus précise de la solution. Le thème développé à travers cet article porte sur la détermination du géoïde gravimétrique en adoptant l'approche de Stokes-Helmert pour résoudre le problème de valeurs aux limites et exprimer les anomalies de gravité dans l'espace d'Helmert. Dans la détermination de la solution, nous tiendrons compte des effets directs topographiques et atmosphériques sur le potentiel de pesanteur, des corrections ellipsoïdales et du prolongement descendant des anomalies de pesanteur. Les tests effectués ont porté sur la détermination du géoïde gravimétrique au nord de l'Algérie par la méthode de Stokes-Helmert. Les données utilisées sont constituées de 2064 points gravimétriques, du modèle géopotentiel EGM96, du modèle global d'élévation TUG87 et du modèle numérique de terrain GTOPO30. Les différents résultats obtenus sont illustrés.

Mots-clés: Anomalie de pesanteur, Effet atmosphérique, Effet topographique, Géoïde, Co-géoïde, potentiel.

Abstract: One of the most advantageous methods is the approach of Stokes-Helmert developed at the University of New Brunswick (UNB) in Canada. In Stokes's theory, the geodetic boundary value problem (GBVP) of third kind is formulated under the conditions of harmonicity of the disturbing potential and absence of topographical masses outside the boundary surface which is the geoid. In practice, these conditions cannot be carried out exactly and, so of the simplifying assumptions on the density of topographical masses and the Poisson's integral are introduced for obtaining the solution of the problem. The reformulation of the GBVP in "Helmert's space" allows modeling better of topography and thus leads to a more precise estimate of the solution. The objective of this article consists in using the Stokes-Helmert scheme for the definition of the BVP and expressing the gravity anomaly in Helmert space. This will require holding account rigorously, in the determination of the solution, the direct topographic and atmospheric effect, the ellipsoidal corrections and the "downward continuation" of the gravity anomaly. The made tests concerned the determination of the geoïd in the North of Algeria by the method of Stokes-Helmert. The used data are constituted by 2064 points, of the geopotential model EGM96, of the global model of rise TUG87 and the digital model of ground GTOPO30.

Key words: gravity Anomaly, atmospheric effect, topographic effect, Geoid, Potential, Co-Geoid.

1. Introduction

Le processus le plus adéquat à la définition de la forme réelle de la Terre se base sur le "troisième problème de valeurs aux limites géodésiques". Ce problème dans la théorie du potentiel gravitationnel consiste à déterminer une fonction harmonique (potentiel perturbateur) sur une superficie limite (le géoïde) par l'intermédiaire d'une combinaison linéaire de cette fonction ainsi que de ses dérivées normales. La théorie de Stokes-Helmert présentée dans cet article étudie en détail la méthode de condensation de Helmert pour une détermination précise du géoïde.

Dans ce contexte, le 3ème problème de valeurs aux limites géodésiques est ramené au 1er problème de valeurs aux limites géodésiques qui est résolu dans l'espace de Helmert. La solution est obtenue alors sur le co-géoïde et sera de nouveau transformée dans l'espace réel (géoïde) par l'évaluation précise de l'effet topographique indirect primaire.

Le but principal de la méthode de Stokes-Helmert est de fournir une théorie assez précise pour le calcul du géoïde. Ce but sera atteint dans le cas où toutes les corrections et les transformations de l'anomalie de pesanteur observée dans l'espace de Helmert sont effectuées avec une précision de 10 μGal **[14]**. Cela implique a priori que tous les effets sur la pesanteur supérieurs à 10 μGal doivent être pris en compte.

2. Problème de valeurs aux limites géodésiques

Un problème de valeurs aux limites en géodésie physique peut être exprimé comme suit :

$$\begin{cases} \Delta T = 0 & \text{à l'extérieur de } \Sigma \\ BT = f & \text{sur } \Sigma \\ T = O(r^{-1}) & \text{à l'infini} \end{cases}$$

Où T est le potentiel perturbateur, B est un opérateur défini sur la surface limiteΣ, et f est une fonction définie sur Σ résultant des mesures gravimétriques, des observations de nivellement, des systèmes de positionnement globaux (GPS), etc.

Selon les différences des données, on énonce le problème de valeurs aux limites géodésiques sous diverses formes:

- *Problème de 1ère espèce (Dirichlet):*

$$\begin{cases} \Delta T = 0 & \text{à l'extérieur de } \Sigma \\ T = W - U & \text{sur } \Sigma \\ T = O(r^{-1}) & \text{à l'infini} \end{cases}$$

Avec :

W : potentiel de pesanteur

U : potentiel normal.

- *Problème de 2ème espèce (Neumann):*

$$\begin{cases} \Delta T = 0 & \text{à l'extérieur de } \Sigma \\ \dfrac{\partial T}{\partial h} = -\delta g & \text{sur } \Sigma \\ T = O(r^{-1}) & \text{à l'infini} \end{cases}$$

Où $\frac{\partial T}{\partial h}$ et δg représentent respectivement la dérivée normale et la perturbation de pesanteur.

- *Problème de 3ème espèce (mixte) :*

$$\begin{cases} \Delta T = 0 & \text{à l'extérieur de } \Sigma \\ \dfrac{\partial T}{\partial h} - \dfrac{1}{\gamma}\dfrac{\partial \gamma}{\partial h} T = -\Delta g & \text{sur } \Sigma \\ T = O(r^{-1}) & \text{à l'infini} \end{cases}$$

Δg est l'anomalie de pesanteur.

Ce problème représente le problème fondamental de la géodésie physique dont la formulation est donnée, selon l'approche de Stokes par l'équation **[3]**:

$$\frac{\partial T(r_t)}{\partial h} - \frac{1}{\gamma}\frac{\partial \gamma}{\partial h} T(r_t) + \Delta g(r_t) = 0 \qquad (2.1)$$

Une approximation sphérique à cette équation est donnée par :

$$\frac{\partial T(r_t)}{\partial r} + \frac{2}{R} T(r_t) + \Delta g(r_t) = 0 \qquad (2.2)$$

Où R est le rayon moyen de la Terre.

Rappelons que les mesures de pesanteur sont effectuées à la surface du sol ou à une certaine hauteur de celui-ci; Ce qui nous amène à utiliser une méthode de réduction pour le calcul de la pesanteur au géoïde. Cependant, le manque d'informations précises sur la densité de la masse topographique ne permet pas de calculer correctement la pesanteur au niveau du géoïde. Pour pallier à ces inconvénients, plusieurs approches ont été proposées dont la méthode de Helmert **[4]** que nous décrirons en détail dans ce qui suit.

3. Théorie de Stokes-Helmert

La deuxième méthode de condensation de Helmert est appliquée en même temps qu'à la théorie de Stokes comme étant la méthode la plus simple pour résoudre le problème de valeurs aux limites géodésiques. La combinaison de ces deux méthodes est dite Théorie de "STOKES-HELMERT" qui est basée d'une part, sur l'idée de condensation de Helmert pour la détermination précise du géoïde, et d'autre part, sur les propriétés théoriques de la solution de Stokes dans l'espace de Helmert.

Le potentiel perturbateur T^h dans l'espace de Helmert devient :

$T^h(r_l) = T(r_l) - \delta V(r_l)$ (3.1)

et $\delta V(r_l) = \delta V^t(r_l) + \delta V^a(r_l)$ (3.2)

- δV^t est le potentiel topographique résiduel, tel que : $\delta Vt(r_l) = V^t(r_l) - V^{ct}(r^l)$ (3.3)

Où V^t et Vct représentent respectivement le potentiel des masses topographiques et le potentiel des masses topographiques condensées

- δV^a est le potentiel atmosphérique résiduel : $\delta V^a(r_l) = V^a(r_l) - V^{ca}(r_l)$ (3.4)

Où V^{ca} et V^a représentent respectivement le potentiel de la couche atmosphérique condensée et le potentiel des masses atmosphériques.

La fonction T^h est harmonique en tout point à l'extérieur du co-géoïde (le géoïde décalé) :

$\Delta T^h(r) = 0 \qquad r \geq r_g$ (3.5)

r_g est le rayon géocentrique du co-géoïde.

Le co-géoïde de Helmert est décalé de quelques mètres du géoïde sous l'effet indirect de condensation de Helmert.

Ce dernier est connu sous le nom de l'effet topographique indirect primaire (PITE) **[3]**.
La pesanteur de Helmert $g^h(r_l)$ à la surface de la Terre est la somme de la pesanteur observée $g(r_l)$ à la surface de la Terre, de l'effet topographique direct $\delta A^t(r_l)$ et de l'effet atmosphérique direct $\delta A^a(r_l)$ référé à la surface de la Terre, telle que :

$$g^h(r_l) = g(r_l) - \delta A^t(r_l) - \delta A^a(r_l) \qquad (3.6)$$

La forme sphérique de la pesanteur observée peut être écrite en termes d'anomalies de pesanteur de Helmert de la manière suivante :

$$\Delta g^h(r_l) = \Delta g^{FA}(r_l) + \delta S^t(r_l) + \delta S^a(r_l) + \delta A^t(r_l) + \delta A^a(r_l) + \delta S^\xi(r_l) \qquad (3.7)$$

- $\delta S^t(r_l) = \frac{2}{R}\delta V^t(r_l)$: Effet topographique secondaire indirect sur la pesanteur .

- $\delta S^a(r_l) = \frac{2}{R}\delta V^a(r_l)$

Effet atmosphérique secondaire indirect sur la pesanteur.

- $\delta S^\xi(r_l) = \frac{2}{R}H^\circ(r_l)\,\Delta g^{SB}(r_l)$ Correction du géoïde au quasi-géoïde.

- $\Delta g^{FA}(r_l)$: L'anomalie complète de Bouguer

3.1 Effets des masses topographiques sur la pesanteur

- Effet topographique direct

L'effet topographique direct des masses topographiques sur la pesanteur, créé en un point à la surface de la Terre, est donné par **[8]**:

$$A^t(r_l) = \left.\frac{\partial V^t(r)}{\partial r}\right|_{r=R+H^\circ(\Omega)} \qquad (3.8)$$

$$= G \iint_{\Omega'\in\Omega_0} \rho(\Omega') \int_{r'=R}^{R+H^\circ(\Omega')} \left.\frac{\partial N(r,\psi,r')}{\partial r}\right|_{r=R+H^\circ(\Omega)} r'^2 dr' d\Omega'.$$

$\rho(r',\Omega)$ Densité des masses topographiques.
$N(r,\psi,r')$ Forme spatiale du noyau de Newton.
$H^\circ(\Omega')$ Altitude horthométrique.

L'effet topographique direct des masses topographiques condensées sur la pesanteur, compté également sur la surface de la Terre, est représenté par **[8]** :

$$A^{ct}(r_l) = \left.\frac{\partial V^{ct}(r)}{\partial r}\right|_{r=R+H^\circ(\Omega)} \qquad (3.9)$$

$$= GR^2 \iint_{\Omega'\in\Omega_0} \sigma(\Omega') \left.\frac{\partial N(r,\psi,R)}{\partial r}\right|_{r=R+H^\circ(\Omega)} d\Omega'.$$

Où $\sigma(\Omega')$ représente la densité de la couche topographique condensée.

- Effet topographique secondaire indirect

L'application de la correction topographique à l'anomalie de pesanteur donne l'origine de l'effet topographique indirect secondaire. Il est donné par l'équation suivante **[9]** :

$$\delta V^t = G \iint_{\Omega'\in\Omega_0} \rho(\Omega') \int_{r'=R}^{R+H^\circ(\Omega')} \left. N(r,\psi,r')\right|_{r=R+H^\circ(\Omega)} r'^2 dr' d\Omega' -$$

$$G \iint_{\Omega'\in\Omega_0} \rho(\Omega') \frac{r'^3(\Omega') - R^3}{3} N(r,\psi,R)\, d\Omega'. \qquad (3.10)$$

3.2 Effet des masses atmosphériques sur la pesanteur

- Effet atmosphérique direct

L'effet atmosphérique direct sur la pesanteur rapporté à la surface terrestre est **[14]** et **[11]**:

$$\left.\frac{\partial \delta V^a(r)}{\partial r}\right|_{r=R+H^\circ(\Omega)} = \left.\frac{\partial V^a(r)}{\partial r}\right|_{r=R+H^\circ(\Omega)} - \left.\frac{\partial V^{ca}(r)}{\partial r}\right|_{r=R+H^\circ(\Omega)} \qquad (3.11)$$

- Effet atmosphérique secondaire indirect

L'effet atmosphérique secondaire indirect sur la pesanteur définie sur la surface de la Terre, peut être décrit par l'expression suivante **[11]** :

$$\frac{2}{r_l}\delta V^a(r) = \frac{2}{r_l}V^a(r) - \frac{2}{r_l}V^{ca}(r). \qquad (3.12)$$

3.3 Prolongement descendant des anomalies de pesanteur de Helmert

Dans la formulation standard du problème de valeurs aux limites géodésiques de Stokes, la solution (potentiel perturbateur T) est déterminée au-dessus de la surface limite (géoïde) alors que les observations (valeurs de pesanteur g) sont mesurées à la surface de la Terre. Pour obtenir ces valeurs aux limites, les observations doivent être réduites de la surface terrestre au géoïde. Cette réduction est appelée le prolongement descendant d'anomalie de pesanteur.
L'outil mathématique standard utilisé pour l'étude des prolongements descendant et ascendant est basé sur le théorème de Poisson qui définit une fonction f, connue sur une sphère de rayon R et harmonique en dehors de cette sphère. Le calcul des valeurs de la fonction $f(r,\Omega)$ s'effectue sur n'importe quel point à l'extérieur de la sphère $(r > R)$ par l'intégrale de Poisson selon **[6]** :

$$f(r,\Omega) = \frac{1}{4\pi}\int_{\Omega'} f(R,\Omega')K(r,\psi,R)d\Omega', \qquad (3.13)$$

Où K est le Noyau de l'intégral de Poisson défini par **[15]** :

$$K(r_l,\psi,R) = \sum_{n=2}^{\infty}(2n+1)\left[\frac{R}{r_l}\right]^{n+1} P_n(\cos\psi) \qquad (3.14)$$

Puisque les masses topographiques et atmosphériques sont condensées sur le géoïde, l'espace de Helmert, au-dessus du géoïde (rapproché par la sphère géocentrique de rayon R ($r_g \approx R$)), est harmonique. L'anomalie de pesanteur de Helmert Δg^h multiplié par le rayon géocentrique de la surface terrestre r_i satisfait l'équation de Laplace au-dessus du géoïde, $r_i \phi R: \nabla^2 \left| r_i \Delta g^h(r_i) \right| = 0$ **[16]**.

L'intégrale de poisson pour Δg^h est donnée par la formule suivante **[6]** :

$$\Delta g^h(r_i) = \frac{R}{4\pi r_i} \iint_{\Omega \in \Omega_0} K(r_i, \psi, R) \Delta g^h(R) d\Omega, \quad (3.15)$$

Où $\Delta g^h(r_i)$ est le vecteur des anomalies de pesanteur de Helmert sur la surface de la Terre et $\Delta g^h(R)$ est le vecteur des anomalies de la pesanteur de Helmert sur le Co-géoïde (rapprochée encore par la sphère de référence de rayon R).

La forme discrète de l'équation de l'intégrale de Poisson dont la forme générale est l'équation de l'intégrale de Fredholm de première espèce, peut être exprimée comme suit **[10]** et **[4]** :

$$\Delta g^h(r_i) = K(r_i, \psi, R) \Delta g^h(R), \quad (3.16)$$

Selon l'itération approchée de Jacobi **[12]** pour la solution d'un système d'équations algébriques linéaires, on obtient le système d'équations algébriques suivant **[10]** :

$$\Delta g^h(R) = \Delta g^h(r_i) + B(r_i, \psi, R) \Delta g^h(R). \quad (3.17)$$

B est la matrice creuse déduite de la matrice K par suppression des termes de la diagonale.

Ce système d'équation (3.17) peut être résolu itérativement. On commence par le vecteur d'anomalies à l'air libre de pesanteur à la surface terrestre Δg^{FA} (car ces dernières sont semblables aux anomalies de pesanteur de Helmert sur le géoïde), tel que :

$$\Delta g^h(R)\Big|_0 = \Delta g^{FA}(r_i). \quad (3.18)$$

La $k^{ième}$ étape d'itération (k>0) $\Delta g^h(R)|_k$, est effectuée selon l'équation suivante **[10]** :

$$\Delta g^h(R)\Big|_k = B(r_i, \psi, R) \Delta g^h(R)\Big|_{k-1} + \Delta g^h(r_i) \quad (3.19)$$

Ainsi, lorsque la différence des résultats de deux itérations $|\Delta g^h(R)|_k - \Delta g^h(R)|_{k-1}|$ est inférieure à la tolérance ε, le processus itératif s'arrête. Le résultat de cette opération est la solution de l'équation (3.7), **[10]** :

$$\Delta g^h(R) = \Delta g^h(r_i) + \sum_{k=1}^{\bar{k}} \Delta g^h(R)\Big|_k, \quad (3.20)$$

Où $\bar{k}$ est la valeur de la dernière itération.

Les différentes étapes de cette étude sont illustrées dans le schéma suivant :

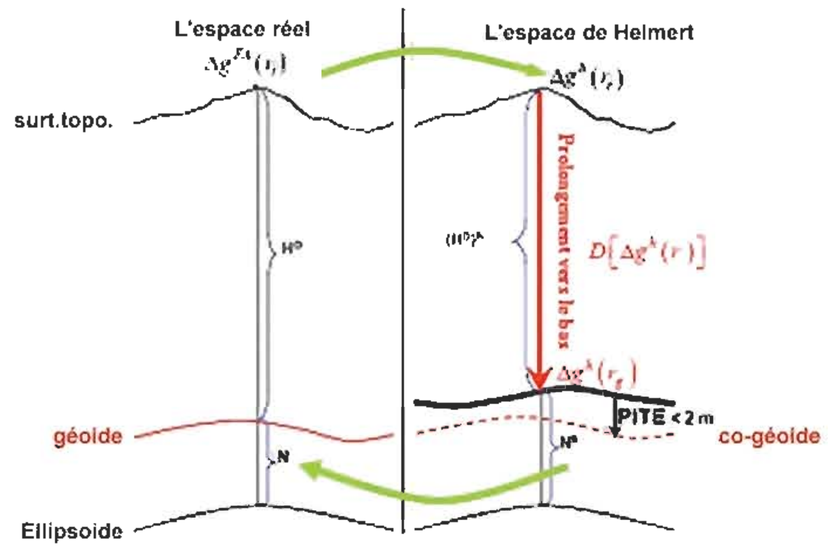

FIg. 1 Schéma des deux espaces (Réel, Helmert).

4. Problème de valeurs aux limites de Stokes

Le potentiel de pesanteur de référence $W^h_{ref}(r)$ dans l'espace de Helmert peut être exprimé par la formule suivante **[15]**:

$$r > R: \; W^h_{ref}(r) = \frac{GM}{r}\left[1 + \sum_{n=2}^{n}\left(\frac{a_0}{r}\right)^{n+1} \sum_{m=-n}^{n} W^h_{n,m} Y_{n,m}\right] \quad (4.1)$$

Cette relation est valable au niveau du co-géoïde. Comme cette surface est inconnue, l'approximation appropriée du géoïde $(r_g \approx r_0)$ peut être utilisée avec **[15]**:

$$r_g \approx r_0 \equiv a(1 - f\sin^2\varphi)$$

Le potentiel de pesanteur de référence de Helmert au niveau du co-géoïde devient :

$$r > R: \; W^h_{ref}(r_g) \approx \frac{GM}{r_0}\left[1 + \sum_{n=2}^{n}[1 + (n+1) f \sin^2\varphi] \sum_{m=-n}^{n} W^h_{n,m} Y_{n,m}\right] \quad (4.2)$$

Tel que :

$$n = 1,2,\ldots, \bar{n}: \; \left[\frac{a_0}{r_g}\right]^{n+1} = 1 + (n+1) f \sin^2\varphi - \ldots,$$

Selon la condition aux limites **[3]**, l'anomalie de pesanteur de référence de Helmert peut être exprimée comme suit :

$$\Delta g^h_{ref}(r_g) \approx \left.\frac{\partial T^h_{ref}(r)}{\partial r}\right|_{r=r_0} + \frac{2}{R} T^h_{ref}(r_g) \quad (4.3)$$

Où $T^h_{ref}(r_g) \cong T^h_{ref}(r_0) = W^h_{ref}(r_g) - U_0(\phi)$ décrit le potentiel perturbateur de référence de Helmert.

La surface limite équipotentielle dans l'espace de Helmert est donnée par l'ondulation co-géoïdale $N^h(\Omega)$. Cette surface peut être évaluée à partir des anomalies de pesanteur de Helmert $\Delta g^h(R)$ rapportée à la sphère de référence de rayon R par l'application des formules de Stokes et Bruns dans l'équation suivante **[3]** :

$$N^{h}(\Omega) = \frac{R}{4\pi\,\gamma_0(\phi)} \iint_{\Omega' \in \Omega_0} \Delta g^{h}(R) S(\psi)\, d\Omega'. \qquad (4.4)$$

4.1 Fonction sphéroïde modifiée de Stokes

Les valeurs de la fonction sphéroïde de Stokes $S_{n>\bar{n}}(\psi)$ varient proportionnellement par rapport à la distance sphérique ψ. Le domaine d'intégration Ω_0 de l'intégrale de Stokes peut être décomposé *en deux* domaines. L'un concerne les zones proches $\Omega_{\psi 0}$ ($\psi \in [0,\ \psi_0]$) *et* l'autre les zones éloignées Ω_0-$\Omega_{\psi 0}$ ($\psi \in [\psi_0, \pi]$), tel que **[13]** :

$$\iint_{\Omega \in \Omega_0} d\Omega = \iint_{\Omega \in \Omega_{\psi 0}} d\Omega + \iint_{\Omega \in \Omega_0 - \Omega_{\psi 0}} d\Omega \qquad (4.5)$$

Les contributions des zones proches et éloignées, à haute fréquence, aux altitudes co-géoïdales $N^{h}_{n>\bar{n},\Omega'_{\psi 0}}$ et $N^{h}_{n>\bar{n},\Omega'-\Omega'_{\psi 0}}$ sont données respectivement, par :

$$N^{h}_{n>\bar{n},\Omega'_{\psi 0}}(\Omega) = \frac{R}{4\pi\,\gamma_{0\,\Omega'}} \iint \Delta g^{h}(R) S_{n>\bar{n}}(\psi)\, d\Omega' \qquad (4.6)$$

$$N^{h}_{n>\bar{n},\Omega'-\Omega'_{\psi 0}}(\Omega) = \frac{R}{4\pi\,\gamma_{0\,\Omega' \in \Omega - \Omega_{\psi 0}}} \iint \Delta g^{h}(R) S_{n>\bar{n}}(\psi)\, d\Omega' \qquad (4.7)$$

La fonction sphéroïde modifiée de Stokes $S_{n,\bar{n}}(\psi_0,\psi)$ peut alors être exprimée comme suit :

$$S_{n>\bar{n}}(\psi_0,\psi) = \begin{cases} 0, & \psi \in \langle 0,\psi_0 \rangle, \\ S_{n>\bar{n}}(\psi), & \psi \in \langle 0,\psi_0 \rangle \end{cases} \qquad (4.8)$$

Le développement en série de polynômes de Legendre est donné par :

$$\forall \psi \in \langle 0,\pi \rangle:$$

$$S_{n>\bar{n}}(\psi_0,\psi) = \sum_{n=\bar{n}+1}^{\infty} \frac{2n+1}{2} Q_n(\psi_0,\psi)\, P_n(\cos\psi) \qquad (4.9)$$

Où $Q_n(\psi_0, \psi)$ décrivent les coefficients de troncation pour la fonction sphéroïde modifiée de Stokes $S_{n\ \bar{n}}(\psi_0,\psi)$. La contribution de la zone proche des anomalies de pesanteur à haute fréquence de Helmert à l'altitude géoïdale $N^{h}{}_{n>\bar{n},\Omega'\psi 0}$ co-géoïdale peut être décrite par :

$$N^{h}_{n>n,\Omega'_{\psi 0}} = \frac{R}{4\pi\,\gamma_{0\,\Omega' \in \Omega_{\psi 0}}} \iint \Delta g^{h}_{n>\bar{n}}(R)\, S_{n>\bar{n}}(\psi)\, d\Omega' \qquad (4.10)$$

La contribution de la zone éloignée à haute fréquence des anomalies de pesanteur de Helmert $\Delta g^{k}_{n>\bar{n}}(R)$ l'altitude co-géoïdal $N^{h}_{n>n\Omega'_{\psi 0}}$ est donnée par :

$$N^{h}_{n>n\Omega'_{\psi 0}} = \frac{R}{4\pi\,\gamma_0} \iint_{\Omega' \in \Omega'_{\psi 0}} \Delta g^{h}_{n>\bar{n}}(R)\, S_{n>\bar{n}}(\psi)\, d\Omega' \qquad (4.11)$$

Si les anomalies de pesanteur ne sont pas disponibles au-dessus de la Terre entière, le calcul numérique peut être fait en employant l'équation suivante :

$$N^{h}_{n>\bar{n}\,\Omega'_{\psi 0}}(\Omega) = \frac{R}{4\pi} \sum_{n=\bar{n}+1}^{\infty} Q_n(\psi_0,\psi) \sum_{m=-n}^{n} T^{h}_{n,m} \qquad (4.12)$$

La relation entre l'ondulation du géoïde N (Ω) et l'ondulation du co-géoïde $N^{h}(\Omega)$ est présentée par la formule suivante :

$$\delta N(\Omega) = N(\Omega) - N^{h}(\Omega) = \frac{\delta V^{t}(R)}{\gamma_0(\phi)} - \frac{\delta V^{a}(R)}{\gamma_0(\phi)} \qquad (4.13)$$

$\frac{\delta V^{t}(R)}{\gamma_0(\phi)}$ et $\frac{\delta V^{a}(R)}{\gamma_0(\phi)}$ sont respectivement l'effet topographique indirect primaire sur la hauteur géoïdale et l'effet atmosphérique indirect primaire sur la hauteur géoïdale.

4.2 Effet topographique indirect primaire

L'effet topographique indirect primaire sur la hauteur géoïdale prend la forme suivante **[7]** :

$$\begin{aligned} \frac{\delta V^{t}(R)}{\gamma_0(\phi)} = {} & \frac{G}{\gamma_0(\phi)} 4\pi\,\rho_0 \left[RH^{\circ} + \frac{[H^{\circ}]^2}{2} - \frac{r_t^3 - R^3}{3R} \right] + \\ & \frac{G}{\gamma_0(\phi)} \rho_0 \iint_{\Omega' \in \Omega_0} \int_{r'=R+H^{\circ}}^{R+H'} N(R,\psi,r') r'^2\, dr'\, d\Omega' - \\ & \frac{G}{\gamma_0(\phi)} \rho_0 \iint_{\Omega' \in \Omega_0} \frac{r_t'^3 - r_t^3}{3} N(R,\psi,R)\, d\Omega' + \\ & \frac{G}{\gamma_0(\phi)} \iint_{\Omega' \in \Omega_0} \delta\rho(\Omega') \int_{r'=R}^{R+H^{\circ}} N(R,\psi,r') r'^2\, dr'\, d\Omega' - \\ & \frac{G}{\gamma_0(\phi)} \iint_{\Omega' \in \Omega_0} \delta\rho(\Omega') \frac{r_t'^3 - R^3}{3} N(R,\psi,R)\, d\Omega'. \end{aligned} \qquad (4.14)$$

4.3 Effet atmosphérique indirect primaire

L'effet atmosphérique indirect primaire sur l'altitude géoïdale peut être décrit par la forme de base suivante **[11]** :

$$\begin{aligned} \frac{\delta V^{a}(R)}{\gamma_0(\phi)} = {} & \frac{G}{\gamma_0(\phi)} \iint_{\Omega' \in \Omega_0} \int_{r'=R+H^{\circ}(\Omega')}^{r'_{\lim}} \rho^{a}(r') N(R,\psi,r') r'^2\, dr'\, d\Omega' - \\ & \frac{G}{\gamma_0(\phi)} \iint_{\Omega' \in \Omega_0} \int_{r'=R+H^{\circ}(\Omega')}^{r'_{\lim}} \rho^{a}(r') N(R,\psi,R) r'^2\, dr'\, d\Omega'. \end{aligned} \qquad (4.15)$$

L'ordre de grandeur de l'effet atmosphérique indirect primaire sur l'altitude géoïdale est relativement plus petit que l'effet topographique indirect primaire sur la hauteur géoïdale.

Une fois le potentiel perturbateur réel déterminé sur le géoïde, sa conversion en hauteurs géoïdales peut être effectuée par la formule de Bruns.

Le potentiel perturbateur réel $T(r_t)$ à l'extérieur de l'atmosphère est obtenu à l'aide d'un prolongement continu de $T(R)$. Le potentiel de pesanteur réel W, pour n'importe quel point donné, en dehors de l'atmosphère, est alors simplement calculé à partir de la formule de Bruns.

5. Application : Nord de l'Algérie

La détermination du géoïde, tenant compte des noyaux modifiés de Stokes, est effectuée à l'aide des programmes du logiciel GRAVSOFT et d'autres programmes réalisés au LAREG (Laboratoire de Recherche en Géodésie de l'Institut Géographique National, Marne la Vallée) et à l'ESGT (École Supérieure des Géomètres et Topographes) **[2]**.

5.1 Description des données utilisées

Les données utilisées sont issues de différentes sources: données gravimétriques, modèle géopotentiel et modèle numérique de terrain.

Données gravimétriques: La zone d'étude est limitée entre [32°, 37°] en latitude et [-3°, 5°] en longitude et comprend 2064 points gravémitriques (Fig1). Ces données sont fournies par le BGI (Bureau Gravimétrique International de Toulouse). Elles sont extraites d'un fichier nommé EOL dont dispose le CTS. Ce choix est dû à la densité de points relativement élevée et à la nature du terrain dans cette région.

Données du modèle géopotentiel : Le modèle géopotentiel utilisé est le modèle EGM96 (Earth Geopotential Model - 1996), développé jusqu'au degré et ordre 360. Il résulte des données issues de l'analyse des orbites des satellites et de la gravimétrie de l'ancienne Union soviétique, l'Amérique du sud et l'Afrique.

Le modèle global d'élévation TUG87 qui contient la représentation harmonique sphérique de la topographie globale au degré et à l'ordre 180 a été également utilisé. Les coefficients pour la puissance de la topographie globale jusqu'au degré et à l'ordre 90 sont également disponibles pour l'évaluation des effets dus aux masses topographiques éloignées.

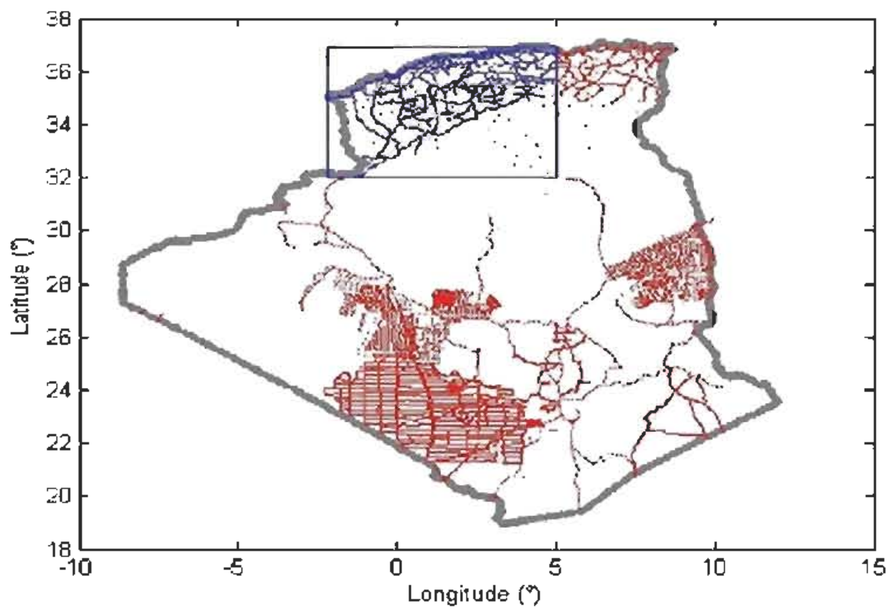

Fig 2. Domaine de calcul du géoïde et la répartition géographique des données gravimétriques.

Modèle numérique de terrain : Le calcul des effets de la topographie nécessite l'existence d'un modèle numérique de terrain de haute résolution. A cette fin et par manque d'un MNT précis sur l'Algérie, un modèle a été généré à partir des informations altimétriques liées aux observations gravimétriques fournies par le BGI. Ce MNT généré n'est pas plus homogène que la répartition des stations gravimétriques et présente quelques lacunes. C'est bien évidemment un handicap pour une solution définitive de géoïde **[1]**.

Dans cette application deux modèles numériques de terrain ont été soustraits du modèle numérique de terrain GTOPO30 employés dans ces calculs numériques: le M.N.T Large (5' x 5') pour les zones éloignées du point de mesure et le M.N.T Fin (30" x 30") pour les zones proches de ce même point. Les surfaces océaniques sont indiquées par les valeurs 9999. Ces deux MNT sont illustrés dans les figures suivantes:

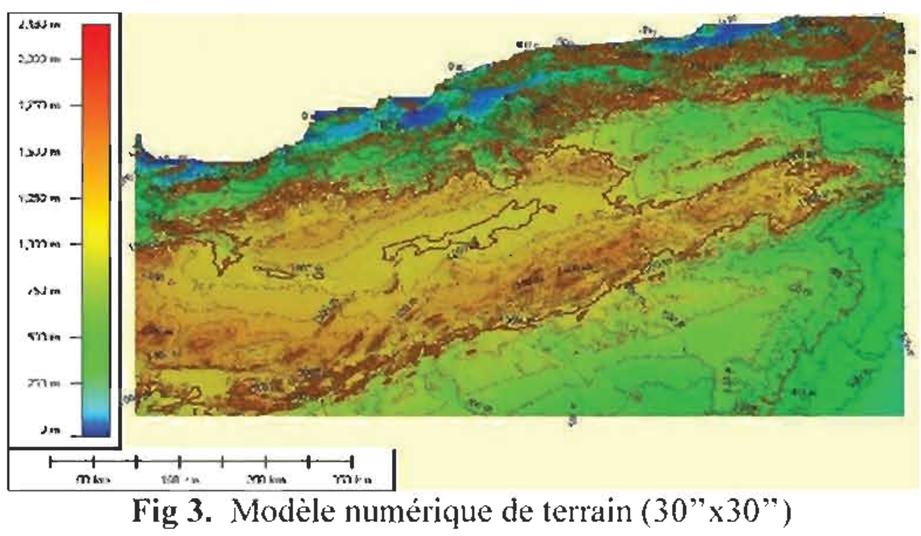

Fig 3. Modèle numérique de terrain (30"x30")

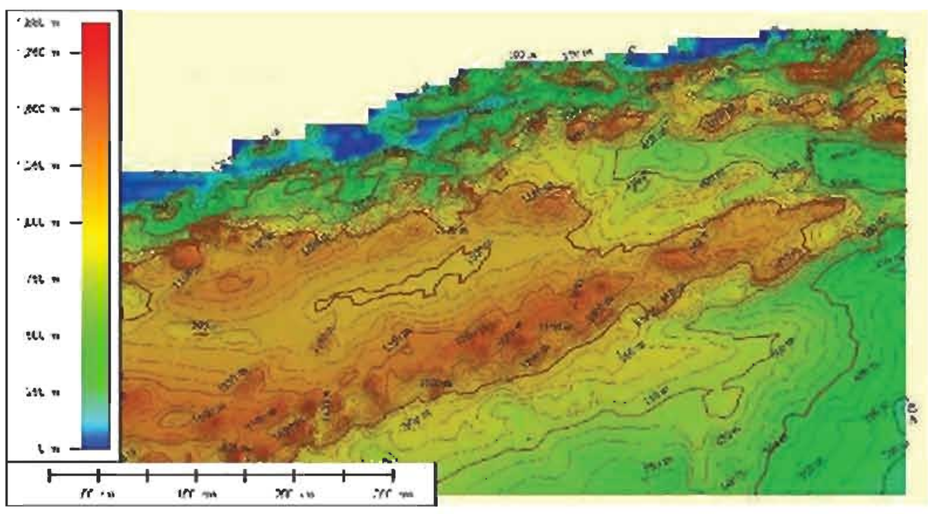

Fig 4. Modèle numérique de terrain (5'x5')

5.2 Traitement des données

Le programme dénommé "**GEOGRID**" et développé dans le cadre de cette application, permet de générer une grille gravimétrique à partir d'un échantillon de données réparties aléatoirement. Il est écrit en langage Fortran et il fait appel à plusieurs routines suivantes :

DTE : calcul de la contribution des zones proches à l'effet topographique direct sur la pesanteur.

DTF : calcul de la contribution des zones éloignées à l'effet topographique direct sur la pesanteur.

DAE : calcul de l'effet atmosphérique direct sur la pesanteur

PTE : calcul de la contribution des zones proches à l'effet topographique primaire direct sur l'ondulation du géoïde.

PTF : calcul de la contribution des zones éloignées à l'effet topographique primaire direct sur l'ondulation du géoïde.

STE : calcul de la contribution des zones proches à l'effet topographique secondaire indirect sur la pesanteur.

STF : calcul de la contribution des zones éloignées à l'effet topographique secondaire indirect sur la pesanteur.
GIN : transforme les anomalies de pesanteur via la formule de Stokes-Helmert en ondulations géoïdales.

5.3 Résultats obtenus et Analyse

Les statistiques des effets topographiques et atmosphériques de pesanteur sont fournies dans les tableaux suivants :

Tableau 1. Effets topographiques de pesanteur "zones proches"

Paramètre	Min	Max	Moy	σ
Effet ter. (mGal)	-0,06	417,06	13.10	41,6
Effet ter. cond. (mGal)	-110,75	468,7	1.69	29,92
Effet dir. (mGal)	-166,99	387,03	11.41	36,17
Effet sec. ind. (mGal)	-0.4721	-0.0009	-0.0250	0.0519
Effet prim. ind.(m)	-1,283	-0,003	-0,136	0,095

Tableau 2. Effets topographiques de pesanteur "zones éloignées"

Paramètre	Min	Max	Moy	σ
Effet ter. (mGal)	-31,38	117,136	60.938	36,529
Effet ter. Cond. (mGal)	-31,43	117,424	61.039	36,628
Effet dir. (mGal)	-0,311	0,066	-0.101	0,105
Effet sec. Ind. (mGal)	-0.059	0.068	-0.007	0.0256
Effet prim. Ind. (m)	-0,079	0,165	0,0615	0,0419

Tableau 3. Effets atmosphériques de pesanteur

Paramètre	Min	Max	Moy	σ
Effet atm. Dir. (mGal)	0,6603	0,9064	0,807	0,0295
Accél. plateau sph. cond. (mGal)	-0,8692	-0,715	-0,787	0,032
Accél. Résid. Atm. Accid. (mGal)	-0,102	0,042	0,0127	0,0063

Le tableau (4) présente les statistiques correspondant aux ondulations du co-géoïde N^h et les ondulations du géoïde N:

Tableau 4. Statistiques des ondulations du géoïde et du co-géoïde

Paramètre	Min	Max	Moy	σ
Ondulation du co-géoïde(m)	6.21	68.91	33,43	13,65
Ondulation du géoïde (m)	5,61	68,69	33,20	13,96

On constate bien que l'ondulation du co-géoïde se rapproche de l'ondulation du géoïde (différence≈23cm), ceci est dû probablement à l'influence des effets topographiques.

Pour mettre en évidence la précision du modèle du géoïde gravimétrique estimé, une étude comparative entre les hauteurs géoïdales calculées par voie gravimétrique et les ondulations du géoïde dérivées à partir des observations GPS et de nivellement de précision (points GPS nivelés), tel que :

$N_{(GPS/Nivellement)} = h_e - H^\circ$

Où h_e et H° représentent respectivement la hauteur ellipsoïdique obtenue par GPS et l'altitude orthométrique déterminée par nivellement. Ces trois quantités doivent être d'une part, référencées au même ellipsoïde, et d'autre part, de précision comparables.

Dans le cas de notre application, l'absence d'informations relatives à la précision des mesures gravimétriques et à l'inexistence d'un modèle numérique de terrain réel, ainsi que l'insuffisance d'observations ne permettent pas d'effectuer une analyse de précision réelle et fiable.

6. Conclusion

La résolution du problème de valeurs aux limites géodésiques dans l'espace de Helmert nécessite une évaluation des valeurs moyennes des anomalies de pesanteur de Helmert sur la surface de la Terre.

Ces valeurs dépendent des valeurs moyennes des anomalies de pesanteur à l'air libre, des corrections ellipsoïdales à la perturbation de pesanteur, de la correction ellipsoïdale due à l'approximation sphérique, des effets topographiques et atmosphériques directs, des effets topographiques et atmosphériques indirects secondaires et de la correction du géoïde/quasi-géoïde.

Les principaux facteurs limitant la théorie de "Stockes-Helmert" sont l'approximation de la densité topographique réelle par la surface topographique de Stokes, la détermination des données de pesanteur pour le prolongement descendant, l'effet topographique direct primaire, et l'approximation sphérique du géoïde dans le cas de l'évaluation des effets topographiques.

Références Bibliographiques:

Aarizou. M., 1995 : "Détermination précise du géoïde par voie gravimétrique", Thèse de magister. C.N.T.S/Arzew.

Duquenne H., 2005: "Le géoïde et les méthodes locales de sa détermination", Ecole francophone sur le géoïde .IGN/Paris.

Heiskanen W., Moritz H., 1967: "Physical geodesy". San Francisco.

Huang J., 2002: "Computational Methods for the Discrete Downward Continuation of the Earth Gravity and Effect of Lateral Topographical Mass Density Variation on Gravity and the Geoid". Ph.D.Theses. UNB, Fredericton.

Helmert, F.R. (1884): "Die mathematische und physikalische Theorien der hoheren Geodasie". Vol.2, B.G.Teubner, Leipzig

Kellogg O.D., 1929: "Foundations of potential theory". Springer. Berlin.

Martinec Z., 1993: "Effect of laterally variations 1of topographical masses in view of improving geoid model accuracy over Canada". Final Report of contract DSS No.23244-2-4356, Geodetic Survey of Canada, Ottawa.

Martinec Z., Vaníçek P., 1994a: "Direct topographical effect of Helmert's condensation for a spherical approximation of the geoid". Manuscripta Geodaetica, No.19. Springer

Martinec Z., Vaníçek P., 1994b: "The indirect effect of topography in the Stokes-Helmert technique for a spherical approximation of the geoid". Manuscripta Geodaetica, No.19: 213-219.

Martinec Z., 1996: "Stability investigations of a discrete downward continuation problem for geoid determination in the Canadian Rocky Mountains". Journal of Geodesy, Vol. 70.Springer.

Novák P., 2000: "Evaluation of gravity data for the Stokes-Helmert solution to the geodetic boundary-value problem". Ph.d. dissertation, Department of Geodesy and Geomatics Engineering Technical Report No. 207, university of New Brunswick, Canada.

Ralston a., 1965: "A First Course in Numerical Analysis". McGraw-Hill/New York.

Vaniçek P., Sun W., Ong P., Martinec Z., Najafi M., Vajda P., Horst B., 1996 : "Downward Continuation of Helmert's gravity". Journal of Geodesy 71: 21-34

Vaniçek P., Martinec Z., 1994:"The Stokes-Helmert scheme for the evaluation of a precise geoid". Manuscripta Geodaetica, No.19., Springer

Vaniçek p., Novàk p., 1999; "Comparison between planar and spherical models of topography" CGU Annual Meeting, Banff, May 9-12, 1999 vol.2.

Establishment of Algerian-Tunisian Unified GPS Network

Mr. M. Haddad
National Institute of Cartography and Remote Sensing.
123, Tripoli Street – P.O.B 430, Hussein Dey. Algiers, Algeria.
E-mail : inct99@wissal.dz Fax : +213 21 23 43 81

ملخّص : تسمح أجهزة تحديد المواقع (GPS) بإعطاء قياس دقيق في أي وقت ، سهل التطبيق و منخفض الكلفة. تجعل هذه المميّزات من أجهزة تحديد المواقع الأداة الملائمة للمواقع و رصد الظواهر الجيوفزيائية بمقاييس مختلفة، (تكتونية الصفائح ، المراقبة الزلزالية ، قياسات الجيود) . في هذا السياق، تكون مدة الأرصاد في أغلب الأوقات جدّ طويلة (بعض الأيام في عدّة سنوات) . أنجزت عملية البحث بالشّراكة بين المعهد الوطني للخرائط و الكشف عن بعد (الجزائر) و المركز الوطني للكشف عن بعد (تونس) حول إنشاء شبكة GPS الموّحدة الجزائرية التونسية و تحسين دقة المواقع ، خصوصاً العمودية ، بإستعمال تقنية GPS .
في هذا السياق ، أرصد في وقت واحد المعهد الوطني للخرائط و الكشف عن بعد (الجزائر) و المركز الوطني للكشف عن بعد (تونس) ثمانية نصب بإستعمال تقنية GPS خلال أسبوع GPS رقم 1502 (من19 إلي 25 أكتوبر 2008). علجت معطيات GPS المجمّعة بالبرنامج برنس 5.0 بالطريقة الآلية بإدماج معطيات IGS و النتائج .تكمن الدقة المحصل عليها لكل الإحدثيات في نظام بعض المليمترات .

الكلمات الأساسية : شبكة GPS الموّحدة الجزائرية التونسية ، برنس ، PCF RNX2SNX ، إحدثيات rms المكررة .

Résumé: Le système de positionnement global (GPS) permet une mesure précise n'importe quand, facile à mettre en application et de coût faible. Ces caractéristiques font du GPS un outil favorisé pour le positionnement et l'observation des phénomènes géophysiques à diverses échelles (tectonique des plaques, surveillance sismique, mesures de géoïde). Dans ce contexte, la durée d'observations est en général très longue (quelques jours dans plusieurs années). L'action de recherche est réalisée conjointement par l'Institut National de Cartographie et de Télédétection (Algérie) et le Centre National de Télédétection (Tunisie) sur l'établissement du Réseau GPS Unifié Algero- Tunisien et l'amélioration de la précision du positionnement, en particulier vertical, en utilisant la technique GPS.
Dans ce contexte, huit bornes (de limite de terrain) Algero-Tunisien ont été observés simultanées par l'Institut National de Cartographie et de Télédétection - Algérie et le Centre National de Télédétection-Tunisie en utilisant la technique GPS pendant la semaine GPS n°1502 (du 19 jusqu'au 25 octobre 2008). Les données GPS collectées ont été traitées par le logiciel scientifique Bernese 5.0 en mode automatique en intégrant les données IGS et les produits. La précision obtenue pour toutes les coordonnées est dans l'ordre de quelques millimètres.

Mots-clés: Réseau GPS Unifié Algero- Tunisien, Bernese, PCF RNX2SNX, coordonnées rms réitérées.

Abstract : GPS allows a precise measure at any time, easy to implement and of weak expense. These characteristics make of GPS a favored tool for positioning and for geophysics phenomena observation with various scales (plate's tectonics, seismic surveillance, measures of geode). In this context, the duration of observations is in general very long (some days in several years).
A research action is jointly performed by the National Institute of Cartography and Remote sensing (Algeria) and the National Centre of Remote sensing (Tunisia) on the establishment of Algerian-Tunisian Unified GPS Network and improvement of the positioning precision, notably vertical, using the GPS technique. In this context, eight Algerian-Tunisian boundary markers were observed by the National Institute of Cartography and Remote Sensing - Algeria and the National Centre of Remote sensing - Tunisia) in simultaneous using GPS technique during the GPS Week n°1502 (from 19th till 25th October 2008). The collected GPS data were processed using Bernese 5.0 scientific software in automatic mode while integrating the IGS data and products. The precision obtained for all coordinates is in the order of some millimeters.

Key words : unified Algerian-Tunisian GPS network, Bernese, RNX2SNX PCF, repeatability coordinates rms.

1. Introduction

In the goal of unification of GPS networks of Algeria and Tunisia, a set of eight Algerian-Tunisian boundary markers (102, 219, 315, 02, 146-01, 17-02, 275 and 005-01) were observed by the National Institute of Cartography and Remote Sensing - Algeria and the National Centre of Remote sensing - Tunisia) in simultaneous using GPS technique during the GPS Week n°1502 (from 19th till 25th October 2008). Considering the precision asked for the data processing, it was necessary to use adapted scientific software. For that, the collected GPS data processing was performed using Bernese software available at level of the National Institute of Cartography and Remote Sensing.

The difficulty of Bernese software manipulation and the tiring character of the preparation of processing as well as the possibility of choosing numerous processing options, forced us to use its BPE automatic mode. This mode allows having the simplicity of use of commercial software while benefiting from advantages of scientific software.

The objective of this paper consists in the presentation of the different stages of data processing and the analysis of acquired precision.

2. Campaign of GPS measurements

The campaign of observations of unified Algerian-Tunisian GPS network took place during all GPS week n°1502 (from 19th till 25th October, 2008). Observations were organized by daily sessions of 24 hours. The cadenza of recording was 30 seconds with an angle of elevation of 5°.

The table (1) represents collected daily GPS observations (in blue by National Institute of Cartography and Remote Sensing - Algeria and in red by National Centre of Remote sensing - Tunisia) and the GPS data of IGS used as reference stations.

Table 1. Collected GPS data.

Num. Station	19 October 2008	20 October 2008	21 October 2008	22 October 2008	23 October 2008	24 October 2008	25 October 2008
102							
219							
315							
02							
146-01							
17-02							
275							
005-01							

The figure (1) represents the geographical distribution of the eight Algerian-Tunisian boundary markers (points in red):

Fig. 1 Geographical distribution of the eight Algerian-Tunisian boundary markers.

Data collected by National Institute of Cartography and Remote Sensing - Algeria and National Centre of Remote sensing - Tunisia were transformed from constructor's format to the international standard format RINEX to be useful by software Bernese. The RINEX observations files are in the form of an ASCII file and decline in two versions: an O file which contains observations and an N file which contains the ephemerides satellites.

3. Preparation data and products IGS files

For the preparation of the group of files necessary for the GPS observations processing by Bernese 5.0, an informatics program "Rin2Sindown" was developed. We note that this program is based on the subroutines of the free program "NetDownload" developed by Dr. Marco Roggero of the polytechnic school of Italy. "Rin2Sindown" allows the automatic downloading from Internet the precise ephemerides (sp3) files, clock information (clk) files and GPS observations files of IGS stations in RINEX format. The figure (2) represents the execution window of "Rin2Sindown" program:

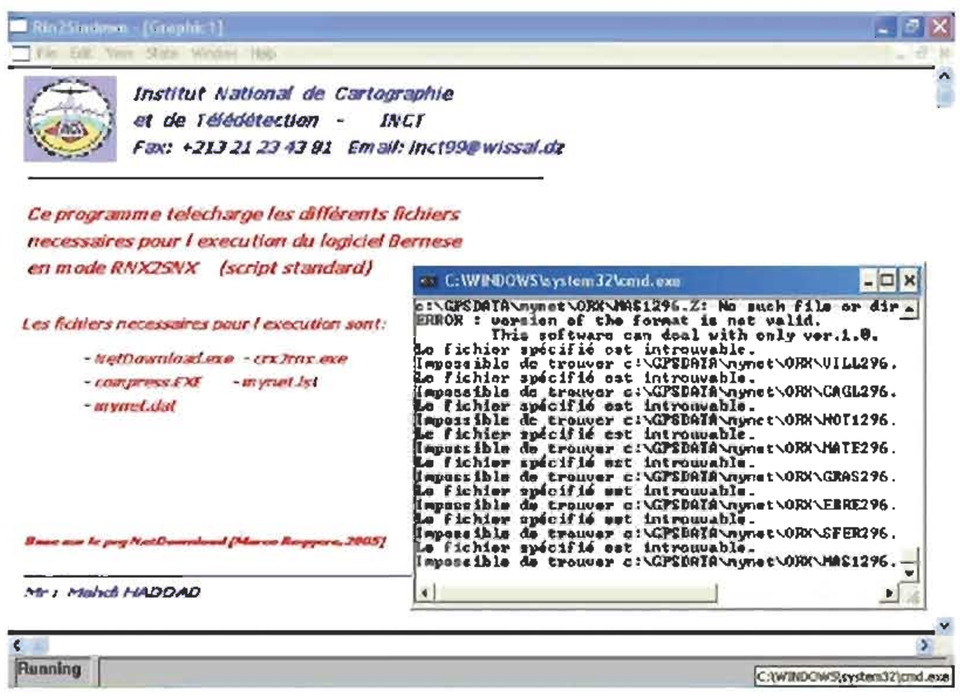

Fig. 2 Execution window of "Rin2Sindown".

4. Data processing

The Bernese GPS Software v5.0 (Dach et al., 2007 & 2004) was used to process the daily observations sessions of unified Algerian-Tunisian GPS network, session by session.

The reference sites used in process are the seven stations of International GNSS Service (IGS): GRAS (France), Cagliari (Italy), Matera (Italy), NOT1 (Italy), MAS1 (Spain), SFER (Spain) and VILL (Spain).

A first process was performed in automatic mode using the PPP PCF of Bernese 5.0. Coordinates acquired from the eight stations, from sub-decimetric precision, were used on one hand, for the preparation of the oceanic tide corrections file and on the other hand, as approached coordinates for the final process using Bernese 5.0 in RX2SNX PCF automatic mode.

The RNX2SNX.PCF is intended for a double-difference based analysis of RINEX GNSS observation data from a regional network. Station coordinates and troposphere parameters are estimated and stored in Bernese and SINEX format to facilitate further processing and combination.

For the seven daily data sessions of unified Algerian-Tunisian GPS network, the basic options of the used RNX2SNX processing strategy are:

The consideration of "absolute" GNSS receiver and satellite antenna phase center offset (I05).

- Observation files with significant gaps or unexpectedly big residuals will automatically be removed from the processing to ensure a robust processing and a reasonable network solution.
- Phase ambiguity fixing is attempted for baselines up to 2000 km length based on the Quasi-Ionosphere-Free (QIF) resolution strategy.
- The final network solution is a minimum constraint solution, realized by three no-net-translation conditions imposed on a set of IGS05) reference coordinates. The coordinates of all involved fiducial stations are subsequently verified by means of a 3-parameter Helmert transformation. In case of discrepancies, the network solution is recomputed based on a reduced set of fiducial stations.

For each session, the corresponding normal equation information is saved for a subsequent multi-session solution.

5. Final coordinates

The Bernese GPS Software allows estimating final site coordinates in a network analysis. The normal equation systems from different sessions are combined in a multi-session solution with ADDNEQ2. All coordinate parameters belonging to the same station are combined to one single set of coordinates.

The seven daily solutions of unified Algerian-Tunisian GPS network were therefore combined by adapting the Minimum Constraint Solution strategy. The IGS stations were considered as fixed stations. The resulting coordinates then refer to the middle epoch (October 22, 2008).

Held count, that we do not dispose enough observations repeated on more than a year, we did not consider the speed dimension in this combination.

To appreciate the quality of results, we are interested to the weekly coordinate repeatability. A bad repeatability indicates possible environmental, station, or processing problems. It also may be caused by geophysical phenomena (e.g., Earthquake).

For that, a seven-parameter Helmert transformation was applied to compare each individual solution of unified Algerian-Tunisian GPS network with the combined solution. The geodetic datum of the network is defined based on minimum constraint solution. The table (3) represents the repeatability coordinates rms values of the combined solution:

Table 3. Repeatability coordinates rms values of the combined solution.

		Weekday	Repeatability (mm)		
Station	#Days	0123456	N	E	U
102	4	XXXX	1.58	0.91	3.15
146-01	3	XXX	0.91	0.32	3.43
17-02	3	XXX	0.71	2.19	2.69
219	7	XXXXXXX	1.51	1.19	5.37
275	3	XXX	6.29	6.75	3.95
315	7	XXXXXXX	1.14	1.17	9.79
005-01	3	XXX	0.72	1.63	4.58
02	7	XXXXXXX	0.41	1.34	3.90
CAGL	7	XXXXXXX	2.15	1.33	4.51
GRAS	7	XXXXXXX	0.95	0.86	1.96
MAS1	7	XXXXXXX	1.23	1.08	2.68
MATE	7	XXXXXXX	1.05	0.84	2.85
NOT1	7	XXXXXXX	0.69	0.88	1.92
SFER	7	XXXXXXX	0.86	1.08	3.06
VILL	7	XXXXXXX	0.85	0.49	3.83
Total	86		1.56	1.57	4.41

The precision of results acquired for all the coordinates' stations is in the order of 1-7 mm for planimetric components and of 2-10 mm for the vertical components.

After verification of the precision of processing, descriptive maps were prepared. Each map contain the coordinates of point expressed in the IGS05 geodetic system at the epoch October 22, 2008, the detailed description of the geodetic monument and extract of topographic map and satellite image.

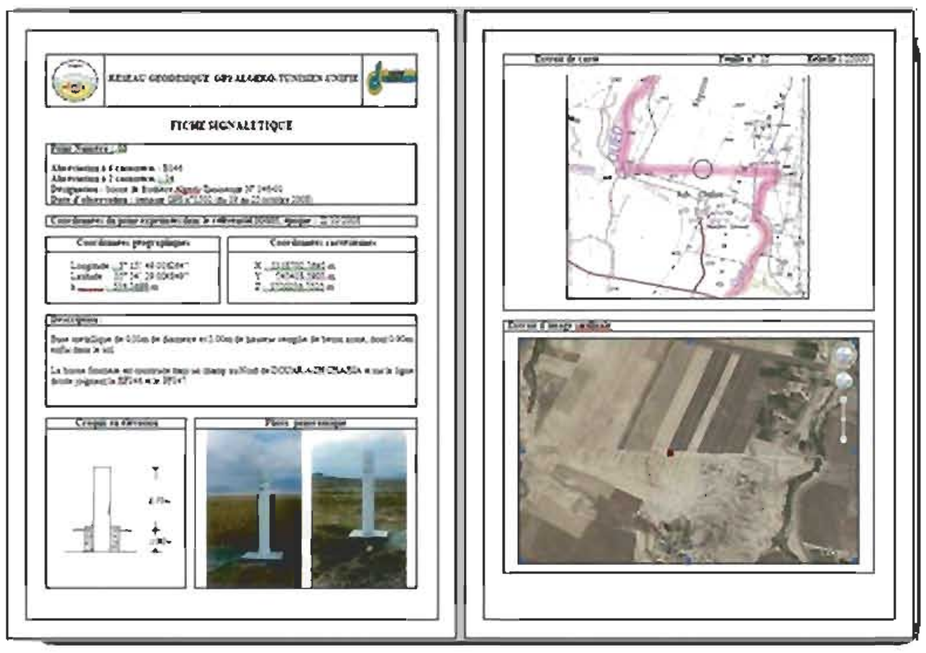

Fig. 3 Example of descreptive map.

6. Conclusion

The essential objective of this project "definition of a unified Algerian-Tunisian GPS network" concerns the mastery of a new technology: positioning by GPS satellites in general and her application at concrete needs having a direct impact on the modernization of Algerian and Tunisian geodetic facilities.

On data processing of Algerian-Tunisian unified GPS network, all our efforts are shared out on two parts:

- Make easier the preparation of IGS files essentials for the GPS data processing by Bernese 5.0 software.
- Data processing of unified Algerian Tunisian GPS network by Bernese 5.0 software.

In the first part, an informatics program was developed and exploited with intent to make easier the preparation of GPS campaigns to be treated by Bernese 5.0. In effect, this program allows recovering automatically the ephemerid files, the satellites clock information files and the GPS observations files of IGS stations in RINEX format.

Concerning the second part, a series of data processing of the eight Algerian-Tunisian boundary markers was made with software Bernese 5.0 while integrating the data of seven IGS stations: GRAS (France), Cagliari (Italy), Matera (Italy), NOT1 (Italy), MAS1 (Spain), SFER (Spain) et VILL (Spain).

The process in PCF RNX2SNX automatic mode has allowed us to get closer to the simplicity of commercial software use while benefiting from advantages of Bernese 5.0 scientific software. The precision obtained after compensation of all the baselines of the seven daily sessions of unified Algerian-Tunisian GPS network in the order of some millimetres is very promising.

In conclusion, we will keep the importance of the densification of the unified Algerian Tunisian GPS network which represents a key stake for the modernization of Algerian and Tunisian national geodetic facilities. This densification will indeed allow the improvement of quality and precision of this network.

Bibliographic references

Z. ALTAMIMI. Systèmes de référence terrestre : Définition et réalisation. Institut Géographique National - Août 2003.

J. ASGARI. Etude de modèles prédictifs dans un réseau de stations GPS permanentes. Thèse de doctorat de l'observatoire de Paris en dynamique des systèmes gravitationnels. Ecole Doctorale Astronomie & Astrophysique d'Ile de France - Novembre2005.

R. Dach, P. Fridez, U. Hugentbler. Tutorial Bernese GPS Software Version 5.0 - Septembre 2004.

H. Dupraz. La méthode GPS. École Polytechnique Fédérale de Lausanne – Cours de topométrie I. Nouvelle Édition - 1994.

J. LEGRAND. Utilisation du logiciel de l'université de Berne pour le traitement de données GPS en production. Automatisation des processus et stratégies de calculs. Mémoire d'ingénieur, Institut Géographique National – septembre 2002.

B. Hofmann-Wellenhof, et al. GPS-Theory and Practise. Second Edition Springer-Verlag- 1993.

New Products of the EPN Time Series Special Project: Status Report

Ambrus Kenyeres
FÖMI Satellite Geodetic Observatory, H-1592 Budapest, POBox 585, Hungary
kenyeres@sgo.fomi.hu

ملخّص : تتمثل المهمة الأساسية للمشروع الخاص بتحليل السلسلة الأحداثية في المراقبة الأسبوعية لـEPN SINEX solutions من أجل تحسين نتائج EPN . تتطلب المراقبة الروتنية تسدية السلسلة الإحداثيات المترابطة للمحطة الفردية و حفظ و نشر إحداثية التعويض و القيم الزائغة المكتشفة . إستعملت كذلك هذه المعلومة لحساب ITRF 2005 و تكاثفه الجهوي . تمّ كذلك حساب و تحليل الحلول الضمّية بإستعمال البرنامج CATREF (Altamimi et al 2004) تحديث و نشرالإحداثيات المقدّرة ، السرعة و قاعدة المعطيات المعوّضة و القيمة الزائغة بإنتظام على الموقع الإلكتروني EPN CB بعد المراقبة الروتنية تمّ إرسال الضوء و التحليل التوافقّي للسلسلة المترابطة EPN. كان التحليل بالبرنامج CATS ، (Williams SD الذي يستعمل (Laboratoire Océanographique Proudman MLE لتحديد ميزة الضوء و التغيّر الفصلي لسلسلة الإحداثيات المترابطة .
تبيّن من تحليل الضوء وجود ضوء ملوّن في السلسلة الأحداثية لـ EPN سمح إستعمال المميّزات الصحيحة للضّوء حساب السرعة المتغيّرة للمحطة الحقيقية .غطّى التحليل التوافقّي تقدير سعة و تأخّر مرحلة الإشارة الفصلية التي قلّما ظهرت في السلسلة الأحداثية . أظهر التحليل السعات الفصلية المعتدلة ، 1-2 ملم بالنسبة للأفقية و 2-4 ملم بالنسبة للمرّكبة العمودية توزيع تأخّر المرحلة بالنسبة للمركبات الأفقية ليس عشوائي ، تمّ إيجاد قيّم تأخّر المرحلة المحددة. يختلف تماما توزيع تأخّرمرحلة المركّبة العليا ، موحّدة الشكل . لم تدرس بعد قيم تأخر المرحلة . تمّ نشر و تحديث النتائج و المنتجات بإنتظام في السلسلة الأحداثية للموقع الإلكتروني EPN CB .

Résumé : La tâche principale du Projet Spécial analyse des Séries chronologiques est le contrôle de l'ENP hebdomadaire combiné SINEX solutions pour améliorer plus la qualité des produits de l'EPN. Le contrôle routine nécessite le lissage des séries chronologiques coordonnées de la station individuelle et l'entretien et la publication de la coordonnée de compensation et des valeurs aberrantes détectées. Cette information a également été utilisée pour le calcul de l'ITRF2005 et sa densification régionale. L'usage du logiciel CATREF (Altamimi et al 2004) qui lisse les solutions cumulatives sont également calculées et analysées. Les coordonnées estimées et les vitesses, ainsi que la base de données de compensation et de la valeur aberrante sont régulièrement mis à jour et publiées sur le site Web EPN CB. Au-delà du contrôle routine le bruit et l'analyse harmonique de séries coordonnées EPN a été lancée. L'analyse est faite avec le logiciel CATS (Williams SD, Laboratoire Océanographique Proudman) qui utilise MLE (Estimation du Maximum de Vraisemblance d'un modèle semi Markovien caché) pour déterminer la caractéristique du bruit et la variation saisonnière des séries chronologiques coordonnées. L'analyse du bruit a prouvé la présence du bruit coloré dans les séries chronologiques de l'EPN. L'utilisation des caractéristiques exacte du bruit a permis le calcul de la vitesse incertitude de la vraie station. L'analyse harmonique a couvert l'estimation des amplitudes et les retards de phase du signal saisonnier peuvent présenter dans les séries chronologiques. L'analyse a montré les amplitudes saisonnières modérés, 1-2 mm pour l'horizontal et 2-4 mm pour la composante verticale. La distribution du retard de phase pour les composantes horizontales n'est pas aléatoire, les valeurs bien déterminées du retard de phase ont été trouvées. La composante supérieure du retard de phase est totalement différente, elle est plus uniforme sans pics. La réalité physique des valeurs du retard de phase n'est pas encore étudiée. Les résultats et les produits sont publiés et mis à jour régulièrement dans la section des Séries chronologiques du site Web EPNCB.

Abstract : The main task of the Time Series Analysis Special Project is the monitoring of the EPN weekly combined SINEX solutions in order to further improve the quality of the EPN products. The routine monitoring involves cleaning of the individual station coordinate time series and the maintenance and publication of the detected coordinate offsets and outliers. This information has also been used for the computation of the ITRF2005 and its regional densification. Using the CATREF software (Altamimi et al 2004) cleaned cumulative solutions are also computed and analyzed. The estimated coordinates and velocities, together with the outlier and offset database are regularly updated and published on the EPN CB website.

Beyond the routine monitoring the noise and harmonic analysis of the EPN coordinate series has been started. The analysis is being done with the CATS software (Williams SD, Proudman Oceanographic Laboratory), which uses the MLE (Maximum Likelihood Estimator) approach to determine the noise characteristic and seasonal variation of the coordinate time series.

The noise analysis proved the presence of the coloured noise in the EPN time series. The use of the right noise characteristics allowed the computation of more realistic station velocity uncertainties. The harmonic analysis covered the estimation of the amplitudes and phase lags of the seasonal signal may present in the time series. The analysis has shown moderate seasonal amplitudes, 1-2 mm for the horizontal and 2-4 mm for the vertical component. The phase lag distribution for the horizontal components are not random, well determined phase lag values were found. The up component phase lag distribution is totally different, it is more uniform without peaks. The physical reality of the phase lag values is not yet studied. The results and products are published and regularly updated at the TimeSeries section of the EPNCB website.

1. Computation of the EPN cumulative solution

The primary product of the EPN analysis is the series of the combined weekly SINEX files created at the BKG Combination Centre. The combination is based on the subnetwork solutions of the 16 EPN Local Analysis Centres. The combined solutions are tied to the actual ITRF realization by tightly constraining a subset of EPN-ITRF sites. Since GPS week 1330, the new ADDNEQ2 program (Beutler et al 2006) and the more favourable minimum constraint (MC) approach is used.

During the 10 years of operation both the network of reference sites and the reference frame realizations were changed resulting in inhomogeneous coordinate series.

To eliminate part of the inconsistencies (reference frame changes and misalignment) the EPN Time Series Special Project computes monthly a cumulative solution using CATREF. This software applies the minimum constraint approach to align the EPN to the latest ITRF realization (by the end of 2006 we used ITRF2000 and the following reference sites: BOR1, JOZE, GRAS, MATE, NYA1, MAS1, METS, ONSA, VILL, POTS, WTZR). The main advantage of the minimal constraint approach is that the influences of the site specific, non-stationary coordinate variations of the reference sites on the results are minimized.

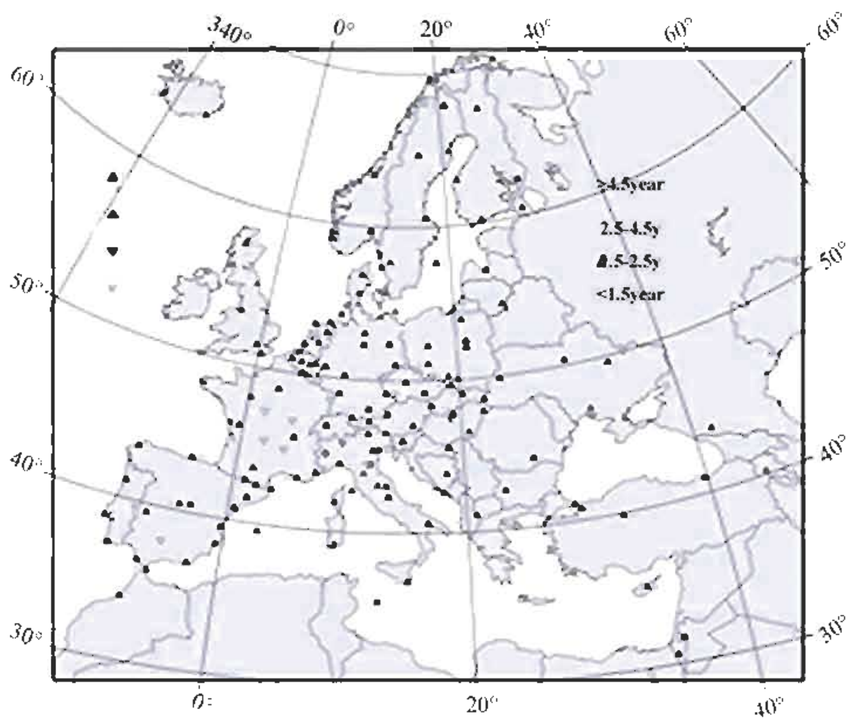

Fig. 1 Distribution and 'age' of the EPN sites (status 30.11.2006). The orientation and grey shades of the triangles indicate the length of the available data series.

The final step of the combination is a series of 7-parameter Helmert transformations, performed between the cumulative and each of the individual weekly solutions. The transformation residuals represent the time series that will be analysed. As a by-product, the values of the weekly transformation parameters are saved and plotted in Fig. 2. All parameters show a drift and an annual periodicity. The periodicity of the rotation parameters appears only for the X and Z components, while the translation parameters only have a periodicity for the Y component!

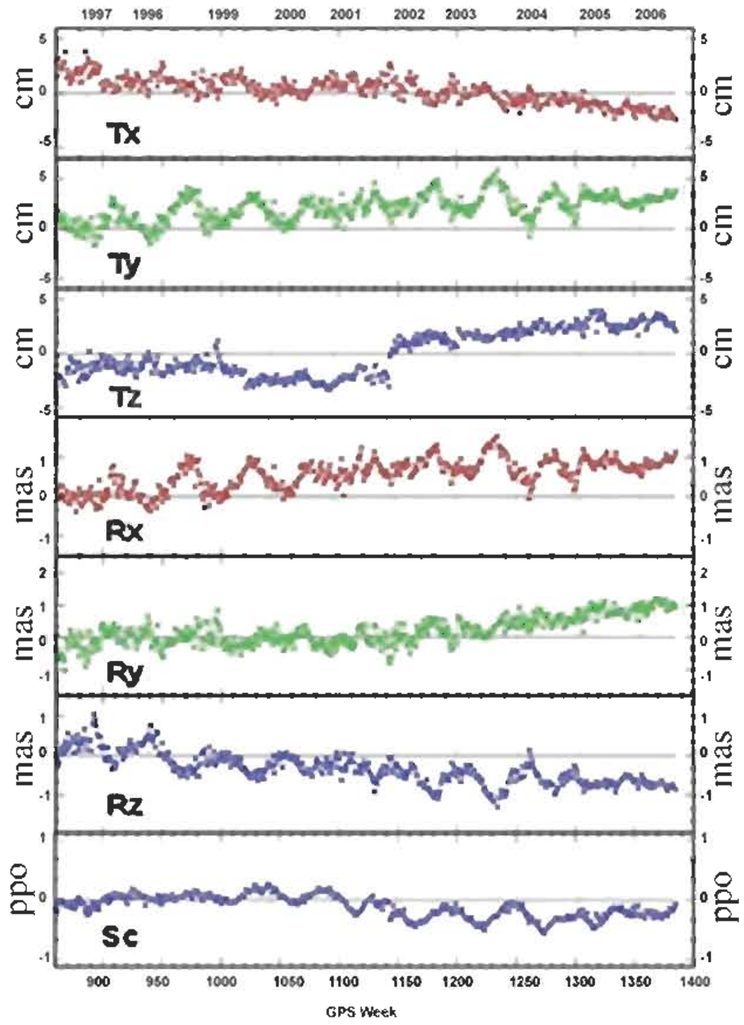

Fig. 2 The Helmert translation, rotation and scale parameters between the multiyear and the weekly solutions.

The positive offset in the Z translation at GPS week 1303 corresponds exactly to the epoch, when the ITRF2000 was introduced. The offset is caused by the reference frame difference between ITRF96 and ITRF2000 implicitly present in the EPN solutions through the IGS orbits, which are kept fixed in the EPN analysis. Similarly the new ITRF2005 also has, but a negative (-5.8 mm) Z offset with respect to ITRF2000 (Altamimi, 2006) – not yet seen on the plot. The temporal appearance of the seasonal variation of the scale between GPS weeks 1020 and 1280 caused by the tidal bug of the Bernese software. Before starting any further interpretation of the discussed transformation parameter series it must be emphasized that the evolution of the series reflects the time variable recovery of the global reference frame by the regional network and is not necessary related to real physical phenomenon.

During the routine analysis the coordinate offsets related to equipment change and the outliers caused by short or long term inconsistencies (e.g. snow coverage, antenna problems) are manually identified and removed from the time series.

The database of the outliers and offsets are published at the EPNCB website both in a simple text file and in the internationally recognised SINEX format. An extract of the outlier datafile is presented below in Table 1.

Table. 1 An extract of the EPN_outliers.www file available at the EPNCB website

```
Status: 2006:288
  Station ID      GPSweek    Estimated outlier value(*)      explanation
---------------from--to -----North-----East-----Up-----------------------
BUKK_20005M002 1023 1040      [-3,3]     [0,3]    [-15,0]  Izmit EQ
BUKK_20005M002 1054 1054         -3         x         66    single_outlier
BUKK_20005M002 1266 1281          x         x     [15,55]   antenna_malfunction?
LOCO_12207M002 0860 0898          x         x     [-5,-15]  station_start
LOCO_12207M002 1123 1125      [3,21]        x          x    single_outlier
LOZ1_12205M002 0943 0944          x         x   [-14,-22]   single_outlier
LOZ1_12205M002 1307 1307          x         x          13   single_outlier
LOZK_14263M001 1212 1221          3         x    [-8,-23]   antenna_malfunction
LOZK_14263M001 1222 1224          x         x           5   temporary_antenna
LRST_10004M004 1033 1033          6       -16         -13   single_outlier
LRST_10004M004 1237 1237          x         x          14   single_outlier
LRST_10004M004 1317 1324      [5,13]       -6           x   antenna_malfunction
LRVS_13101M004 1059 1059         -3        -2          13   single_outlier
LVCV_11401M001 1002 1021          4        -3           x   station_start
LSZG_12751M001 1123 1161    [0,-30]     [0,9]   [10,-13]   antenna_malfunction
...
...
SEOK_12351M001 0935 0935          x         x         -34   equipment_change
SIMK_14001M004 0886 0886          x         x         -11   single_outlier
SOVE_12763M001 1301 1301         -4         x         -38   equipment_change
SWEN_12330M001 1057 1066 [-34,-55]     [20,44]      [-20]  antenna_malfunction
SWEN_12330M001 1078 1080         10      [15]      [-40]   temporary_equipment
SWEN_12330M001 1115 1123        [-9]  [-6,-20]     [1,18]   antenna_malfunction
SWEN_12330M001 1210 1210          x         x         27    single_outlier
SWEN_12330M001 1274 1288      [36,0]      [10]      [10]   fragment
SWEN_12330M001 1289 1296          x         x       [-10]    fragment
```

(*) Explanation of outlier value designations:
x : no significant outliers for the component single value : well determined single value for the week(s)
[single value] : typical, well determined average value for the interval
[from, to] : the outliers vary between the given range

The quality of a single weekly solution is characterized by the weighted RMS (root mean square) values (see Fig. 3a,b) obtained from the multiyear combination. The quality improvement after the removal of the offsets and outliers, especially for the height component is quite remarkable. However, still some seasonal variation of the WRMS (weighted RMS) remains, with peaks around winter time; these are clearly correlated with the snow coverage of some GPS antennae.

The reason of the temporary drops in the horizontal WRMS values is not yet understood, but we suspect that it caused by the improperly removed constraints from the combined solution.
The WRMS plots, given in Fig. 3a-b, stress the importance of the offset and outlier elimination from the time series. After the cleaning we obtained an RMS of 1.4, which is an improvement of 40% compared to the results obtained without any offset and outlier elimination.

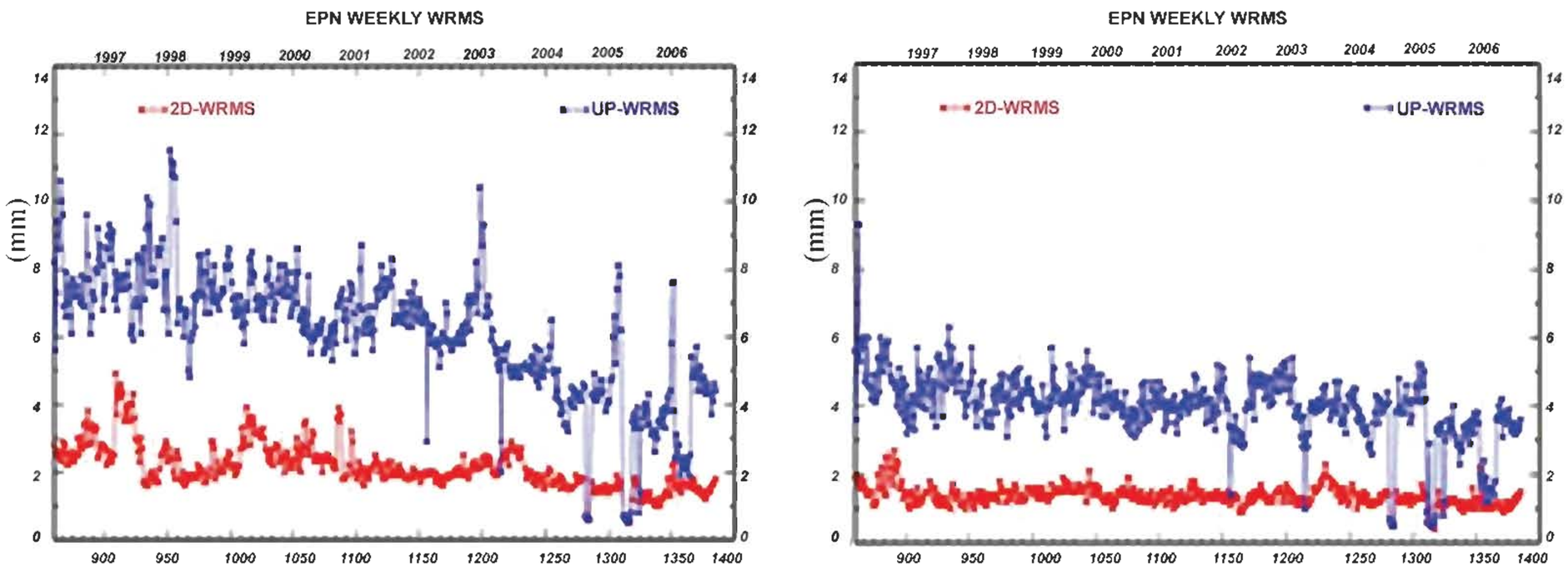

Fig. 3a-b Weighted RMS of the weekly EPN solutions before and after the elimination of the coordinate offsets and outliers. The improvement is more than 40 %!

2. Noise analysis of the EPN series

The power spectra of the noise present in the coordinate time series is characterized by a power-law dependence on frequency f:

$$P(f) = P_o f^{\kappa}$$

where κ is the spectral index and P_o is a normalizing constant. The spectral index can get any floating number, but as the natural processes mostly have more power at low frequencies they are characterized by negative indices. Some integer values are assigned to special processes, κ=-2 is called random walk, κ=-1 is flicker noise and κ=0 is white noise. The right modelling of the real noise spectra of the GPS time series is critical, especially when station velocities are estimated. According to previous studies (Mao et al, 1999, Williams, 2003) it is incorrect to assume, like in most of the GPS processing and combination softwares, that the time series containes white noise only. A direct consequence of this mismodeling is the over-optimistic estimation of the coordinate and velocity uncertainties.

In our study we used the MLE (Maximum Likelihood Estimation) approach of the CATS software.

After the removal of the linear and annual terms we estimated the spectral indices of each EPN station (Fig. 4). The obtained spectral indices ranged between [0;–2]; the average index for all coordinate components was near –1 (flicker noise), clearly indicating the presence of coloured noise in the EPN coordinate solutions.

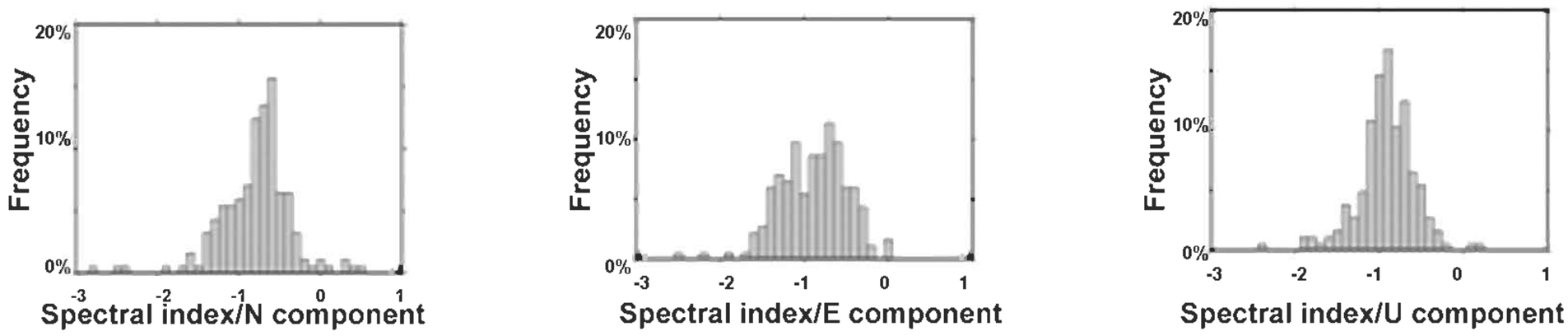

Fig. 4a-b-c Histograms of the distribution of the estimated spectral indices for the North (a), East (b) and Up (c) coordinate components. The 'extreme' values (-2> k > 0) are from short series (> 1 year).

This result is in full agreement with the ones derived for other regional networks (e.g. Williams et al, 2004). In addition, the spectral indices do not show random walk type noise, which indicates the longterm monument stability of the sites.

The histograms of the spectral indices for each of the components are characterized by slightly different distributions. Remarkable is the diagram of the East component, which shows a less significant peak around k=-1. When the linear and seasonal terms are not removed the flicker noise is much more dominating.

Using the above discussed white+coloured noise model, we estimated the velocity uncertainties of each EPN station. The computed uncertainties were 4-6 times larger than the values coming from the white noise-only model. Since they are based on a well-determined statistical model, our values are considered more realistic. All results are available from the EPN CB website (www.epncb.oma.be) for anyone interested in geophysical interpretation.

3. Harmonic analysis

The stacking of the weekly SINEX files eliminates the inconsistencies caused by the reference frame changes and also removes a regional signal related to the time variable alignment of the regional network to the global frame. This latter can be studied through the series of the parameters of the 7-parameter Helmert-transformation (see Fig. 2). All transformation parameters show seasonal variation caused by the common movement of the EPN with respect to the global frame. However these parameters are not helpful to extract real, station-specific information. The residual coordinate time series, which are obtained after the stacking, reflect better the local behaviour of the individual stations and will be studied in the following. Using the CATS_MLE software, the phase lags and amplitudes of the annual periodic terms were estimated. Considering the results of the previously described noise analysis the estimation was done assuming the white+flicker noise model. We found average amplitudes of 1 mm both for the North and East components and 2 mm for the Up component. The estimated harmonic parameters were used to create new time series plots. The existing cleaned plots, showing the coordinate development of the stations in the ETRS89 frame (with respect to the Eurasian plate) has been retained, but the de-trended plots were replaced with two additional plot sets. One is the extension of the existing de-trended plots with the estimated annual sinusoidal coordinate variation and the other is the same plot, but the annual term is removed from the original one (see the examples in Fig. 5). This latter residual time series may more clearly show the variations in the series.

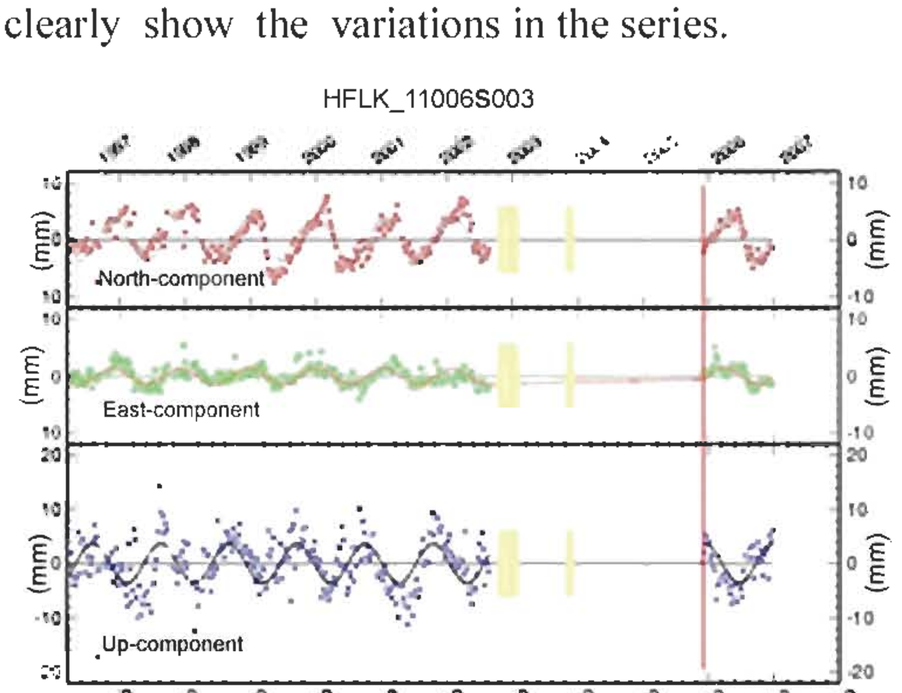

Fig. 5 De-trended time series plots of HFLK (Hafelekar, Austria). The estimated amplitude and the phase lag values of the annual signal are given at the bottom of the plots. The annual sinusoidal terms are indicated on both plots, but at the right plot the annual term is removed from the series. Similar plots are available for all EPN stations at the EPN CB website.

In Fig. 6a-b-c the normalized polar histograms of the North, East and Up components of the estimated annual periodic terms are shown. The histograms give a clear insight into the distribution of the estimated phases and amplitudes. The horizontal and vertical annual signals have a completely different phase lag distribution. While the horizontal components show two representative phase lag values of about +30 and -150 degrees (corresponding to +1 and -5 months) the vertical component exhibits a more uniform phase distribution. The geophysical models describing the temporal variation of the solid Earth do not indicate a significant annual periodicity in the horizontal components and therefore the observed distribution is most probably due to an artificial signal caused by e.g. processing and modelling shortcomings. It is expected, that when the whole EPN observation dataset will be re-processed with better and uniform models for the antennae phase centres and the atmosphere, the horizontal seasonal signal will be highly reduced.

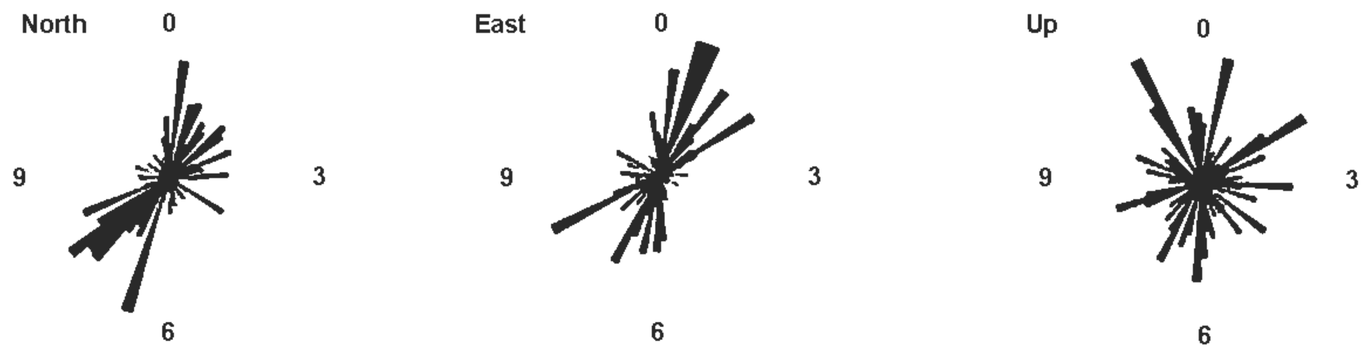

Fig. 6a-b-c Normalized polar histograms of the estimated phase lag distribution for the North, East and Up coordinate components. The phase lags are expressed in months.

Considering the vertical component on the regional scale statistically we may not expect one representative phase lag group, because the loading variation depends on the latitude, longitude and time. However according to independent investigations (King et al, 2005) the phase lags estimated from the GPS data do not agree with the geophysical model predictions. Therefore the estimated EPN vertical phase lags also suggest modelling shortcomings.

4. Velocity estimation

Beyond the station performance, the quality of the estimated coordinates and velocities is also dependent on the length of the observation series. A significant portion of the EPN sites has less than 3 years (see Fig. 1) observation history. Due to the apparent noise and annual periodicity in the series those sites should be treated with caution when coordinates and velocities are estimated (Blewitt and Lavallee, 2002). Fig. 7 shows an example of the dependence of the estimated velocity on the length of the observation series.

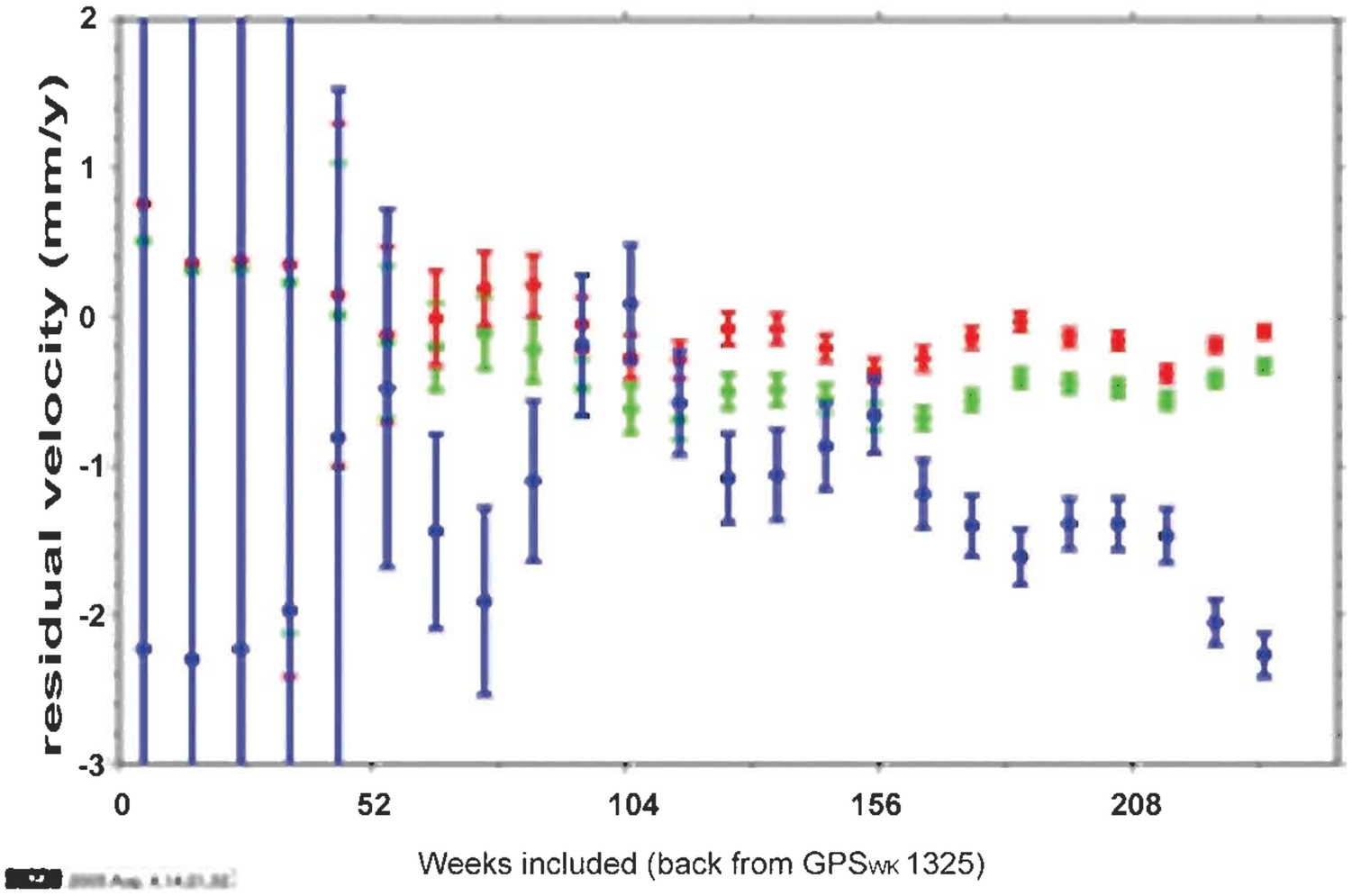

Fig. 7 Dependence of the estimated velocity on the available observations, when annual periodicity is present. This example is derived from the time series of CHIZ (Chize France), which has an annual periodic signal with 2cm amplitude at each component.

As a compromise between targeting the highest accuracy and responding to user needs, we decided not to publish any velocities for sites having data for less than 18 months. Using the procedures explained in this paper, we compute and publish reference coordinates and velocities of the EPN stations at the EPN CB website. This information is regularly updated.

Finally the map with the estimated horizontal residual velocities is presented in Fig. 8. All velocities are relative to the Eurasian plate, where the NUVEL1A-NNR model velocities - modified by Altamimi to better fit to ITRF2000 - are used to derive the intraplate velocities. The velocity uncertainty ellipses are derived from the values we computed by CATS_MLE taking the coloured+white noise model into account.

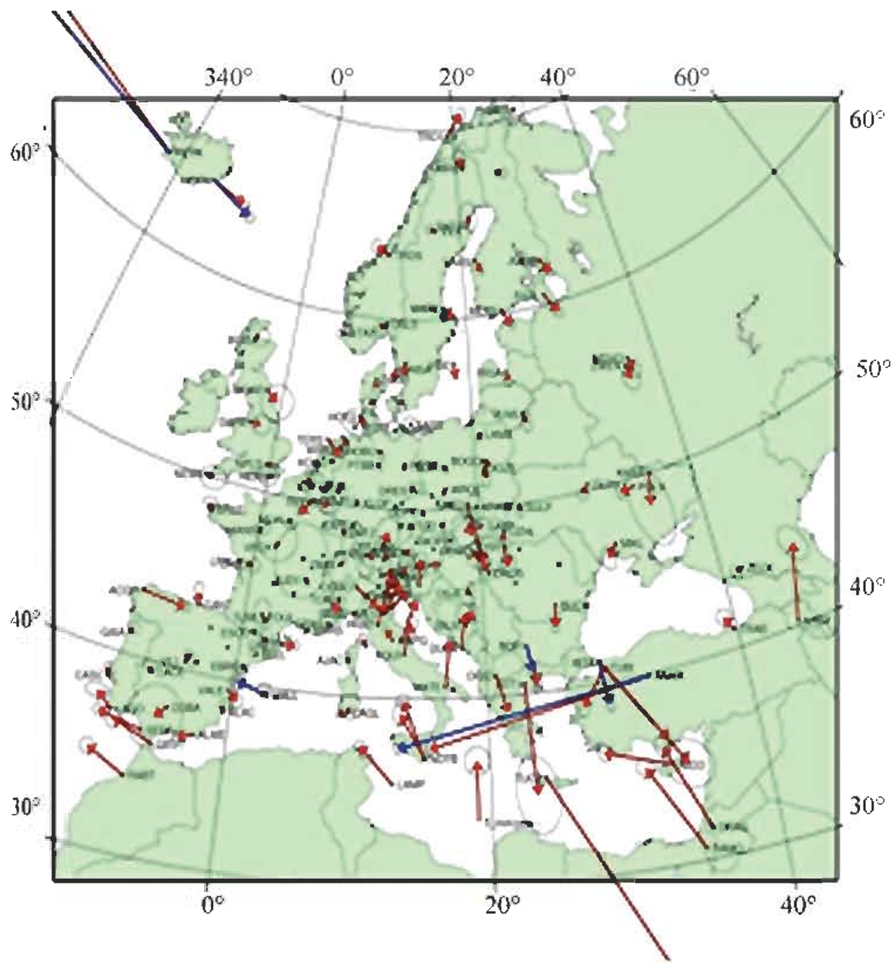

Fig. 8 The estimated EPN residual velocities wrt the Eurasian tectonic plate. Some sites has double velocity estimations, where following an event (equipment change, earthquake) the station had apparently different behaviour.

5. Summary

The EPN Time Series Special Project monitors the weekly SINEX files, eliminates the observed offsets and outliers and maintains a database including the detected inconsistencies. This database is harmonized with the IGS discontinuity table used for the computation of ITRF2005. The discontinuities of the non-IGS EPN stations are used to generate an EPN solution delivered for the regional densification of ITRF2005. Using the cleaned weekly SINEX files monthly updated ITRS coordinate and velocity solutions are published on the EPNCB website.

Until the regional densification of ITRF2005 will be published, these solutions are considered as the most accurate and up-to-date source of the ETRF coordinates and velocities for the EPN stations.

In this paper we presented new results of the detailed studies concerning the analysis and improvement of the EPN's long-term products as coordinates and velocities. We have shown how the performance of all stations are monitored and how the station problems are kept track and the combined weekly SINEX files are cleaned. The handling of the offsets and outliers makes 40 % overall improvement of the cumulative solution. We proved the presence of the coloured noise and we computed reliable velocity uncertainties. A general harmonic analysis was done, which just called our attention for the existing modelling problems. In the future we plan to validate our estimation of the vertical annual periodicities with information from independent processing approaches (PPP by Bernese or GIPSY) and by comparing them with real environmental and satellite based models. We should note here that the unavoidable global and regional GPS reprocessing will provide more realistic coordinate time series for the further studies.

Acknowledgements

The stacking of the EPN weekly SINEX files has been done by the CATREF software developed by *Z. Altamimi* (IGN, France). The velocity uncertainties and spectral indexes were computed with the CATS software kindly provided by *SD. Williams* (Proudman Oceanographic Laboratory, UK). The maps and histograms were created by the GMT 3.4 software.

Bibliographical References

Altamimi Z., P. Sillard P, C. Boucher (2004). CATREF software: Combination and analysis of terrestrial reference frames. LAREG Technical Note SP08, Institut Géographique National, France.

Altamimi, Z. (2006). Strengths and Limitation of the ITRF: ITRF2005 and beyond. Paper presented at the GRF2006 Symposium, 9-14 October, 2006, Munich, Germany.

Beutler G, Bock H, Brockmann E, Dach R, Fridez P, Gurtner W, Habrich H, Hugentobler U, Ineichen D, Jaeggi A, Meindl M, Mervart L, Rothacher M, Schaer S, Schmid R, Springer T, Steigenberger P, Svehla D, Thaller D, Urschl C, Weber R (2006) Bernese GPS software

version 5.0 (draft). ed. Urs Hugentobler, R. Dach, P. Fridez, M. Meindl, Univ. Bern, 464 pp.

Blewitt G, Lavallee D: Effect of annual signals on geodetic velocity. JGR, Vol.107/B7, doi: 101029/2001JB00570, 2002.

Mao A, Harrison CGA, Dixon TH: Noise in GPS coordinate time series. JGR, Vol.104, 2797-2816, 1999.

Kenyeres A Bruyninx C. : EPN coordinate time series monitoring for reference frame maintenance. GPS Solutions, Vol.8 pp.200-209, doi:10. 1007/s10291-004-0103-9, 2004

T.vanDam - Wahr J. - kING m.: Geophysical and Non-geophysical Annual Signals in European IGNHeight time Series.Presented at the IAG Scientific Assembbly, August, 2005,, Cairns, Australia.

Williams SDP et al.: Error analysis of continuous GPSposition time series.JGR,Vol.109/B03412, doi: 101029/2003jboo2741,2004.

Williams SDP: The effect of coloured noise in the uncertainities of rates estimated from geodetic time series. Journal of Geodesy, 76(483-494), doi. 10.1007/s00190-002-283-4, 2003.

Wessel, P. - Smith,W.H.F.: New, improved version of Generic Mappig Tools released, EOS Trans. AGU, Vol.79(47), pp.579, 1998.

LiDAR Imagery and its Critical Evaluation for Vegetation Management and Transmission Power Lines

R. Ansari & H. Sarkar
Pogung Baru, D-34, Yogyakarta, Indonesia
amu_gmu@yahoo.com

ملخص : لتلاقي خط نقل الطاقة الكهربائية و النباتات إنعكاس جدّ فعّال على الخطوط الكهربائية . واجه مليون من الأشخاص مشكلة الشحنة الكهربائية الناجمة عن دارة كهربائية قصيرة بين النباتات و الخطوط الكهربائية . في هذه الدراسة تمّ إستعمال صوّر ليدارلحل المشاكل المذكورة أعلاه .
في حين أن كل تصنيف قد تمّ بالماكرو (macros) لكن نظرا للتصنيف السيئ للأصناف صنّفت الأصناف يدويا. تمّ إيجاد صعوبات كبرى في النقاط المنخفضة للنباتات التي إختلطت بنقاط الأرض و لا تحتاج هذه النقاط المنخفضة للنباتات إلى التسيير بما أن إرتفاعها لا يلمس الخطوط الكهربائية . تمّ إيجاد المشكلة الكبرى في النباتات المتوسطة التي تجاوزت الخطوط الكهربائية و تحتاج إلى تسيير حسن . يقدّر الإرتفاع الحالي لخط الكهرباء بـــ 8.5 mu و الإرتفاع المتوسط للنباتات في بعض الأماكن بـــ <14.00mu بالنسبة للأرض. غير أن الخطوط الكهربائية ذات شدّة التوتر العالي و الخطوط الكهربائية ذات شدّة التوتر المنخفض تحتاج إلى حماية حيث لا يمكن للنباتات أن تجتاز منطقة الحماية كما تحتاج إلى قياس على أساس دقيق و أولويّ.
مع ذلك ، تبيّن الدراسة بأن ليدار تعطي مقاييس إرتفاع دقيقة و كاملة ومعلومة ثلاثية الأبعاد للخطوط الكهربائية و النباتات .

Résumé: L'impact de ligne de transmission d'énergie électrique avec la végétation a une incidence très efficace sur les lignes électriques. Un million de personnes ont confronté le problème d'hachure de charge électrique dû à de court-circuit entre végétation et lignes électriques. Dans cette étude les images LIDAR ont été utilisées pour résoudre les problèmes prescrits ci-dessus.
Cependant toute la classification ait été faite par les macros mais dû à la mauvaise classification de classes, la classification manuelle a aussi été faite. Les difficultés maximales ont été trouvées en bas points de végétation qui sont mélangés avec les points au sol et ces bas points de végétation n'ont pas besoin d'être dirigé comme leur hauteur n'allait pas toucher les lignes électriques. Le problème maximal a été trouvé dans la végétation moyenne qui dépasse les lignes électriques et a besoin d'une bonne gestion. La hauteur exacte de ligne électrique est de 8.5 mu et la hauteur moyenne de végétation dans certaines places est respectivement > 14.00 mu du sol. Non seulement que, les lignes électriques à haute tension et les lignes électriques à basse tension ont besoin de tampon jusqu'a où la végétation ne traversera pas la zone tampon et a besoin d'être levé sur des bases régulières et prioritaires.
Cependant, l'étude montre que le levé LIDAR fournit les détails d'altitude réelle, complète et l'information 3D de lignes électriques et de végétation.

Abstract : The impact of electric power transmission line and vegetation has very effective significance for the power transmission lines. Million of people faced electricity loadshading problem due to short circuit between vegetation and transmission power lines. In this study LiDAR imagery were used in solving the above stated problems. However all the classification was done by macros but due to misclassification of classes manual classification were also done. The maximum difficulties were found for the low vegetation points which get mixed with ground points and these low vegetation points don't need to be managed as their height were not going to affect transmission lines. The maximum problem was found with the medium vegetation which encounters power lines and needed proper management. The actual height of the power line is 8.5 mu and average height of vegetation in certain places is > 14.00 mu respectively from the ground. Not only that, high Voltage transmission power lines and low voltage transmission power lines need to buffer unto where vegetation will not cross the buffer zone and need to survey on regularly and priority basis.
However, the study reveals that LiDAR surveying provides actual, complete and finest elevation Details and 3D information of power lines and vegetation.

1. Introduction

The use of laser technology have been developed since the 1960s. Most of people are aware with the use of laser technology in electronic distance measurement devices. LiDAR sensors mounted in airborne platforms began to achieve more consistent and accuracy of data. LiDAR represented Light Detection and Ranging (LiDAR) systems. There are two basic types of LiDAR systems like topography and bathymetry. LiDAR is one of the most recent airborne remote sensing technology and 'a GPS and

an Inertial Measurement Unit (IMU) are the integral parts of the equipment, provide for continuous monitoring of the position of the aircraft and its attitude' (Réjean and Pierre, 2006). In this study LiDAR data are used for the vegetation management and Transmission Power lines where long trees are crossed transmission power lines and create load shading problem for the million of people and such of problem affects daily life and faces heavy losses. To maintain such kind of problem new researches come into existence. Remote sensing depending upon its resolution according to Susanto (2004) remote sensing resolution have four types: Spatial, spectral, temporal and radiometric where as airborne remote sensing used point resolution which measure the distance of an object. However time changes, technique of data collection and accuracy also improved. LiDAR makes direct physical measurements and provide high accuracy data (Rejean and Pierre, 2006). In a word LiDAR a better understanding technology have greatly revolutionized in Remote Sensing Era and the usefulness of LiDAR as a valuable mapping tool and have a Potential applications.

2. Formulation problem

The impact of electric transmission line and vegetation have significant role for power transmission. Million of people faced electricity load shading problem due to short circuit between vegetation and transmission power lines.

3. Benefit of this Research

This research will beneficiary for the area where dense vegetation and thousands of hundred kilometer long transmission power line passes and manage the power load shading problem. It also help to proper management of Vegetation basically in highly dense tropical vegetation. This is a scientific approach, less time consuming as well as for human well being.

4. Research objectives

The main objectives of this research are:

1- 3D mapping of vegetation and power transmission lines.
2- Find out the electricity power supply problem and its proper management.

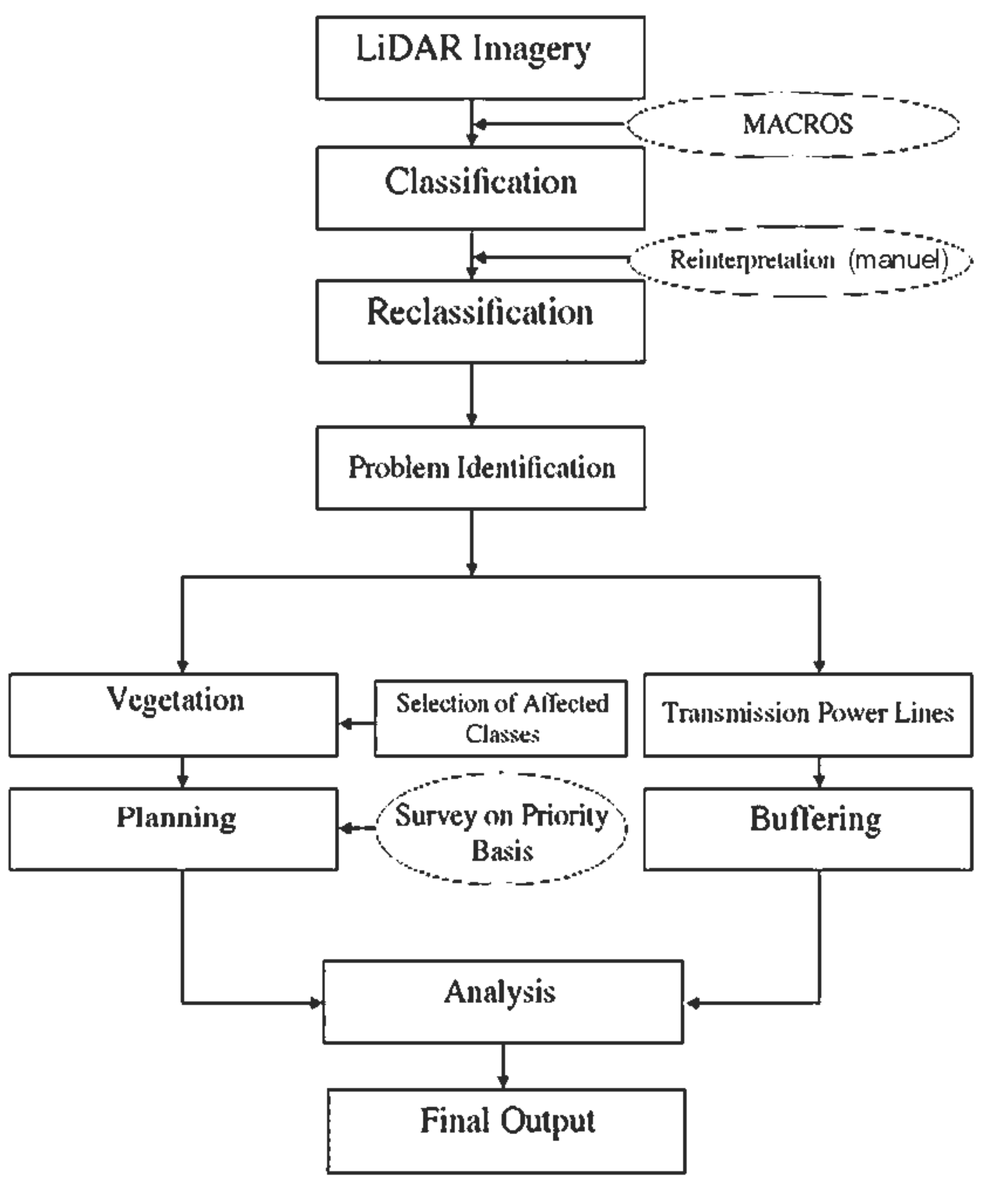

Fig. Flow Chart of the Research Method.

5. Analysis and Its Evaluation

As LiDAR captured the point data and points directly measures the object's distance. So it is very useful to classify the 3D objects. In the following figure1 cross section of low vegetation and ground points were well classified and TIN model was generated from ground points which shows 3D surface. Even there are some difficulties for the interpretation because with some extent it is difficult to identify that which point refers to which classes because vegetation point height is lying same with ground point height.

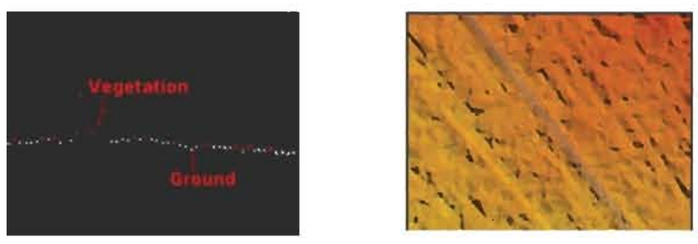

Fig. 1 Front View of Ground Class and Vegetation Class With TIN Ground model.

In this study more then ten (10) classes were taken into consideration for detail studies and each class was clearly defined. However in the class divination, MACROS were used but manual checking was done for maximum accuracy purposes. The figure 2 clearly represent that each class was well defined but there are few classes which get mixed with another classes. Though it is a quite difficult job to identify the class without priori of knowledge.

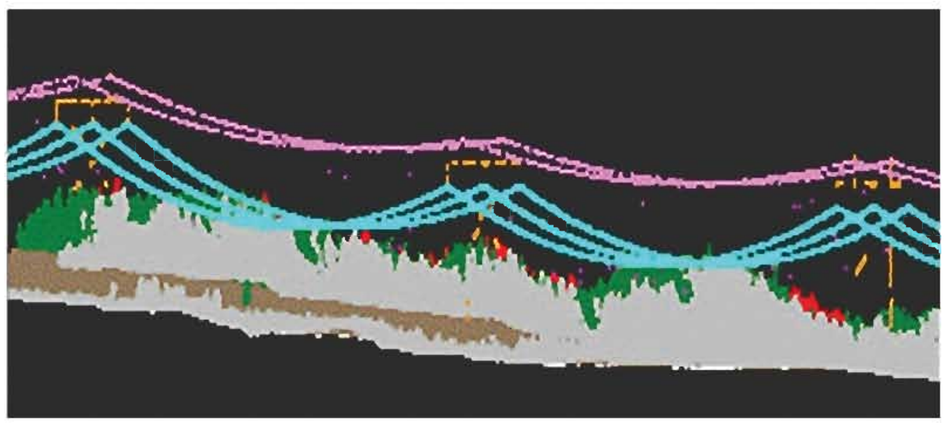

Fig. 2 Front View of diffrent Classes.

However our main task in this study is to identify the vegetation classes which overtake the transmission power lines and find the solution for proper management of vegetation detail study shows that the medium vegetation classes are the most affected trees which crosses transmission power lines.

The medium vegetation were measured averagely 14mu where as the transmission power lines height 8.5mu. from the ground. It is assumed that in a such condition it will create short circuit for certain areas where vegetation crosses the transmission power lines.

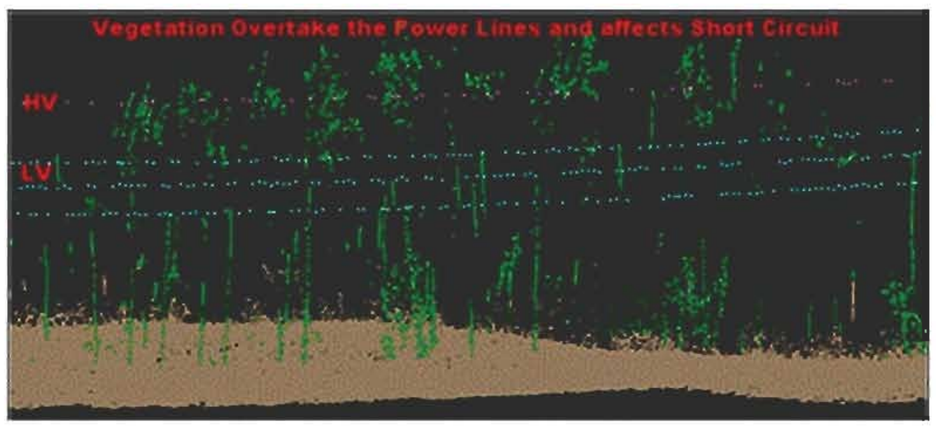

Fig. 3 Vegetation Overtake the Transmission Power Lines.

Here medium vegetation taken into consideration for management purposes. It is quite difficult to measure the frequency of electricity and up to which level it will affect vegetation so cut down the vegetation canopy top at certain level which will not affect the low voltage power transmission line not only that need to proper survey on regular priority basis.

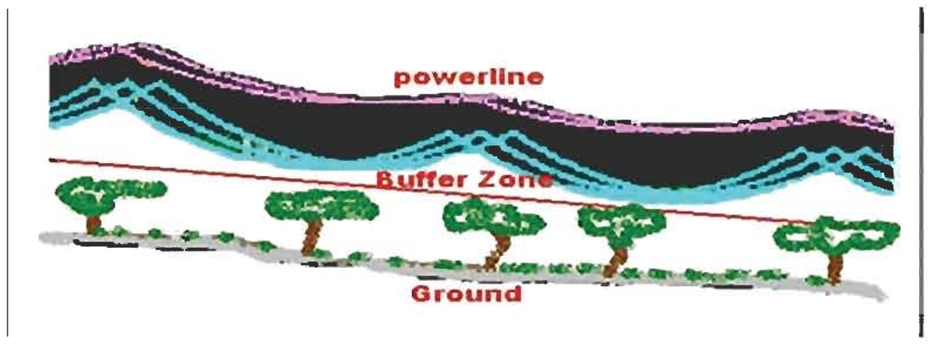

Fig. 4 Vegetation and assumed buffer zone.

6. Conclusion

LiDAR surveying provides actual, complete and precision elevation data. LiDAR data is more enough to identify vegetation class which encounter transmission power line and as a result short circuit and load shading problem and could be managed through proper managerial task. It is hoped in near future LiDAR technology will replace the photogrammetry.

Going to Shawbak (JORDAN) and getting the data back: toward a 3D GIS dedicated ta medieval archaeology

P. Drap[1], J. Seinturier[1], J-C. Chambelland[1], G. Gaillard[2], H. Pires[3],
G. Vannini[4], M. Mucciotti[4], E. Pruno[4]
[1], LSIS umr CNRS 6168, Marseille, France
(Pierre.Drap@esil.univmed.fr)
[2]Stratos Documentation, Cadenet, France
(gillouxGaillard@wanadoo.fr)
[3]Superficie, Porto, Portugal
(hpires@superficie.pt)
[4]Dipartimento di Studi storici e Geografici dell'Università degli Studi, Florence, Italy
(elisa.pruno@unifi.it)

Résumé: L'article présente un projet interdisciplinaire en cours proche du Système d'Information Géographique 3D consacré à l'Héritage Culturel avec le centre d'application spécifique sur le Château de Shawbak, aussi connu par le " Crac de Montréal", un des sites médiévaux ruraux bien conservé dans le Moyen-Orient entier.
Nous développons un ensemble des outils pour l'analyse archéologique médiévale qui va de la présentation de la documentation graphique traditionnelle comme orthophotos et les modèles 3D à basse-résolution (VRML) à l'usage de SIG à 3D/2D par la création de l'outil du stockage de l'objet exhaustif et centralisé des deux données archéologiques et photogrammétriques.
En utilisant ces outils les archéologues seront capables de produire, conserver, visualiser et diriger les données 3D et archéologiques, d'après leurs besoins. Le projet archéologique de Shawbak est un projet intégré et spécifique entre restauration conservatrice, recherche archéologique médiévale et valorisation de site.
Se concentrer principalement sur l'analyse stratigraphique de structures bien bâties fournies aux archéologues, un taux énorme de données pour collecter sur le site et des archives utiles qui seront utilisés pour étudier les structures à travers les points de vues technologiques et stratigraphiques.

ملخّص : يعرض المقال مشروع فروع من العلم مشتركة العمل في قيد الإعداد شبيه بنظام المعلومات الجغرافية الثلاثي الأبعاد المخصّص للإرث الثقافي مع مركز التطبيق الخاص حول قلعة Shawbak ، المعروفة أيضا بـــ " Crac de Montréal " ، واحدة من معالم القرون الوسطى الريفية المحفوظة جيّدا في الشرق الأوسط كله .
نعرض مجموعة أدوات علم الآثار القديمة للقرون الوسطى بتقديم التوثيق الخطي التقليدي مثل مرئيات ذات الإسقاط العمودي و النماذج الثلاثية الأبعاد 3D ذات دقة تمييز منخفضة (VRML) إلى إستعمال نظام المعلومات الجغرافية 3D/2D بإنشاء أداة تخزين الأشياء الإستقصائية و المركزية لمعطيات علم الآثار القديمة و المساحة التصويرية .
بإستعمال هذه الأدوات يكون بإمكان علماء علم الآثار القديمة عرض، حفظ ، تصوّر و تسيير المعطياتD3 وعلم الآثار القديمة، حسب إحتياجاتهم. يعّد مشروع علم الآثار القديمة لـــ Shawbak مشروع كامل و خاص بين الترميم المحافظ ، البحث في علم الآثار القديمة للقرون الوسطى و تقويم المعلم .
بعد التمعن في الدراسة المتعلقة بمبحث الطبقات الأرضية للبنيان المتين البنية يحصل علماء علم الآثار القديمة على نسبة كبيرة من المعطيات لجمعها عن المعلم و الأرشيف المفيد الذي يستعمل لدراسة البنيان من خلال المفاهيم التكنولوجية و مبحث الطبقات الأرضية .
يعّد حجرأساس هذا المشروع دراسة الوثائق المقدّمة و المستعملة من قبل علماء علم الآثار القديمة من أجل تعيين متطلبات علم الآثار القديمة الخاصة تتمثل المرحلة الأولى في إعطاء أدوات المساحة التصويرية التقليدية لعلماء علم الآثار القديمة لكي يتمكّنوا من عرض الوثائق الخطية بإستقلالية (التصوير الضوئي ، توجيه الصورة و توليد الصور ذات الإسقاط العمودي التقليدي). أما المرحلة الثانية فتتمثل في عرض بنيان من نموذج مشترك لتخزين معطيات علم الآثار القديمة و المساحة التصويرية بإستعمال قاعدة المعطيات الوحيدة وتسمح بربط معطيات علم الآثار القديمة بالنماذج 3D.
لم تتطوّر بما فيه الكفاية أدوات المساحة التصويرية المخصّصة للقياس منذ سنة 2000 لتساعد علماء علم الآثار القديمة على قياس المساحة التصويرية بسهولة. أدمجت في الوقت الحاضر هذه الأدوات في نظام جدّ معقّد يسمح بالعرض الآلي للصوّر ذات 2D أو 3D من قاعدة معطيات علم الآثار القديمة .
تبدو الوثائق الخطية 2D المقدمة في هذه المرحلة من طرف علماء علم الآثار القديمة اللذين يستعملون صوّر ذات الإسقاط العمودي وكأنّها مرسومة بالأيدي.
تهدف آخر مرحلة و هي نظام المعلومات الجغرافية 3D إلى العرض الآلي لنماذج 3D من قاعدة معطيات علم الآثار القديمة :

أما النماذج 3D هي في الواقع صورة خطية لقاعدة المعطيات وفي نفس الوقت جهاز الترابط الذي من خلاله يمكن للمستعمل تعديلها.
تسمح هذه المقاربة للصورة الموضوعية 3D الآلية و الدراسة الجديدة لعلم الآثار القديمة بالربط الثنائي الاتجاه المباشربين الصورة 3D و معطيات علم الآثار القديمة .
كل هذه الصوّر مدوّنة في Java داخل بنيان مسّاح الأراضي (مسّاح الأراضي 2008).

الكلمات الأساسية : علم الآثار القديمة للقرون الوسطى ، مبحث الطبقات الأرضية ، نمذجة ، تبصّر، مرئيات ذات الإسقاط العمودي، نظام المعلومات الجغرافية .

La pierre de fondation de ce projet est l'analyse de documents présentés et utilisés par les archéologues afin d'identifier des exigences archéologiques spécifiques. La première phase est de donner des outils photogrammétriques traditionnels aux archéologues afin qu'ils puissent être autonomes à présenter des documents graphiques (prendre des photographies, orientation de la photo et génération de l'orthophoto traditionnelle). La deuxième étape est de développer un modèle commun de structure pour le stockage des données archéologiques et photogrammétriques en utilisant une base de données unique et permettant de lier les données archéologiques avec les mesures 3D.

Les outils de photogrammétrie spécifique consacrés pour mesurer par mesure de pierre ont été insuffisamment développés depuis 2000 pour aider les archéologues à faire facilement des levés photogrammétriques. Ces outils sont maintenant intégrés dans un système plus complexe qui permet la production automatique des représentations de 2D ou 3D de l'interrogation de base de données archéologiques. Les documents graphiques 2D présentés dans ce processus par des archéologues qui utilisent les orthophotos semblent comme des dessins faits à la main.

La dernière étape de cette chaîne est Le SIG 3D qui vise la production automatique de modèles 3D par l'interrogation de base de données archéologiques: ces modèles 3D sont en fait une image graphique de la base de données et en même temps l'interface par laquelle l'utilisateur est capable de la modifier.

Cette approche permet à la représentation thématique 3D automatique et la nouvelle analyse archéologique la liaison-bidirectionnelle directe entre la représentation 3D et la donnée archéologique.

Toutes ces présentations sont écrites à Java dans la structure Arpenteur. (Arpenteur, 2008)

Mots-clés : Archéologie médiévale, stratigraphie, modélisation, visualisation, Orthoimage, SIG

Abstract: The paper presents an interdisciplinary project which is a work in progress towards a 3D Geographical Information System (GIS) dedicated to Cultural Heritage with a specific focus application on the Castle of Shawbak, also known as the "Crac de Montréal", one of the best preserved rural medieval settlements in the entire Middle East.

We develop a set of tools for medieval archaeological analysis ranging from the production of traditional graphical documentation like orthophotos and low-resolution 3D models (VRML) to the use of 3D/2D GIS through the creation of centralized and exhaustive object storage tool both for archaeological and photogrammetric data.

Using these tools archaeologists will be able to produce, store, visualize and manage both archaeological and 3D data, according to their needs. The Shawbak archaeological project is a specific and integrated project between medieval archaeological research, conservative restoration and site's valorization.

Focusing mainly on stratigraphical analysis of upstanding structures provides archaeologists with a huge amount of data to collect on site and useful records that will be used to understand the structures from stratigraphical and technological point of views.

The foundation stone for this project is the analysis of documents produced and used by archaeologists in order to identify specific archaeological requirements

The first phase is to give archaeologists traditional photogrammetric tools so that they can be autonomous in producing graphical documents (taking photographs, photo orientation and traditional orthophoto generation). The second step is to develop a common model structure for both photogrammetric and archaeological data storage using a unique database and allowing to link archaeological data with 3D measurements.

Specific photogrammetry tools dedicated to stone by stone measurement have been under development since 2000 to help archaeologists to easily produce photogrammetric surveys. These tools are now integrated in a more complex system which allows automatic production of 2D or 3D representations from archaeological database queries. The graphical 2D documents produced through this process look like the handmade drawings done by archaeologists using orthophotos.

The 3D GIS is the last step of this chain and aims the automatic production of 3D models through archaeological database queries: these 3D models are in fact a graphical image of the database and at the same time the interface through which the user is able to modify it.

This approach enables automatic 3D thematic representation and new archaeological analysis through bidirectional-links between 3D representation and archaeological data.

All these developments are written in Java within Arpenteur framework. (Arpenteur, 2008)

key words : Medieval Archaeology, Stratigraphy, Modelling, Visualization, Orthoimage, GIS

1. Archaeological context : The need

The archaeological research of the Castle of Shawbak, also known as "Crac de Montréal", (Figure 1) one of the best preserved rural settlements in the entire Middle East (Drap et al 2007, Vannini et al. 2007) has been chosen to develop a new documentation system. In fact the site is very huge stratigraphically complex both in deep stratigraphy and in upstanding structures stratigraphy. Because its features and in accordance with the University of Florence research in Petra Valley (Vaninni et al, 2007), the Shawbak analysis starts from upstanding structures (Vannini et al. 2002). First of all this allows to collect many archaeological data in relatively short time. Only later on the archaeologists have decided to open some excavation areas to better understand the dynamic of settlement.

The stratigraphical analysis of upstanding structures produces a very large amount of data both graphical and stratigraphical. For the first one the common method to collect and to record them on the site is the survey. The survey is achieved in different ways, often it is two-dimensional. Its goal is to define the area, the perimeter and the volume of all the recognized USM (*standing for Unità Stratigrafica Muraria – similar to the stratigraphic unit for digging archaeology*). Every USM is a building homogeneous action which is representative of different building moment. In other words to identify and record the different USM in upstanding structures allows archaeologists to define a relative chronology of the building by the relative position of every USM. (Figure 10)

Fig. 1 The Shawbak castle.

For the second one we use commonly a schedule in which the stratigraphical data is written, that means chronological data and also the technological data of the buildings (lithotype, presence of mortar and its quality, stone measurement), that can lead to summarize the workers technological level and the power of the owner. Hence we must work with both graphical and archaeological data and we need to connect them. We need also to spend less time in the field drawing the survey because we need to spend more time to identify and know all the USM, but, at the same time, we need to produce the best possible graphical data because this is the best way to study and to compare our data to produce historical knowledge. (See Figure 2 below).

Fig. 2 Documents produced by archaeologist USM visualization

2. The traditional photogrammetric results

Several photogrammetric campaigns have been accomplished in Shawbak in the past years allowing the production of several graphic outputs representing archaeological features and constructions. These campaigns are composed of photographic sets acquired with calibrated digital cameras both in convergent and parallel coverage with the survey of control point by Total station and DGPS. These control points are used to reference the photogrammetric models in a common geodetic system. Among the most common outputs achieved in this process are orthophotos, low-resolution 3D models and vector graphic drawings representing constructive features. Orthophotos are two-dimensional projections of physical elements (like walls, pavements or ceilings) (Figure 3) that provides archaeologists with scaled and orthographic representations which can be used for multiple purposes like vector restitution, planar measuring or archaeological interpretation (as in USM definition). Three-dimensional models are the result of 3D shape restitution of built structures in the photogrammetric models. In this case they are low geometric resolution representations although they present high definition photographic texture (Figure 4).

Fig 3. Orthophoto from Ayyubid Palace.

The process of shape acquisition consists in defining the geometric characteristics of buildings or other archaeological elements by defining edges and surface discontinuities in order to achieve a geometric representation of the reality. They provide archaeologists an "absolute" 3D represen tation of all the features on a site, expressing the spatial relationship between them and going one step forward (in this case one more dimension) comparing to orthophotos.

Fig. 4 View from Ayyubid Palace VRML model

Traditional vector graphic drawings correspond to operator assisted restitution of specific features, like blocks perimeters, using photogrammetric models (See Figure 10). In this process photographs are used to interpret and measure morphological characteristics on the objects under study, resulting in drawings that extract or enhance information for archaeologists. Although 3D data is far more complete than 2D planar projections it is not used usually in traditional archaeological workflow as, in most cases, there are not appropriate interfaces for archaeologists to interact with. Two-dimensional outputs are easier to work with because they correspond to the traditional concepts of archaeological or technical drawings (i.e. 2D plans, elevations, etc.).

3. Measuring ashlar blocs

Once all the photographs are oriented The I-MAGE process (Image processing and Measure Assisted by GEometricalprimitive), developed in 2001, is used to support the user during the measuring process in photogrammetric surveys.

Users can make a 3D measurement using one single photograph, without altering precision of the result. This method was already published in CIPA congress, (Drap et al., 2001); it allows the user to concentrate on the archaeological aspects of the survey with less attention to the photogrammetric one. We use this approach also to produce 3D models of building blocks (i.e. ashlars) based on the only observable face. The morphology of each ashlar's block is expressed as a polyhedron with two parallel sides, or faces. In most of the cases, only one side is visible, sometimes two, rarely three. The survey process can inform about the dimensions of one face, then the entire polyhedron is computed accordingly to the architectural entity's morphology (extrude vector) and the data (depth, shape, etc.) provided by the archaeologist (Figure 5).

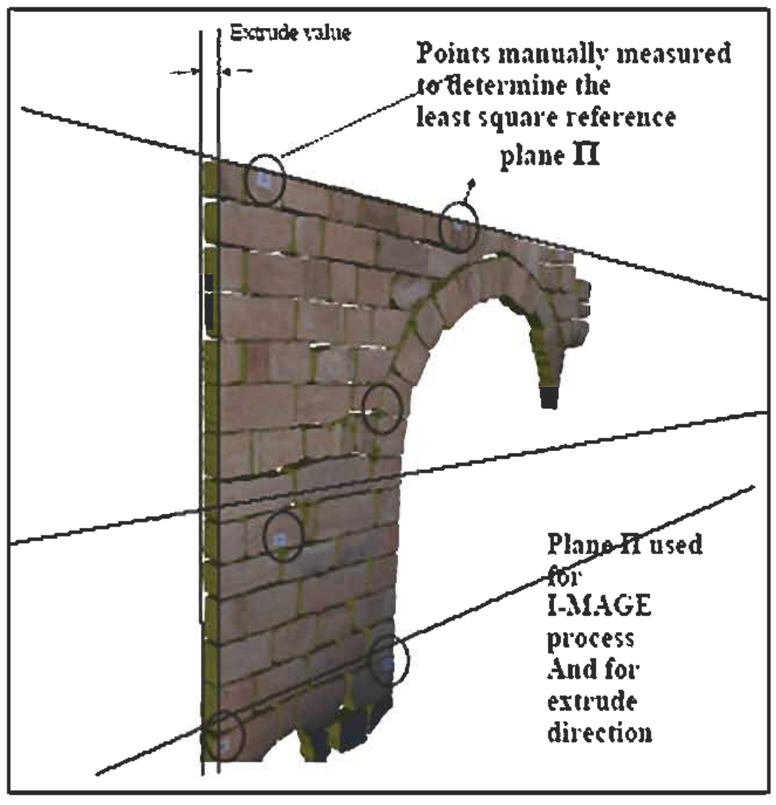

Fig. 5 Ashlars' blocks using a plane as an approximation to algorithm searches iteratively for a minimum scale factor the exterior face of the wall (Drap et al. 2007)

Computing an extrusion vector can be easy in the case where the architectural entity's morphology is obvious; during a wall survey for example an extrusion vector can be computed by a least square adjustment of a plane around the survey zone. This is the plane used by I-MAGE. In this case where the entity's geometrical properties are simple, the extrusion vector is calculated before the survey phase and the block is extruded directly from the measured points. In the case of the survey of an arch the extrusion should be radial and needs the geometrical features of the entity (intrados, radius, axis) and is therefore processes afterwards. This approach for measuring blocks was already published in a VAST congress (Drap et al., 2000) and has been combined with the I-MAGE process in order to obtain an integrated tool.

4. Working with USM – An example, the cement extraction

The example demonstrated below shows the algorithm used to extract the cement from a set of blocs belonging to the same USM. All the computation is performed in 2D, i.e. in the plane defined by the wall. The purpose of this computation is to evaluate the area covered by the mortar between the blocks. This 'cement extraction' enables a visual representation and the evaluation of the area covered by the mortar.

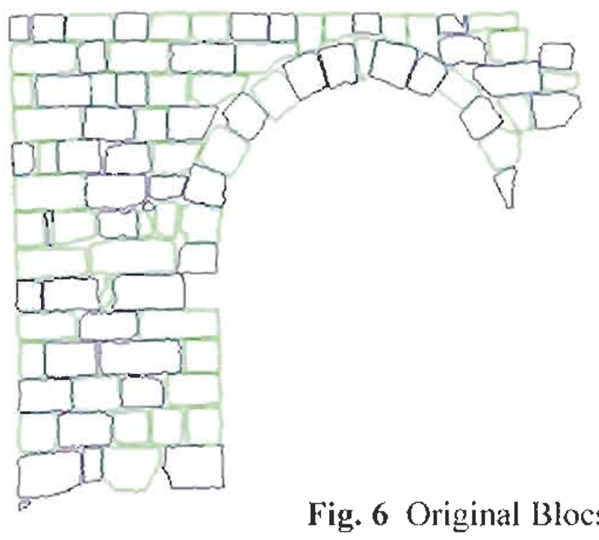

Fig. 6 Original Blocs

The figure 6 shows the original blocks belonging to the USM. Note that the colours have no specific meaning. The algorithm here assumes that an upper limit exists to the distance between blocs and further that this limit can be expressed in term of the size of the blocs. The algorithm also assumes that blocs are represented as closed polygons. All polygon calculations use the GPCJ – java version (Bridenbecker, 2004) – of the General Poly Clipper algorithm developed by (Murta, 1997). Only minor refactoring was made to the Java version.

4.1 Step 1. Find an approximate value for the USM perimeter

In this step, the bounding boxes of the blocs are used. The algorithm searches iteratively for a minimum scale factor enabling the union of all the boxes to be one single polygon 2D.

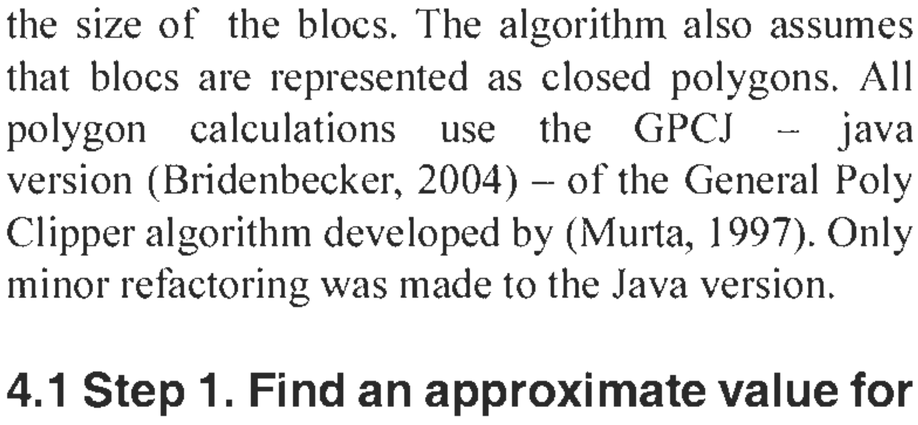

Fig. 7 Blocs bounding boxes scaled at 1.25 (left) and the computed perimeter displayed in magenta (right) superposed with the original blocs.

During iteration, the boxes are *blown* by this factor meaning that they are scaled while their center of mass remains the same before and after scaling. The scale factor is allowed to go from 1.0 to 1.3, incrementing the scale by 0.05 at each iteration.
This step also enables to select the blocs on which the next step will perform: only blocs whose blown bounding box has points on the perimeter are selected. In other words, only the blocs standing on the perimeter of the USM will be used.

4.2 Step 2. Adjust the perimeter to be in contact with the actual blocs

Starting from this step, the perimeter is represented with a B-Spline curve 2D - description in (Blake & Isard, 1998) – and the properties of the curve are used. The points on the curve are resampled and moved to be in contact with the blocs belonging to the perimeter of the USM. The figure 8 below shows the curve perimeter before and after this fitting step.

Fig. 8 (Left) Initial perimeter as a B-Spline Curve 2D (Right) Initial perimeter adjusted to the actual blocs

Note that the curve touches almost all blocs but does not really adhere to the blocs that stand a little bit far from the initial position. See for example, the upper right corner in the right image.

4.3 Step 3 and 4. Fit the perimeter to the USM blocs and cement extraction

Points along the curve perimeter are resampled. For each of these points, the *n* (constant) closest blocs are selected (by their distance between the point and their center of mass). If one of these blocs has a segment whose distance to the point is less than a threshold value, this point is kept as it is. The threshold value is computed as 0.02 x the mean size of blocs. The mean size of blocs is evaluated as the average dimension value of all bounding boxes of blocs. The constant 0.02 has been found to be experimentally acceptable. Otherwise the normal to the curve at this point is calculated and the nearest blocs are scanned to find the closest segment intersecting the normal. The intersection point is added in the curve perimeter. The Figure 9 shows the resulting perimeter.

Note that now the curve better fit to the blocs but further fitting could improve the result. To do that and avoid dealing with an increased number of points it would be needed to add new points only in the regions of the curve where it does not 'touch' the blocs.
Finally the cement can be extracted by performing a difference between the union of all blocs and the found perimeter, as shown in the image below with the mortar in green. (Figure 9)

Fig. 9 (Left) Perimeter fitted to the blocs. (Right) Cement extraction.

5. Archaeological data and 3D measure:a common database

Since 2006 (Drap et al., 2006a) the data produced by Arpenteur is stored both in XML and in a relational database. The main way to store data is a relational database in order to manage a big amount of data but XML is still used to work on subset of data or offline. The database contains geometrical data (photogrammetric measures, oriented photographs and artefact geometry) as well as archaeological data (USM definition, site data and observation on measured artefact as lithotype and so on).
The database is used to generate views on the model according to archaeological requirements. 2D or 3D representations are produced by queries on the database: the projection plane for 2D representation, the subset of blocks according to the requested USM are used to generated geometrical representations with a bidirectional link between the graphics and the database.

6. Automatic 2D document generation

The central database enables to represent various queries into 2D documents. 2D GIS software like ArcGIS (c) or libraries as Geotools can be used for producing specific views of the database and working in a GIS context. This capability is an automation of the manual drawings originally done by archaeologist (Figure 10). As we can see in Figure 11, ArcGIS interface shows a projection plane with USM represented by different colours. User can then work in ArcGIS and export results in other formats suitable for specific works.

Fig. 10 Orthophoto with manual design of USM.

The second kind of 2D database representation is the generation of annotated orthophotos. This representation merges GIS features and real visual information in one document that enables to see the objects as they are on site with the adjunction of information coming from archaeologist's knowledge.

Fig. 11 Database query exported in Arc-Gis software.

Figure 12 shows an orthophoto resulting from the query for the blocs (with texture), the USM (green perimeter) and the cement (yellow) attached to a given projection plane.

Fig. 12 Orthophoto generation on a query related to blocs, with design of USM perimeter and the cement paint in yellow

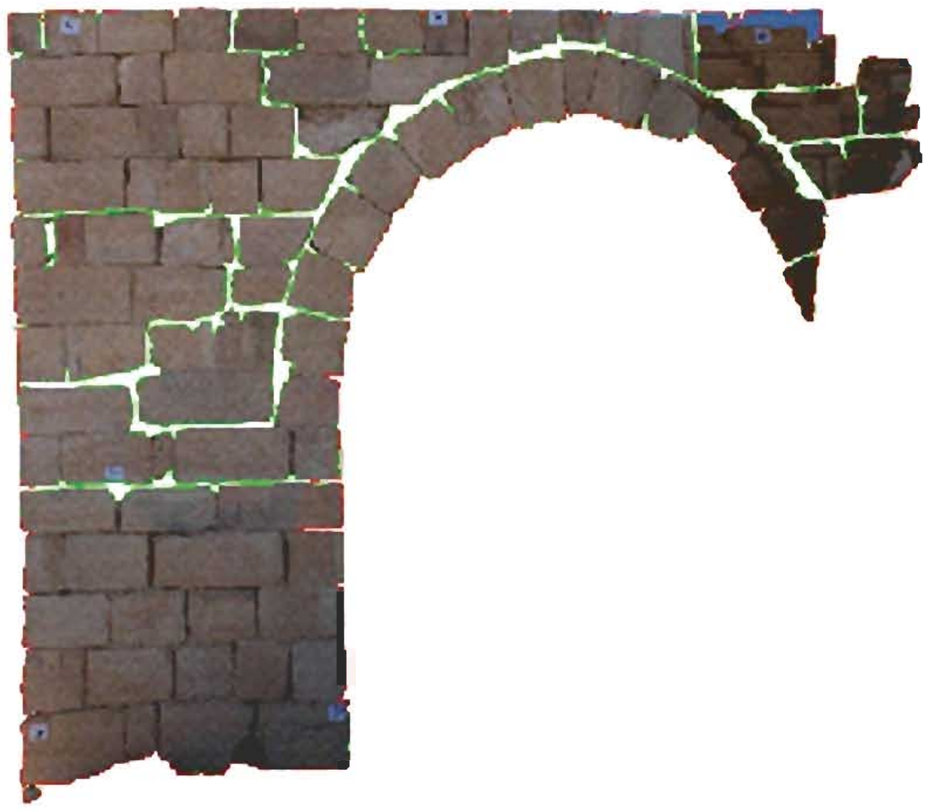

Fig. 13 Orthophoto generation on a query related to USM with cement between USM paint in white

The orthophoto shown in Figure 13 represents the query of the USM and the cement attached to the same projection plane. In this representation, the blocs are not represented individually and the different USM are clearly visible.

Queries resulting in orthophotos can also be close to a static GIS representation. As we can see in Figure 14 both orthophotos represents the same queries used for generating the orthophotos seen in Figure12 and Figure13 but without integrating photographic data related to USM and blocs.

With the two kinds of 2D documents created from the database, archaeologists have two complementary ways for reading the site. The GIS representation is dynamic, enables multiple queries and iterations and can be embedded in dedicated applications while orthophoto generation produces easy to use and handmade-like documentation.

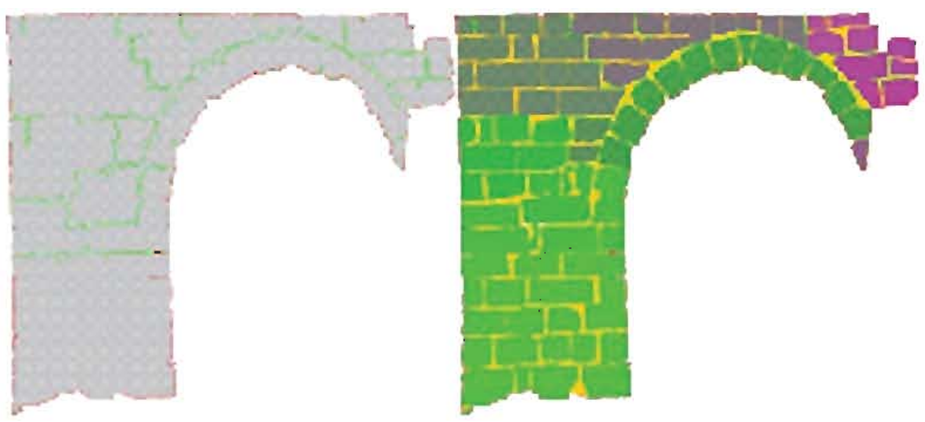

Fig. 14 Orthophoto generation (without texturing) on a query related to USM, with, on the left, the design of USM perimeters and on the right the bloc representation with a colour depending of their USM.

7. A 3D GIS approach

7.1 JReality-based software for interacting with 3D data

Computer tools that enable interactive 3D representation and new analysis of the studied objects through a bidirectional-link between the 3D representation and the archaeological data look very interesting for archaeologists.

In this sense, specific software has been designed for allowing the 3D interactive visualization, the analysis and the enhancement of the archaeological data collected on the Shawbak Castle. This problematic was already addressed on this case study (Drap et al., 2006a) but this time we use a full Java development allowing more integration and interaction. This software has been developed into the Arpenteur framework by means of the jReality (http://www3.math.tu- berlin.de/jreality/) application programming interface which is an Open source Java class library for interactive visualization of a large spectrum of 3D data. The last version of JReality is a light but efficient library offering a wide set of data structures and classes for handling common geometric entities (e.g. point sets, line sets, face sets, parametric curves and surfaces), a rendering engine allowing surface shading and texture mapping, a picking process for selecting 3D scene entities, a native import format (JRS), and several export file formats such as (RIB, VRML 1.0, U3D, PS, STL, Image, Sunflow). Moreover, several Java classes devoted to the design of Java-Swing based programs are available in the JReality package. The latest allows to rapidly producing graphical user interfaces for interacting with 3D data. The communication of JReality with the Arpenteur framework and consequently the object database is a straightforward task. Indeed, since both are fully written in Java code, displaying geometrical entities coming from Arpenteur with JReality simply requires implementing some suitable exchange procedures allowing converting the Arpenteur geometrical data structures to the JReality ones.

7.2 Archeology oriented Java procedures

To fulfill the needs of archeologists, a set of Java procedures have been designed for interacting with the database fields from the 3D representation of the database objects. Since the last development, all attributes of each block stored in the database (e.g. index in the database, name, dimensions …) can be read and/or modified through a devoted panel.

It is notably possible to interactively request and modify the database from its 3D representation by displaying USM spatial distribution of blocks and modifying manually each bloc attribute. This kind of actions can be achieved on a single block or on a block set, and enables archaeologists to work on the chronological building phases of the walls or answer to many questions regarding the masonry's technological aspects.

Since the measurement of the blocks is important information in a statistically approach to a building, procedures for displaying and sorting blocks from their dimensions (block length, block height) have been also implemented. The later notably allows evaluating the spatial distribution of the bloc dimensions and represents a relevant tool, for instance to analyze different chronological building periods in medieval constructions (e.g. chronotypology).

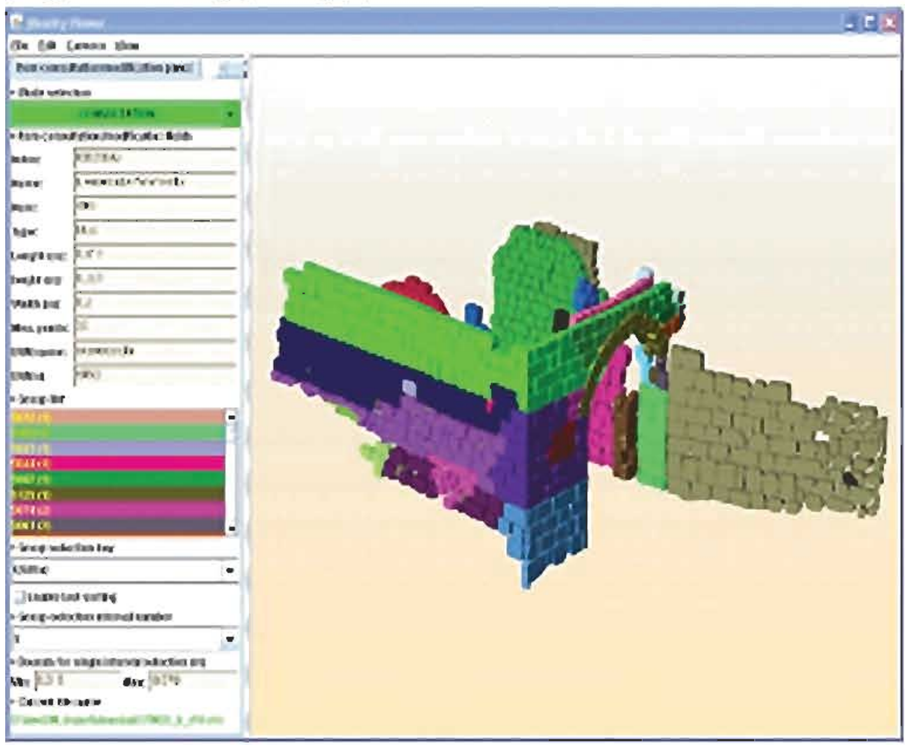

Fig. 15 3D visualisation with a colour panel chosen according to the block height classification.

These procedures also allows archeologists to exactly inspect/adjust each block dimension (collecting these dimensions on the field takes a lot of time and is only possible for easily-accessible blocks), and to gather blocks in different homogeneous classes (Figure 16). This dimensional information is also available for each bloc in the USM schedule through editable text fields. In upstanding structure stratigraphy, this is meaningful because the size is one of the distinctive features to differentiate USM, along with shape and other features (Figure15). Another under construction development aims the area of the mortar which is another distinctive character of the USM. This information is almost neglected in different kind of survey but seems relevant for producing new knowledge and enhancing the database of the studied objects.

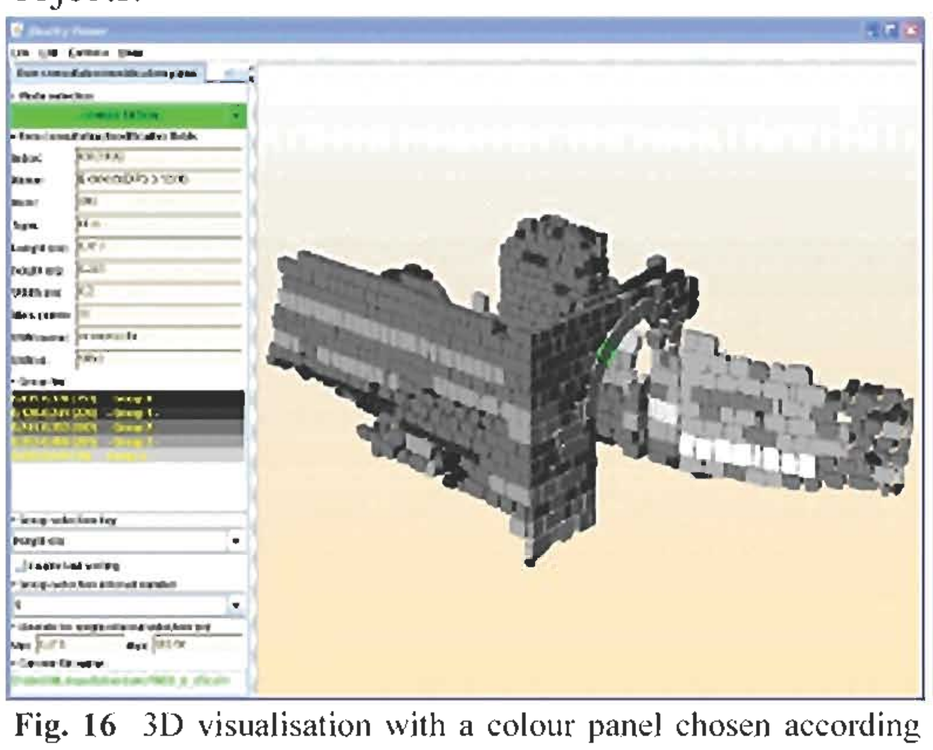

Fig. 16 3D visualisation with a colour panel chosen according to USM.

7.3 A tool to check photogrammetric data

This 3D tool is in fact a tool to visualize the database, from both archaeological and photogrammetry point of view. In the same way can make archaeological interpretation by 3D thematic representation it is also possible to combine artifact visualization with the photogrammetric data (oriented photographs, optical center, 3D point errors, line from 3D points to 2D points, etc…) (See Figure 17).

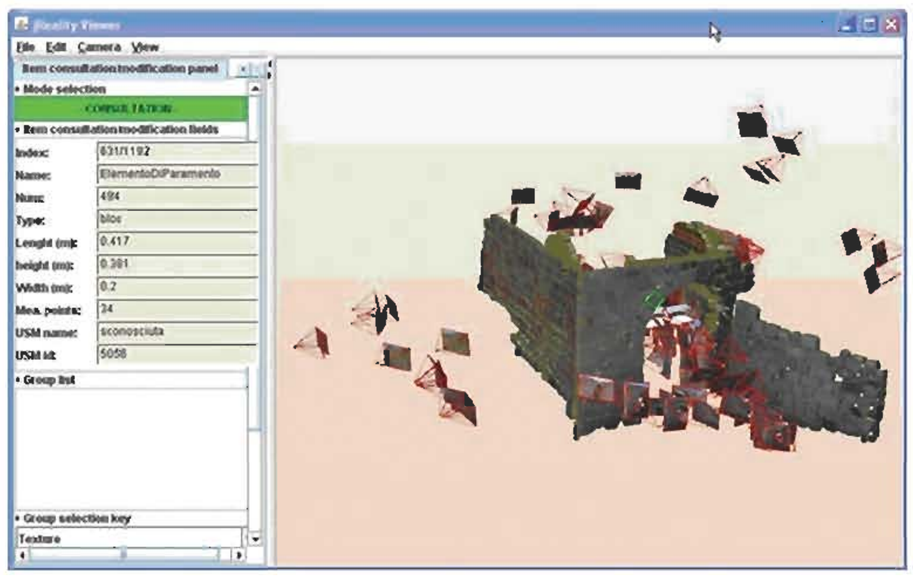

Fig. 17 Photogrammetric data 3D visualization.

Other use of this tool (some of them are currently under development):

- This tool allows to check the final result and to obtain and indicator of quality by artifact. This is the first step of a tool that can make a diagnostic and propose a way to consolidate measures in case of inconsistency.
- This tool allows using texture for each measured bloc: only the measured face is textured and 2D observations are available from this interface.
- Finally this module will be also used as a control for bundle adjustment (photo orientation, RMS on 3D points).

8. Automatic cloud point generation

We use the 3D measured point on the block perimeters and the oriented photographs to compute automatically a set of 3D points by correlation. This surface's densification process uses a mesh build on the 3D points measured manually and can produce a huge quantity of new 3D point only in the specific studied zone. A first version of this software already existed and was published (Drap et al., 2006b) but with a lower number of generated points (also it was not possible to detect false correlations and no texture information was possible).

In the version presented here we have generated more than four million of 3D points on the main door studied here and we export them in VTK - Visualization Toolkit - (VTK 2009) with blend color information (or more generally in ASCII file as XYZRGB).(See Figure 18).

Therefore we start to implement another way to get homologous points, based on SIFT algorithm (Lowe, 2004). This approach is quite different from correlation because it is based on extraction of so-called keypoints. The previous version of the tool was purely correlation based: given an initial set of measured points, a mesh was generated in the 3D space. Then moving on the produced triangles, the process tried to perform correlation between the points projected on the photographs. However, this is highly dependent of the local contrast and frequently fails if images have different orientation or scale.

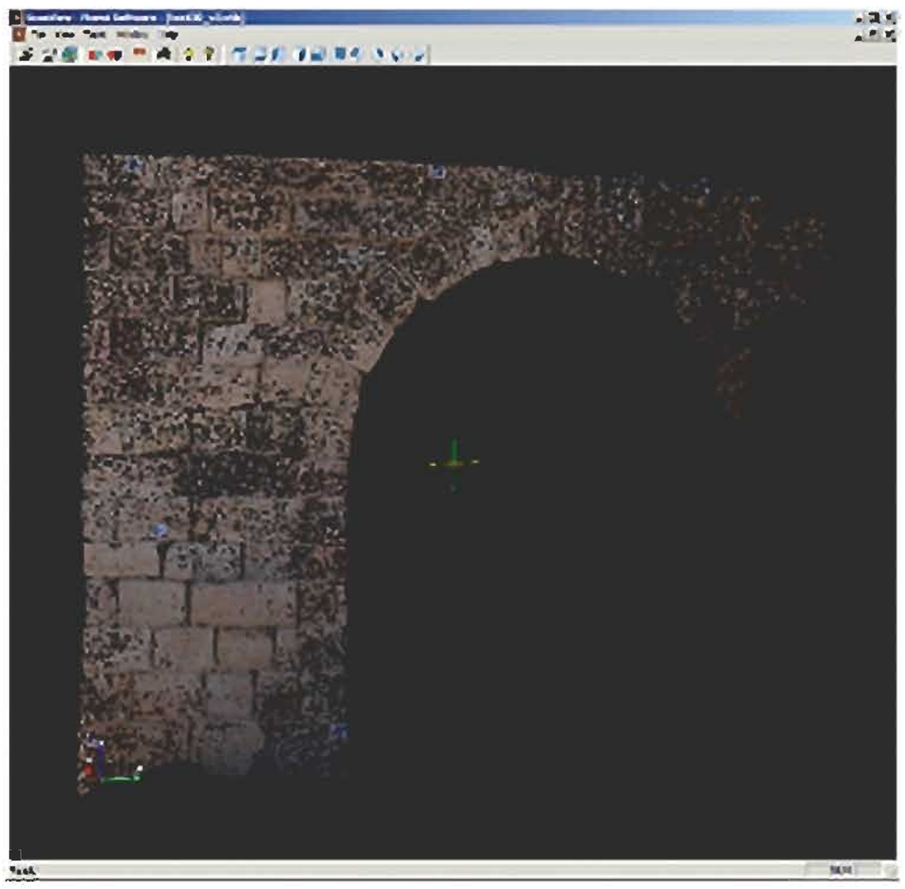

Fig. 18 3D cloud point generation based on autocorrelation and an approximate surface given by the measured blocs.

The keypoint extraction and match operation automatically return a set of homologous points fetched on the basis of the image dynamics. They can be used to define a surface or increase the surface definition (also to make an automatic orientation of the camera). High surface definition is connected with orthophoto generation, as we need to produce, according to archaeological requirements, also 2D representation. We will use this 3 surface definition to produce accurate, georeferenced orthophotos. The way to produce such orthophoto will fully use the 3D data we have produced before: oriented photographs, dense 3D points cloud, dense surface for wall/USM definitionWe have developed an orthophoto generation based on the 3D surface analysis which produces both an image in GeoTIFF format and a set of 3D points with color information gridding the site area.

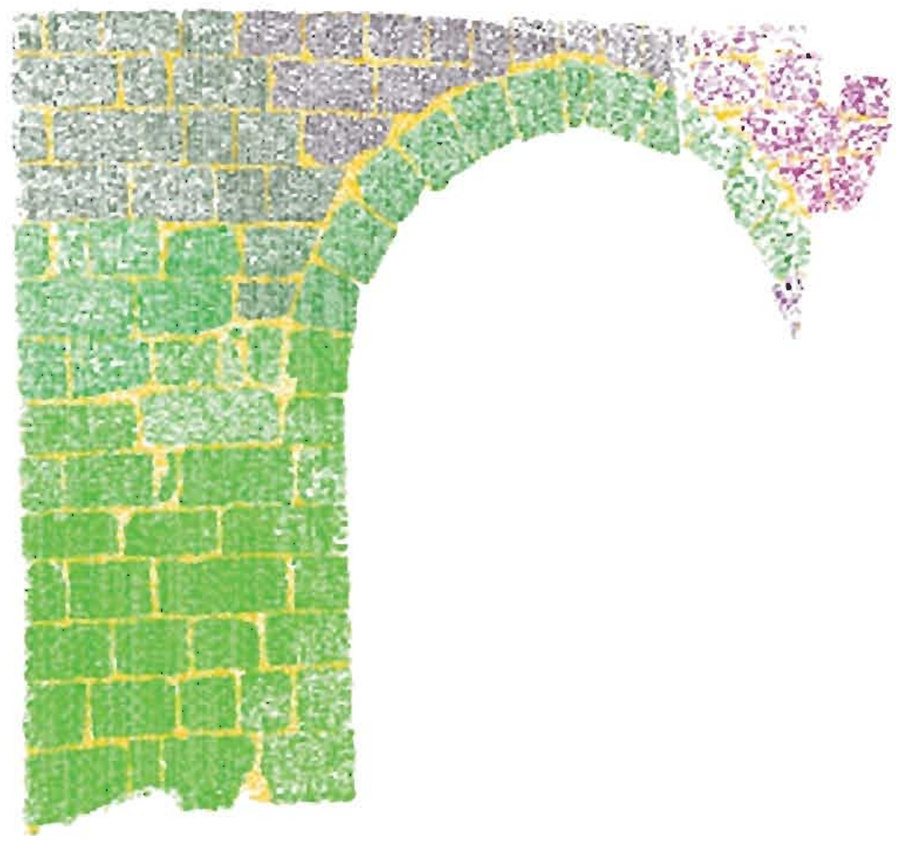

Fig. 19 3D cloud point generation based on autocorrelation where semantic information is used to obtain a colour.

This method will allow combining vector survey, where an expert of the domain, here an archaeologist, is making the survey and cloud of measured points in some zone where a huge quantity of point can help to understand, for example the stability of a wall. Such combined approach is already explored; see for example a study made by Haala and Alshawabkeh
(Haala & Alshawabkeh, 2006) on a famous tomb in Petra, close to Shawbak. Two points are fundamentally different in our approach

- The method is only based on and oriented photographs; in such case (Jordan, desert, etc…) this should be an interesting advantage.
- All the geometrical data obtained are the result of database queries and thus they are linked with archaeological data (See Figure 19).

9. Conclusion and future work

Automatic 3D thematic representation with bidirectional-links between 3D representation and archaeological data allows new archaeological analysis. It is possible to record data and to produce new knowledge about the studied object. We focus on block measurement, developing specific photogrammetric tools which use a priori knowledge to help the operator during the plotting phase. As the main goal of this project is linking measured geometry with archaeological knowledge, we tried to propose a photogrammetric tool that can be used by an archaeologist. In this application 3D measurements are done by using only one photograph through the user interface and automatically computing reprojection and correlation.

The archaeologist-operator can focus his effort on inserting archaeological data instead of spending time and concentration in homologous point determination. It is also important to say that the archaeologist can spend more time on a field to analyze the structure because we can "survey" directly on the 3D model in laboratory and insert in it a lot of different kinds of data.

The 2D/3D GIS context can also be used as a suitable interface for managing survey consistency and session merging. The knowledge driven survey process enables to automatically check consistency of a survey (Seinturier et al, 2006) and to semi-automatically merge different survey sessions of the site. As consistency checking and merge requires expertise, the 2D / 3D GIS can be used for providing experts a global view of the site with geometry, documentation and photographs. With a unique access to all information available, an expert can easily drive the consistency restoration and the merge processes.

Of course archaeologists need some more! Currently the system must be tested with all the buildings already studied in order to compare the results of this method in different examples of structures. The next step will be to find the way to visualize all the chronological aspects of the upstanding structures interpretation, in other words, to visualize the Harris Matrix (Harris, 1989) (Allen, 1983).

Finally, ways for making persistent the documentation of a site have to be explored. New formalisms and specifications such as ontology (Niccolucci F., D 'Andrea A. 2006) and CIDOC-CRM (D'Andrea et al. 2006) (CIDOC-CRM, 2004) are now thoroughly used in the cultural heritage domain. A theoretical study and an implementation of such formalisms and specifications could enhance the current framework.

Acknowledgements

The authors want also to thanks the company Pointstream Inc. for the access to their software, Pointstream 3DImageSuite, used in this work, which is dedicated to represent and manage cloud of 3D point with colour information. (http://www.point-stream.net/).

References and/or selected bibliography

References from Journals

Allen J. F.,. 1983, Maintaining knowledge about temporal intervals. Journal of the ACM, Volume 26 pp 832-843

Lowe D. G., 2004 Distinctive image features from scale invariant keypoints, International Journal of Computer Vision, 60, 2, pp. 91-110.

References from Books:

Blacke, A. and Isard, M., 1998. Active Contour. Vol. 1, Springer, Department of Engeneering Science, University of Oxford, Parks Road, Oxford OX1 3Pj.

Harris E.C., 1989 Principles of Archaeological Stratigraphy. Academic Press; 2 edition (Jun 15 1989) ISBN 978- 0123266514.

Vannini G.(a cura di), 2007, Archeologia dell'insediamento crociato-ayyubide in Trangiordania. Il progetto Shawbak, Firenze, All'Insegna del Giglio.

References from Other Literature

Drap P., Durand A., Nedir M., Seinturier J., Papini O., Gabrielli R., Peloso D., Kadobayashi R., Gaillard G., Chapman P., Viant W., Vannini G., & Nucciotti M.. 2007. Photogrammetry and archaeological knowledge: toward a 3dinformation system dedicated to medieval archaeology: a case Study of Shawbak castle in Jordan. *3D-ARCH 2007: 3D Virtual Reconstruction and Visualization of Complex Architectures,* ETH Zurich, Switzerland. Fabio Remondino Sabry El-Hakim (Ed.).

Drap P., Nedir M., Seinturier J., Papini O., Chapman P., Boucault F., Viant W., Vannini G., & Nuccioti M.. 2006. Toward a photogrammetry and virtual reality based heritage information system: A case study of shawbak castle in jordan. *VIIth International Symposium on Virtual Reality, Archaeology, and Intelligent Cultural Heritage VAST 2006.* M. Loannides and D. Arnold and F. Niccolucci (Ed.), pp.67-74, Eurographics Association and ACM SIGGRAPH, Nicosia, Cyprus(Pub.).

Drap P., Franchi R., Gabrielli R., & Peloso Daniela. 2006. Integrated application of laser scanning techniques and close range photogrammetry. The case study of the ancient water supply system of Petra. *ACN - Archaeological Computing Newsletter,* Vol.:64, pp.12-18, isbn/issn: 0952-3332.

Drap P., Gaillard G., & Grussenmeyer P.. 2001. Simple photogrammetric methods with arpenteur. 3-d plotting and orthoimage generation: the I-MAGE process. *CIPA 2001 International Symposium,* Postdam university, Germany. Isprs (Ed.), Vol.:1, pp.200-212.

Drap P., Gaillard G., Grussenmeyer P., & Hartmann-Virnich A.. 2000. A stone-by-stone photogrammetric survey using architectural knowledge formalised on the ARPENTEUR Photogrammetric workstation. *XIXth Congress of the International Society for Photogrammetry and Remote Sensing (ISPRS),* Geoinformation for all, Amsterdam. Vol.:XXXIII, part 5, 8 isbn/issn: ISSN 0256-1840.

Haala N., Alshawabkeh Y., 2006, Combining laser scanning and photogrammetry – a hybrid approach for heritage documentation. *VIIth International Symposium on Virtual Reality, Archaeology, and Intelligent Cultural Heritage VAST 2006.* M. Loannides and D. Arnold and F. Niccolucci (Ed.), pp.163-170, Eurographics Association and ACM SIGGRAPH, Nicosia, Cyprus(Pub.).

Niccolucci F., D'Andrea A. 2006, An Ontology fo 3D Cultural Object, *VIIth International Symposium on Virtual Reality, Archaeology, and Intelligent Cultural Heritage VAST 2006.* M. Loannides and D. Arnold and F. Niccolucci (Ed.), pp.203-210, Eurographics Association and ACM SIGGRAPH, Nicosia, Cyprus(Pub.).

D'Andrea A., Marchese G., Zoppi T. 2006 Ontological Modelling for Archaeological Data *VIIth International Symposium on Virtual Reality, Archaeology, and Intelligent Cultural Heritage VAST 2006*. M. Loannides and D. Arnold and F. Niccolucci (Ed.), pp.211-218, Eurographics Association and ACM SIGGRAPH, Nicosia, Cyprus (Pub.).

Vannini, G., Nucciotti, M., Tonghini, C., & Desideri, A. V. 2002. Medieval Petra. Archaeology of Crusader-Ayyubid fortified settlements in Trans-Jordan. AA. VV. "Civilisations of the Past, dialogue of the present: Italian Research mission in Jordan, Amman (Jordan).

Seinturier J., Drap P., Papini O., Vannini G., Nucciotti M., 2006, Knowledge representation and data fusion for archaeology: The case study of the castle of shawbak, Proceedings of the IXth Infographie Interactive et Intelligence Artificielle International Conference 3IA'2006, Dimitri Plemenos, XLIM Laboratory of the University de Limoges and Computer Sciences Department of the Sciences and Technics Faculty of Limoges, pp. 169-179, University of Limoges and EUROGRAPHICS-AFIG, Limoges, France, May 23-24 2006.

References from websites

Arpenteur, 2008, Arpenteur web site http://www.arpenteur.net (accessed 30 January 2009).

Bridenbecker Daniel, 2004, General Poly Clipper Algorithm in Java http://www.seisw.com/GPCJ/GPCJ.html (accessed 30 January 2009).

CIDOC CRM consortium, 2008, The CIDOC Conceptual Reference Model, http://cidoc.ics.forth.gr/ (accessed 30 January 2009).

Murta A., 1997, GPC General Polygon Clipper Library http://www.cs.man.ac.uk/aig/staff/ alan/software/ (accessed 30 January 2009).

VTK 2009, Visualization ToolKit http://www.vtk.org/ (accessed 30 January 2009).

Integrating Web GIS and Wireless Network for Secure Transportation

M. Tauhidul Alam[1], M. Phil student[1] & Prof. Dr. Mohammad Shahadat Hossain[2]
[1]Department of Computer Science & Engineering
University of Chittagong, Chittagong- 4331, Bangladesh.
tauhid.cse99.cuet@gmail.com Mobile : 8801819941369

[2]Chairman, Department of Computer Science & Engineering
University of Chittagong , Chittagong- 4331, Bangladesh.
Email: hossain_ms@hotmail.com Tel: 88031726311-14 Extn.: 4297
Mobile : 8801819336660

ملخّص : يعتبر الأمن عامل مهمّ في نظام النقل . يهدف هذا المقال إلى شرح النظام المترابط الذي يؤمّن نظام النقل . لهذا الغرض إستعملت الشبكة المتحركة الحالية لكشف منطقة إتجاه السيارة. تمزج هذه المعطيات التلماتيكية مع مجموعة المعطيات الجغرافية الفضائية لإيجاد المعلومة الجغرافية داخل الخزّان SIG (نظام المعلومات الجغرافية) و خزّان الخريطة الذي يستعمل GPRS أو تكنولوجيا EDGE للدخول إلى شبكة الأنترنيت. حينئذ كل المعطيات الفضائية و الغير الفضائية مرتبطة لتشكيل نظام مترابط و يرسل مخرج هذا النظام إلى جهاز الإستقبال الموضوع في مركز الشرطة المجاور أو في سيارة الشرطة في الطريق السريع الذي يساعد السلطة على التدخل فورا.

Résumé : La sécurité est un facteur important dans le système du transport. L'objectif de cet article est de présenter un système cohérent qui offre une sécurité au système du transport. Dans ce but le réseau mobile actuel est utilisé pour détecter la zone du véhicule en marche et sa direction. Ces données de la télématique sont reliées avec les ensembles de données géo spatiales pour trouver l'information géographique dans le serveur SIG (Système d'Information Géographique) et le serveur de la carte qui utilise GPRS (Service de Communication Radio en mode Paquet) ou la technologie EDGE (Evolution de la Norme GSM Modifiant le Type de Modulation) pour l'accès à Internet. Alors toutes les données spatiales et non spatiales sont reliées pour constituer un système cohérent et la sortie de ce système est transmise au récepteur localisé au poste de police avoisinant ou dans la voiture de police en autoroute qui aide l'autorité à intervenir dans l'immédiat.

Abstract : Security is an important factor in transportation system. The objective of this paper is to present an integrating system which gives an instant security on transportation system. For this purpose existing mobile network is used to detect the vehicle moving area and its direction. These telematics data are accommodated with geospatial data sets to find geographical information from GIS (Geographical Information System) server and map server using GPRS (General Packet Radio Service) or EDGE (Enhanced Data Rates for GSM Evolution) technology to access the internet. Then all spatial and non-spatial data are bind to construct an integrating system and the output of this system is sent to the receiver that resides on neighboring police station or highway police car that helps the authority to take instant action.

1. Introduction

In our everyday life we need to go long distance for different purposes by bus, car etc. On the way to journey the vehicle may be assaulted by the terrorist. So the vehicles' moving area and other geographical informations should be found out and send to proper authority to rescue the passenger. Many transportation applications can be supported by centralized location and navigation systems which utilize communication network, host facilities and other infrastructures together with on-board vehicle equipment to locate and navigate [1]. When a vehicle is attacked by a terrorist, the information of the vehicle can be found by Automatic Vehicle Location Detection system (AVLS).But the problem in this system is that, the vehicle can be recovered after certain time while informing the situation to the service provider. During these time passenger lost their valuable things and even they may attacked by terrorist. So a system should be developed to save passengers instantly. Our goal is to solve this problem.

2. Previous Technologies

Various wireless and web based GIS technologies are used in location detection, Navigation Control and many other fields. Here is a snapshot about previous technologies.

2.1 Wireless Location Technologies

There are three most commonly used location technologies: stand-alone, satellite-based, and terrestrial radio-based [2]. As examples, a typical stand-alone technology is dead reckoning. A typical satellite-based technology is global positioning system (GPS)[3],[4].AVLS system use GPS technology to find vehicles' location. But The GPS receiver is costly and if we use it in mobile phone it reduce the battery life. For wireless E911, the radio-based (satellite and terrestrial) technologies are the most popular ones. Cellular networks are terrestrial-based communications systems. Commonly studied techniques to find location of mobile device are angle-of-arrival (AOA) positioning, time-of-arrival (TOA) positioning, and time-difference-of-arrival (TDOA) positioning [5]. But all of these techniques need multiple BTS to find exact position. Multiple BTS make cumbersome to detect location. This paper concentrate on single BTS and its sectorized antenna to fetch network data such as cell id, cell broadcast name, sector id to find out the location area to overcome the problems of multiple BTS and GPS.

2.2 GIS Web Technologies

GIS Web Services [6], [7] provide commercially hosted spatial data and GIS functionality via the Internet to web applications and users. In a nutshell, GIS Web service provides GIS content and functionalities to applications without having to invest in costly GIS software and platforms. ArcGIS Server [8] provides a standard framework for developing GIS server applications. The world's most popular GIS software (ArcView, ArcEditor, and ArcInfo) is built from this same set of software objects. ArcView GIS Server's ability to leverage web services makes it ideal for integration with other critical IT systems, such as relational databases, web servers, enterprise applications servers. There are different map servers that facilitate the web GIS service. MapServer excels at rendering spatial data (maps, images, and vector data) for the web. DBMAP ASJ Runtime server, ArcIMS etc. is some Map server. ArcIMS provides high performance web geo-publishing of maps and metadata. The proposed system uses ArcView GIS and ArcIMS as GIS and map server respectively.

3. Objective

The objective of this paper is to develop an integrating system which helps the police authority to gives an instant security for the passengers of assaulted vehicle. The system is divided into five phases:

•Phase 1. Collect network data from Base transceiver station (BTS) to find vehicle's moving area and direction using a transceiver that attached to the vehicle dash board.

• Phase 2. Collect geospatial data based on network data from ArcGIS server and ArcIMS server using GPRS or EDGE technology to access the Internet.

• Phase 3. Construct an Integrating System based on phase 1, phase 2 and other vehicle related information.

• Phase 4. Send the output of this system to neighboring police station or highway police.

• Phase 5. To find the updated data refresh total system after few second or few minute.

4. System Design

The system use an onboard hardware and software which is embedded in a vehicle .To find moving area of the vehicle the system use existing GSM network and to find geographical information (like map, image etc)about that area, it use GIS web service using GPRS or EDGE technology. On basis of information provided by the system of the assaulted vehicle, the authority of particular police station or highway police may take necessary steps to rescue the people instantly.

4.1 Hardware

The system needs a transceiver that attached with dash board of vehicle to collect BTS information from network and send vehicle information to the police station. This Vehicle Transceiver (VT) should support GPRS or EDGE to access web for geospatial data from geo-database and map server. Beside this there is also need to receiver device for remote police station which shows the street address and street map of assaulted vehicle.

4.2 Database Design

The system needs two databases for storing different spatial and non-spatial data. First database namely isystem_info is designed for proposed Integrated System Software (ISS) that reside on the vehicle. It contains four tables namely vehicle_info (vid, model_no, passenger_no, start_time, start_place, destination, speed), network_info (cell_id, cell_name, sector_id, sector_direction), ps_info (ps_code, ps_name, receiver_no), and map_info (area_code, street_addr, street_map).

It stores all vehicle, telematic, geospatial and map data collected from different sources. Second database namely isystem_geo_info is designed for spatial data that reside on geo-database in the GIS web server. It contains two tables namely street_info (cell_id, area_code, sector_id, street_addr), ps_info (cell_id, ps_code, ps_name, receiver_no). It provides spatial information about the street at where vehicle is moving on.

3.4 Software Architecture

The software manages all hardware and fabricates information from network and spatial data. The implementing software works automatically after pushing the interfacing button that attached with vehicle board. No other information is provided by the user. Therefore no other user interface is needed on the software. Its main tasks are divided into four sections which implements the four phases of the total system.

• Section 1: It collects network data from the vehicle transceiver and stores it in 'network_info' table of 'isystem_info' database. Data flow is shown on Figure 1.

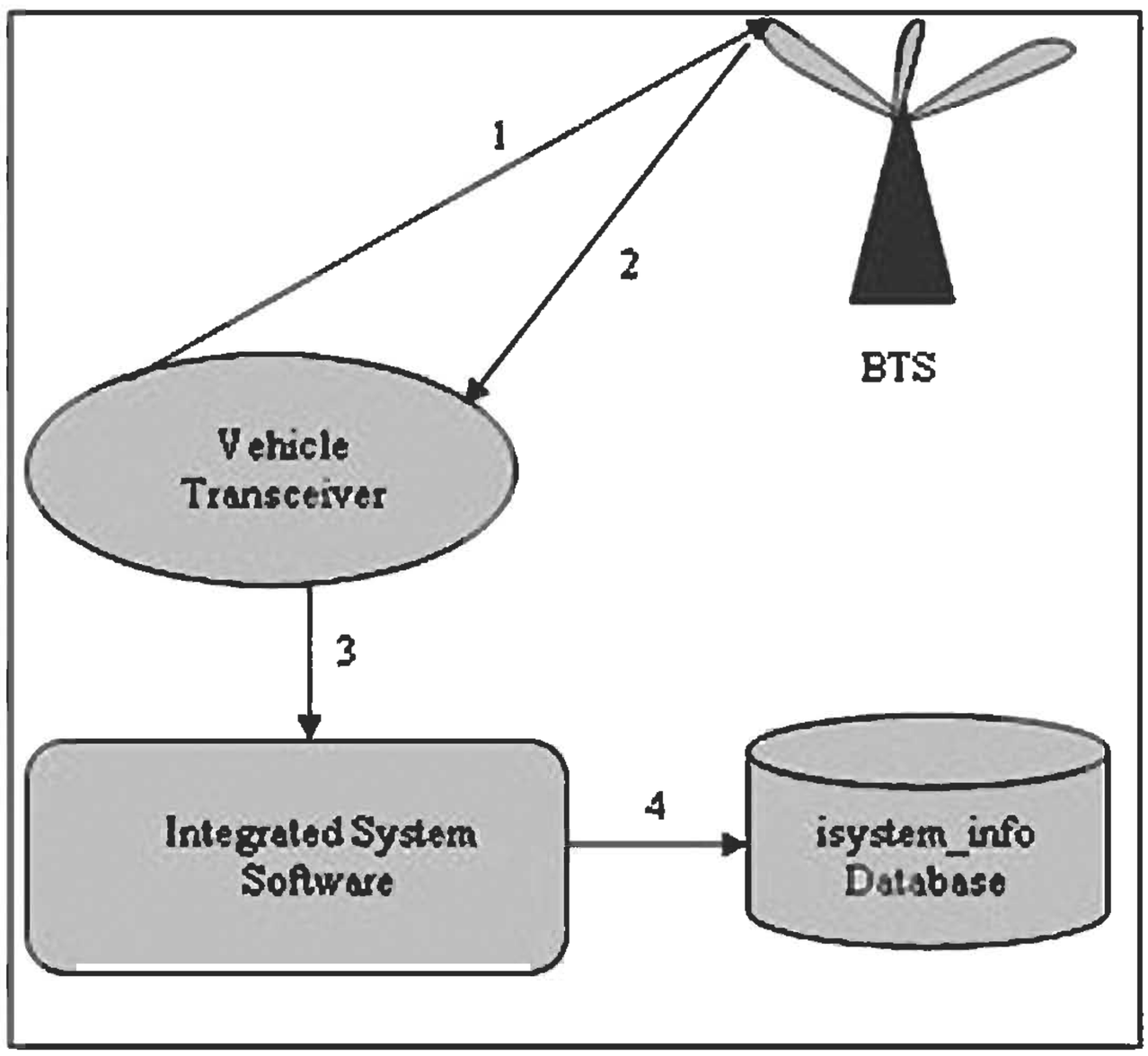

Fig. 1 Collect network data and store into isystem_info database.

• Section 2: It connects to GIS server and sends cell_id and sector_id as parameter. Using both parameter GIS server fetch street address and area code from 'street_info' table of 'isystem_geo_info' database. Also GIS server fetches PS Code, PS Name and PS Receiver No from 'ps_info' table of 'isystem_geo_info' database. Then all the street, area and PS information send back to ISS and stored in 'map_info' and 'ps_info' table of 'isystem_info' database. Data flow is shown on Figure 2.

• Section 3: After fetching information from GIS server it connect with ArcMap server and send a request for map of vehicle moving street address using 'area_code' and 'street_addr parameter'. Arc_Map server then fetches map from map database and sends back to ISS. Then update the 'map_info' table of 'isystem_info' database. Data flow is shown in Figure 3.

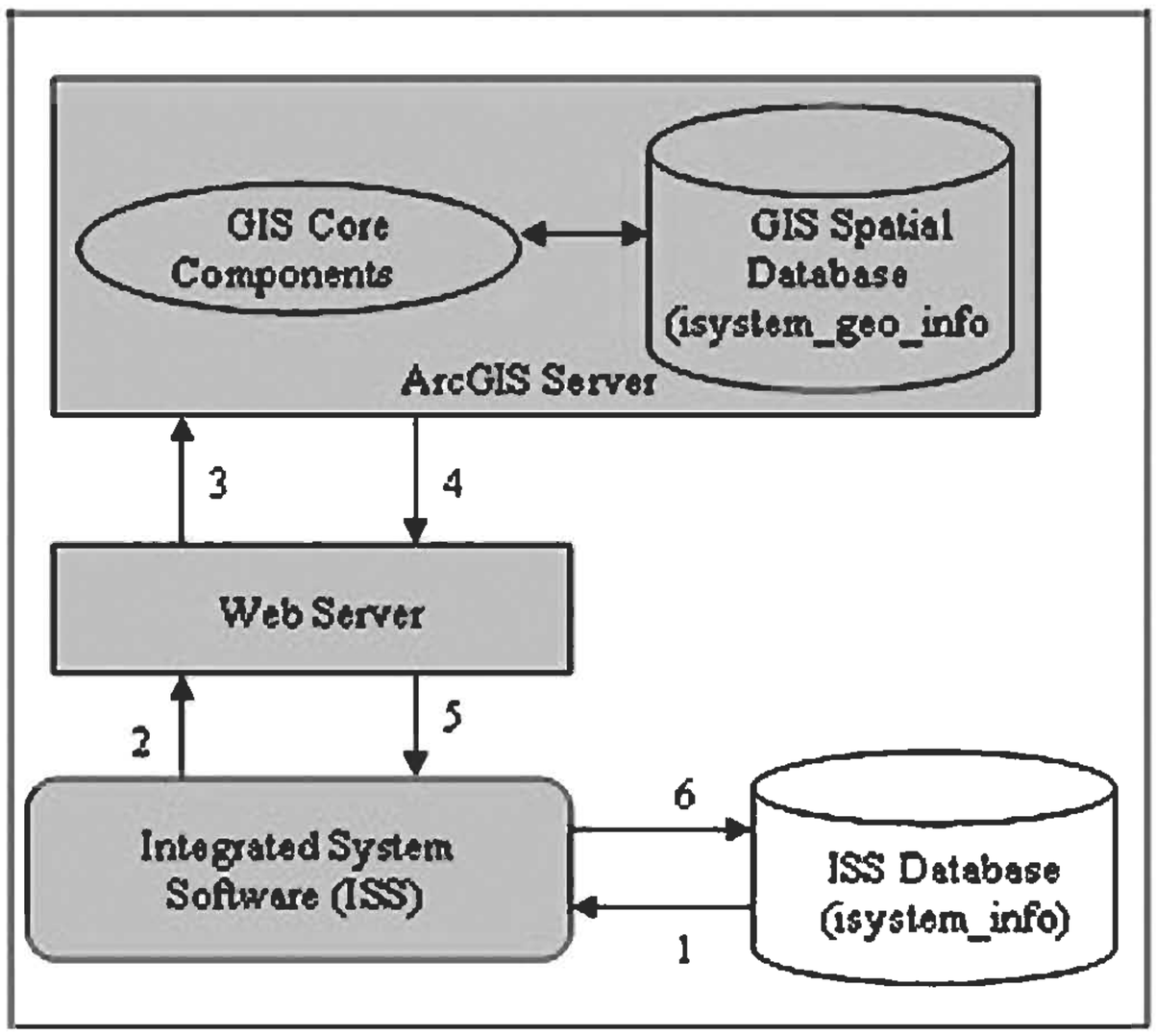

Fig. 2 Collect spatial data from ArcGIS server and store into isystem_info database.

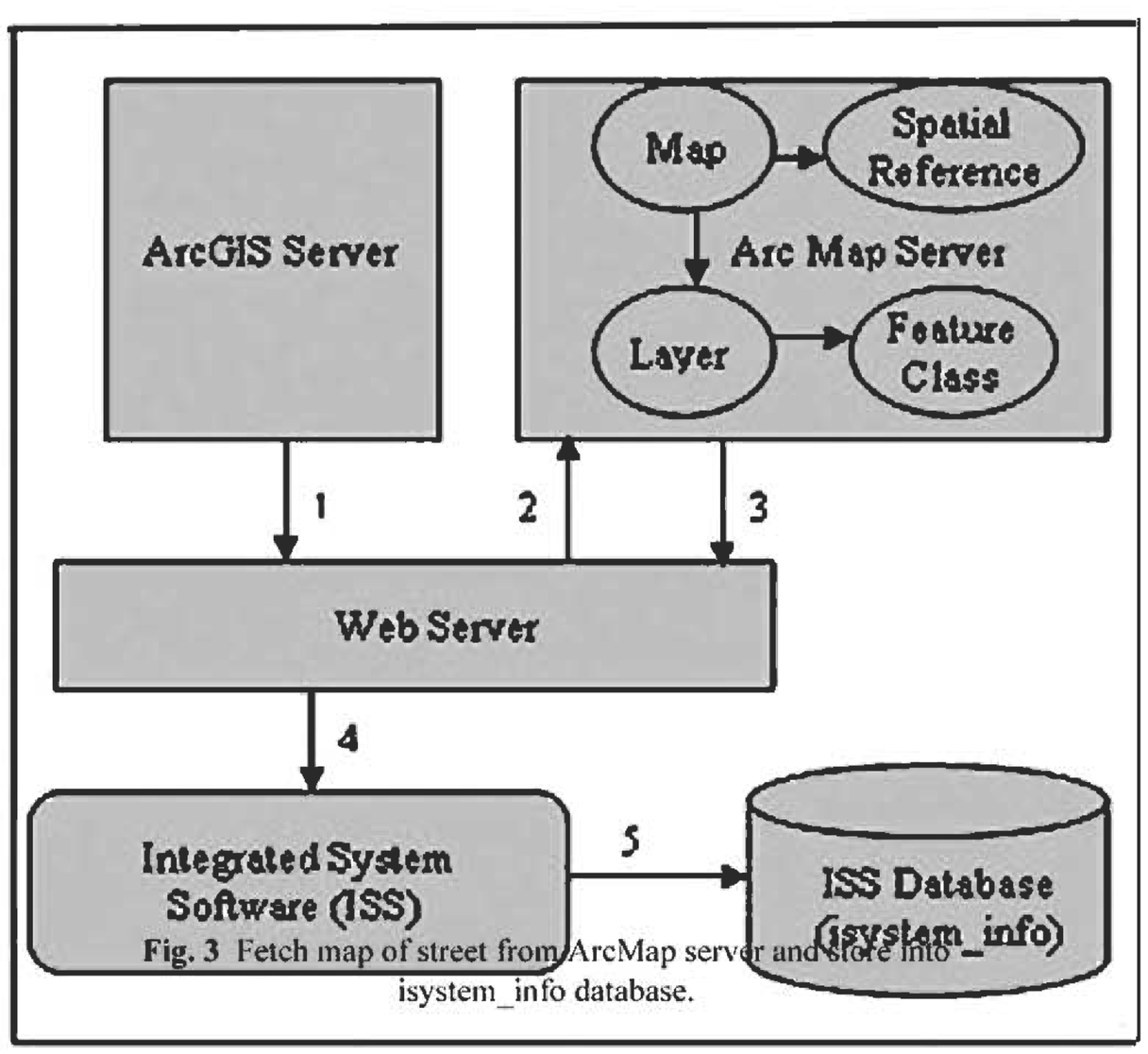

Fig. 3 Fetch map of street from ArcMap server and store into isystem_info database.

• Section 4: Finally it bind the vehicle information , street address and street map from 'vehicle_info' and 'map_info' table of 'isystem_info' database and send to receiver of particular police station or Highway police using 'receiver_no' from 'ps_info' table of 'isystem_info' database. Data flow is shown in Figure 4. While implementing section 1 and section 4, ISS uses GSM to access network and while implementing section 2 and section 3, it uses GPRS or EDGE to access the web.

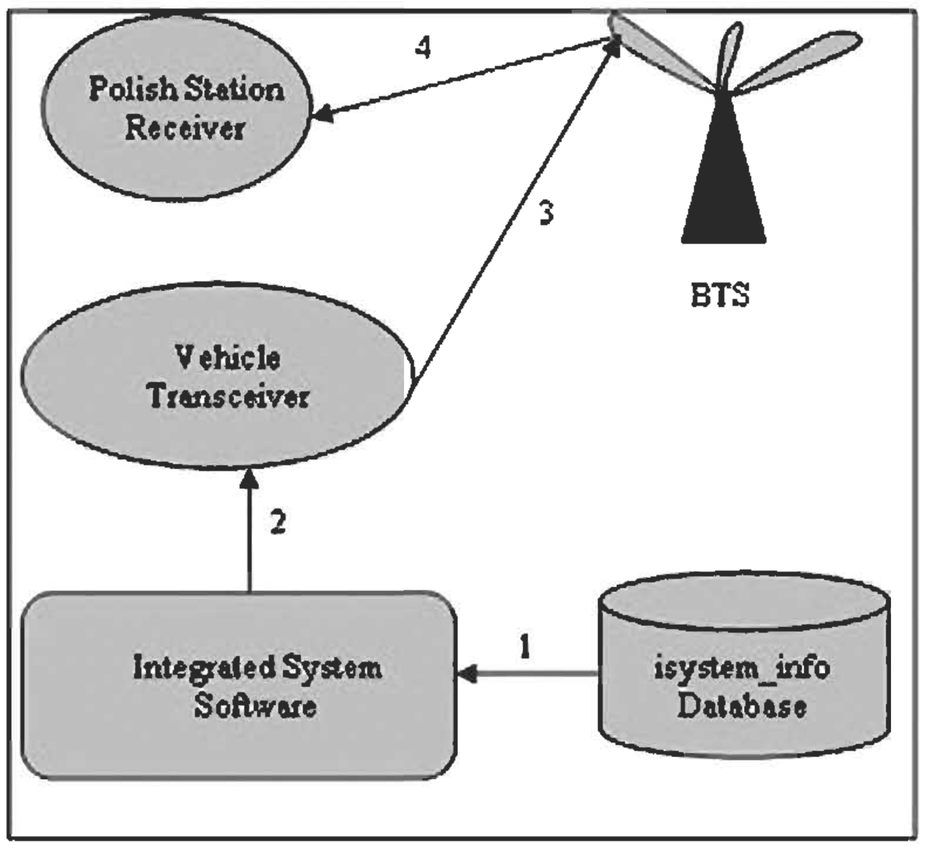

Fig. 4 Collect all spatial & non-spatial data about vehicle and send to the police station receiver.

5. Methodology

When a vehicle is assaulted by the terrorist the driver or security personnel push the button of Vehicle Transceiver (VT) that attached on the board. This transceiver connects with neighboring BTS and collects the following network data.

- Cell Id (CI) and Cell Broadcast (CB) Name
- Sector Id (SI) of GSM sectorized antenna.

After acknowledge from the BTS the system connected with GIS Server through VT to find out the geographical information (street address, neighboring police station etc) about the location where the vehicle is moving on. Then it connected with map server to find out street map. While the system connecting to map server, VT send all other non spatial data such as street address, vehicle info etc. to PS receiver to alert the authority. Then after fetching the map it bounded with other information and send to PS receiver. When the receiver alerts the authority, they will rush to the spot and save the passenger from a hazard situation.

Vehicle may reside at one position or moving continuously. While moving it change the sector of BTS also change the BTS itself. Therefore Street, Police Station also changes dynamically. So all the collected data of the system should be modify. To update all the data automatically the system refresh the software after few second or few minutes. No need to push the button again.

The Highway police or Authority of the certain police station always monitoring the receiver either it change its location or not after 1st alarm from vehicle. If the location is same for a certain time the vehicle is stopped on that street. If the location is changed they need to change their root to chase the vehicle. Two successive change of street give the direction of the vehicle. It helps them to chase the vehicle quickly. Each sectorized antenna has multiple sectors. Each sector is uniquely identified by Sector Id under a particular BTS. There are multiple BTS under a police station. Each BTS is uniquely identified by Cell Id. So while the vehicle changes the sector under same BTS and BTS under same police station it will not hamper the police authority to finish their task. But if the vehicle changes its BTS to new one which is under another PS, the responsibility is handover to that PS. The ISS stop transmitting the information to the previous PS and start transmitting the information to new PS. Then new PS takes responsibility to chase the assaulted vehicle. Thus particular police station is alerted by network automatically while moving the assaulted vehicle. Figure 5 shows the total architecture.

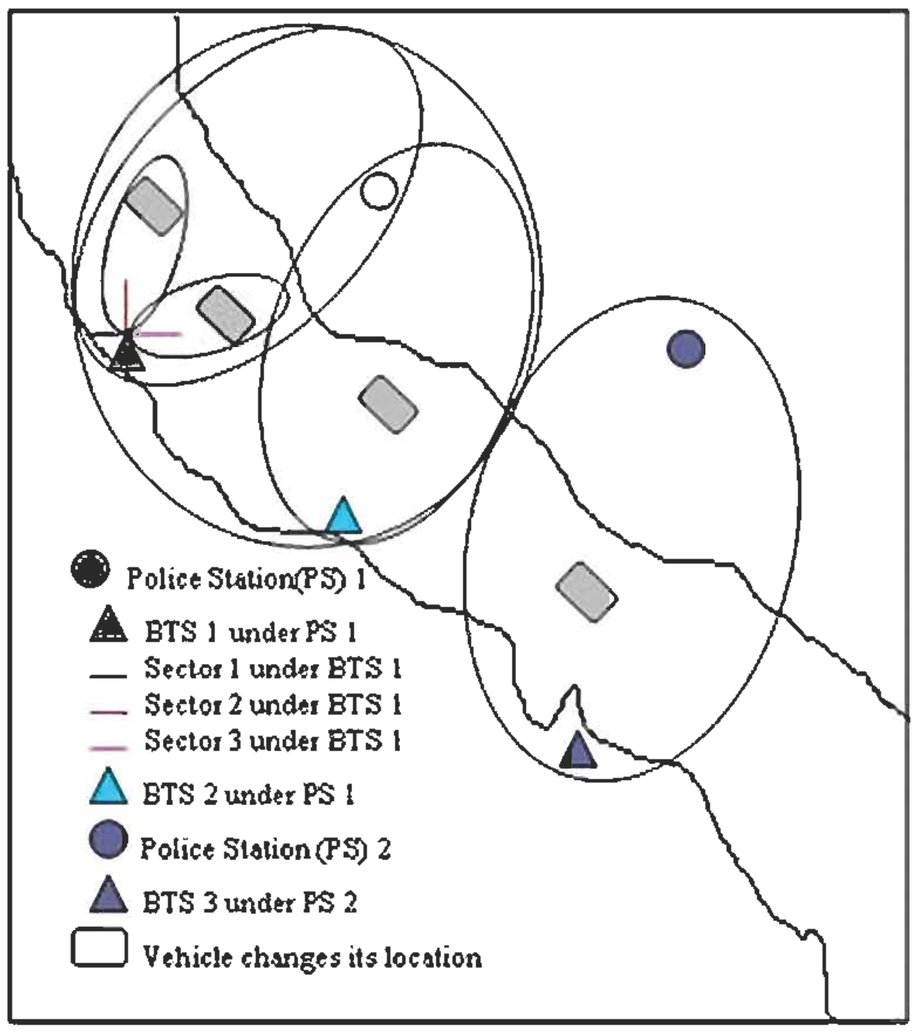

Fig. 5 BTS and Police station handover for the vehicle while moving

6. Conclusion

Many foreigners, tourist and aristocrat people rides on luxurious vehicles that move on the high ways. So the terrorist target the highways or big roads rather than small or branch roads to attack. Therefore this paper focuses on building integrating system that gives the security to vehicles on the highways or big roads. By implementing this system passengers fell more secure while roaming.

7. Limitations and Future Work

This research emphasizes an interactive system for vehicle tracking and rescue passengers are built for only high ways or big roads. Because only high ways street address are placed in geo-database.

In near future branch street address are included in geo-database. The system uses GSM antenna of three sectors. By increasing the sector (six sectors), precise location about vehicle moving area can be found. After little modification this system assures better security in transportation.

Performance is one of the most important limitations in the development of WebGIS and wireless technology. It is mainly because most spatial data including raster and vector data are large in volume [9], and also involve moving large spatial objects over the network between server and client. Though this proposed system is used GPRS or EDGE for web access for spatial data, it may slow the system if proper bandwidth cannot be found. At that case street map can not be supplied in proper time. In near future this system will be integrated with higher bandwidth wireless technology.

References bibliographical

Zhao, Y.: Vehicle Location Navigation Systems. MA :Artech House ,Norwood (1997)

Zhao, Y.: Vehicle Navigation and Information Systems. In: J.G. Webster (ed.): of Electrical and Electronics Engineering, Vol. 23. Wiley, New York, (1999) 106–118

Parkinson, B. W., Jr. Spilker, J. J., Axelrad, P., Enge, P. (eds.): Global Positioning System: Theory and Applications, Amer.Inst. Aeron. Astron., Washington, DC (1996)

E. Kaplan (ed.): Understanding GPS: Principles and Application. MA: Artech House, Norwood, 1996

Zhao, Y.: Mobile Phone Location Detection and Its Impact on Intelligent Transportation Systems, In: IEE Transaction on Intelligent Transportation Systems, Vol. 1, No. 1, March (2000)

Sugumaran, V., Sugumaran, M.: Web-based Spatial Decision Support Systems (WebSDSS): Evolution, Architecture, and Challenges. In: 3rd Annual SIGDSS pre- ICIS Workshop: Designing Complex Decision Support: Discovery and Presentation of and Knowledge, Las Vegas, Nevada (2005) 9-13.

White paper: GIS Web Services: The Changing GIS Landscape, Totonto,Canada(2003). http://gisfactory.com/whitepapers/wp_giswebservices.pdf

Bader, E. et. al: ArcGIS Server Administrator and Developer Guide, Redlands: Environmental System Research Institute,Inc.(2004)

Peng, Z-R., Tsou, M-H.: Internet GIS – Distributed Geographic Information Systems for the Internet and the Wireless Networks. John Wiley & Sons, New York (2003).

Espace Littoral et Dynamique Paysagère (Littoral Oranais, Algérie)

D. Bouras[1], L. Delaby[2], K. Hussein[1], S. Mouffok[1], & F. Abdelghani[1]
[1] : BP. 1524 El Mnaouar, [2] : DLIC, Paris, France
Université d'Oran, Dép. Biologie, Fac. Sciences, Oran Es Sénia Algérie.
E-mail : djilaloran@yahoo.fr;

ملخّص : لإعادة النظر في مسألة المناظر الطبيعية الساحلية الجزائرية و خصوصا المناظر الطبيعية بوهران يتطلب إعداد تقرير عام عن مستقبل السواحل الجزائرية . يعود تحديد عوامل الإختلال إلى تقدّم الساحل. تستند دراستها و علم الخرائط الخاص بها على إستعمال المعطيات التاريخية ، و المخططات المورفولوجية و الخسائر التي حدثت كتدمير السكان ، هبوط المنحدرات خاصة الصخرية يخلق مخاطر للإنسان ، كما على الإفريز وسفح المنحدر الصخري ، الذي يتعرض لتساقط الصخور ، سريان الوحل أو إنزلاقات التربة (إفريز وهران ، كريستل و كناستل) يمكن تعيين هذه المخاطر على الخريطة برؤية زمانية ذات مقاييس مختلفة .

الكلمات الأساسية : المناظر الطبيعية ، وهران ، الساحل ، تقدّم .

Résumé : La question relative aux paysages côtiers algériens et en particulier oranais est à replacer dans un rapport plus général sur le devenir des littoraux algériens. L'identification des facteurs de déséquilibre est très attachante dans l'évolution du trait de côte. Leur examen et leur cartographie reposent sur l'utilisation des données historiques, des tracés morphologiques et des désavantages causés tels que les destructions d'habitats. Le recul des côtes particulièrement à falaises, engendre des risques pour l'homme, aussi bien sur la corniche qu'en pied de falaise, qui s'expose aux chutes de blocs, aux écoulements boueux ou aux glissements (corniche d'Oran, de Kristel et Canastel). Ces aléas peuvent être cartographiés dans une vision spatio-temporelle à différentes échelles.

Mots clés : paysage, Oran, trait de côte, évolution.

Abstract : The issue of coastal landscapes and especially Algeria Oran is put in a more general report on the fate of the Algerian coasts. Identifying factors of imbalance is very attractive in the evolution of the coastline. Their review and mapping based on the use of historical data, tracks morphological and disadvantages that caused such destruction of habitats. The decline of coastal cliffs creates particular risks for humans, both on foot ledge in the cliff, which is exposed to rock falls, mud flows in landslides or (cornices Oran, Kristel and Canastel). These hazards can be mapped in a vision and different spatiotemporal scales.

Keywords : landscape, Oran, coastline, evolution.

1. Introduction

L'idée est d'examiner la corrélation entre les paysages littoraux et les sociétés qu'elles occupent. Chaque configuration côtière est caractérisée par son énergétique et sa dynamique en fonction des conditions environnementales et de l'empreinte écologique (action anthropique) [1] et [2]. L'homme s'est adapté aux paysages mixtes (littoraux) où se multiplient les conflits et concurrences des groupes naturelles et ceux sociaux. En effet, ceci impose à l'évidence, le rapports qui doit être mis entre les paysages, les groupes sociaux et le fonctionnement du littoral.

En effet, les sociétés littorales, simplifient généralement la fonction des périls mixtes à ceux d'une activité séparée comme l'intervalle continental. Avec l'évolution continue du système littoral, une bande côtière (plage, dunes, falaise....) n'indique pas une portion droite du trait de côte limitant la bande régionale. Cet agencement enfante habituellement des déséquilibres dans la dynamique des reconfigurations côtières et par conséquent dans le développement socio-économique littoral. L'explication du personnage d'une forme côtière (naturelle, bâti et mixte) la classe comme une importante source de matériaux et comme un élément fixateur et d'enregistrement de l'évolution des paysages littoraux. Les interactions entre les différentes formes côtières sont à suivre à l'échelle de l'unité morphobiosédimentaire. Elles ne correspondent pas à une phase spatiotemporelle stable, mais à des facteurs morphologiques protagonistes dans le fonctionnement du littoral [1].

2. Identification et stabilisation des formes côtières

Une zone côtière est communément liée à une appellation de lieu, généralement en rapport avec la portion continentale du paysage, octroyère par les différents usagers. Les paysages ne sont donc pas des emplacements ignorés. Ceci montre l'importance

de l'observation que les groupes sociaux ont donné à la définition de ces dénominations de lieux et explique leurs dotations. Ces attributions peuvent être des noms historiques (Montagne des lions), des noms de tribus, d'une ville ou village, par exemple, la falaise de kristel (Est d'Oran), Maddagh (entre Oran et Ain Temouchent), ou selon la forme caractérisent le paysage (par exemple Pointe ou Cap de l'aiguille, Arzew). Parfois, en fonction de la fréquentation (Plage des mouches, Ain Témouchent), ou encore la nature singulière du site côtier (Plage sablette) [3].
Depuis leur occupation des paysages côtiers, les hommes combattent contre le recul des côtes avec différents processus de défense et de reconfiguration et d'adaptation (Epis, murs, enrochements pour la protection des habitations, des routes ou encore un champ cultivé...). En effet, le recul du trait de côte s'exprime par une régression du continent et des pertes aux biens de l'homme, de la faune et de la flore.

D'une manière générale deux types de protection sont prévus :

- Une protection défensive qui se porte sur la fixation du trait de côte par des enrochements ou des quais, lorsqu'on a une menace directe des sites. Dans le cas des côtes meubles et des plages, la protection, vise les effets humains et naturels, alors qu'au niveau de la base des falaises, elle intéresse les effets de l'érosion marine.
- Une protection offensive qui traite les origines de l'érosion. En premier lieu, l'impact des actions prises doit être bien étudié afin de prévenir toute sorte de complication comme le cas de l'amont et l'aval (sens de migration des zones d'érosion). En effet, sur les côtes basses meubles, on peut envisager et discuter des constructions d'épis, de brise-lames. Egalement le rechargement de plage par les sédiments d'apport, conduit aux résultats suivants [4] et [5] :

• Protéger et favoriser la sédimentation devant le trait de côte ;

• Affaiblir l'énergie des houles ;

• Briser la capacité érosive des vagues.

Le traitement de l'érosion dunaire des côtes par l'action anthropique (exemple : circulation de véhicules, vol des sables, construction, route, désenclavement de sentiers,...) peut être envisagé sur le plan législatif.
L'organisation paysagère oranaise a largement été perturbée en raison des aménagements effectués (Macta, Kristel, Ain El Turk.....), et qui ont affaibli voire brisé l'apport en alluvions des différents cours d'eaux, en particulier au niveau de la région de la Macta.
Par ailleurs, les besoins augmentés en sable et en gravier pour les nombreux projets d'aménagements, de l'industrie et les différentes constructions entraînent une surexploitation des réserves des lits des cours d'eau et celle du domaine côtier (cas de Terga, Ain Témouchent).
De plus, de nombreux cours d'eaux ont été déviés de leur trajectoire initiale (Macta, Kristel, Oued El Halouf), provoquant une déstabilisation de l'alimentation des eaux côtières. Signalons également l'intensité des travaux de construction sur des espaces non constructibles, engendrant un fort danger sur l'homme et une fragilisation et dégradation des reliefs et de l'écosystème. En conclusion, ces aménagements ont perturbé les conditions hydrodynamiques et ont favorisé une forte érosion actuelle de la sédimentation.
De même, des aménagements tels que les tracés de routes, les projets d'aménagements et construction des agglomérations ont aggravé les glissements, d'autant plus que les sols, d'une bonne partie du littoral oranais, (Canastel, Kristel, Terga) sont formés par des argiles et des sables gréseux. Ainsi, sur la falaise de Canastel, toutes les conditions sont rassemblées pour que de graves déplacements de terrain puissent avoir lieu à n'importe quel moment (cas de la corniche d'Oran).
Une situation pareille nous impose de retracer la dynamique du trait de côte pour une durée bien déterminée. L'empilement événementiel diversifié, de faible fréquence, (érosion, éboulement, glissement), dont l'origine marine ou continentale collabore dans la dynamique et l'évolution du littoral. Ceci, repose sur le rapprochement des documents anciens comparés à ceux plus récents, donnant une information intéressante sur une durée de l'ordre d'un siècle. Ces informations permettent l'estimation de la vitesse de changement des traits de côte, particulièrement à falaises. L'évolution des côtes à falaise est plus faible et plus lente par rapport à celle des côtes basses meubles.
Les falaises sableuses ou sablo gréseuses de faible hauteur (pas plus de 10 m), reculent comme les côtes basses meubles (Madrague et Terga). En revanche, que les falaises à matériaux résistants et hautes, changent selon leur état (falaise vive, falaise morte.....), ainsi qu'en fonction de leurs natures, résistance, pendage, fracturation, ... L'exemple peut être donné par la corniche oranaise qui est plus résistante par rapport à celle du secteur côtier témouchentois, ceci est causé essentiellement par la nature sédimentaire.
Dans le cas des glissements locaux comme Kristel, l'analyse du rôle des facteurs géodynamiques du versant est meilleure (nature, pendage,

superposition, etc.), des facteurs externes (précipitations, ruissellement, l'occupation de la bande, séismes, etc.) et de l'action érosive des facteurs marins. Toutefois, il est important de comprendre et d'estimer cette érosion marine par rapport aux facteurs intervenants (action anthropique, climatique, hydrologiques,...).

3. Fonctionnement côtier et impact

Les différentes formes côtières sont des éléments de la carcasse paysagère littorale pilotant la dynamique du trait de côte. De ce fait, c'est une concordance de facteurs dessinant et enregistrant toute phase de reconfiguration côtière. Il existe un lien direct entre les positions respectives des diverses formes : si une forme recule de A à A' et A", l'autre reculera de B a B' et B" [1] et [6].

Une forme côtière (dune, falaise, cordon,...) n'est pas un espace littoral isolé mais un enchaînement faisant partie d'un appareil d'ensemble (Fig. 1). Intervenir sur une partie littorale c'est modifié aussi, par contrecoup, les autres éléments. Donc le risque est éminent de déséquilibrer l'ensemble du système morphobiosédimentaire et par conséquent tout le patrimoine paysager côtier.

Les différentes figures d'urbanisation et d'installation de nombreux groupes sociaux (Fig. 1), sur tout ou une partie du trait de côte, brisent la connectivité qui existe entre les divers fragments des accumulations littorales. L'érosion de certaines portions côtière alimente l'estran en sédiments, assure une part importante de l'alimentation des plages et contribue dans l'équilibre du budget sédimentaire.

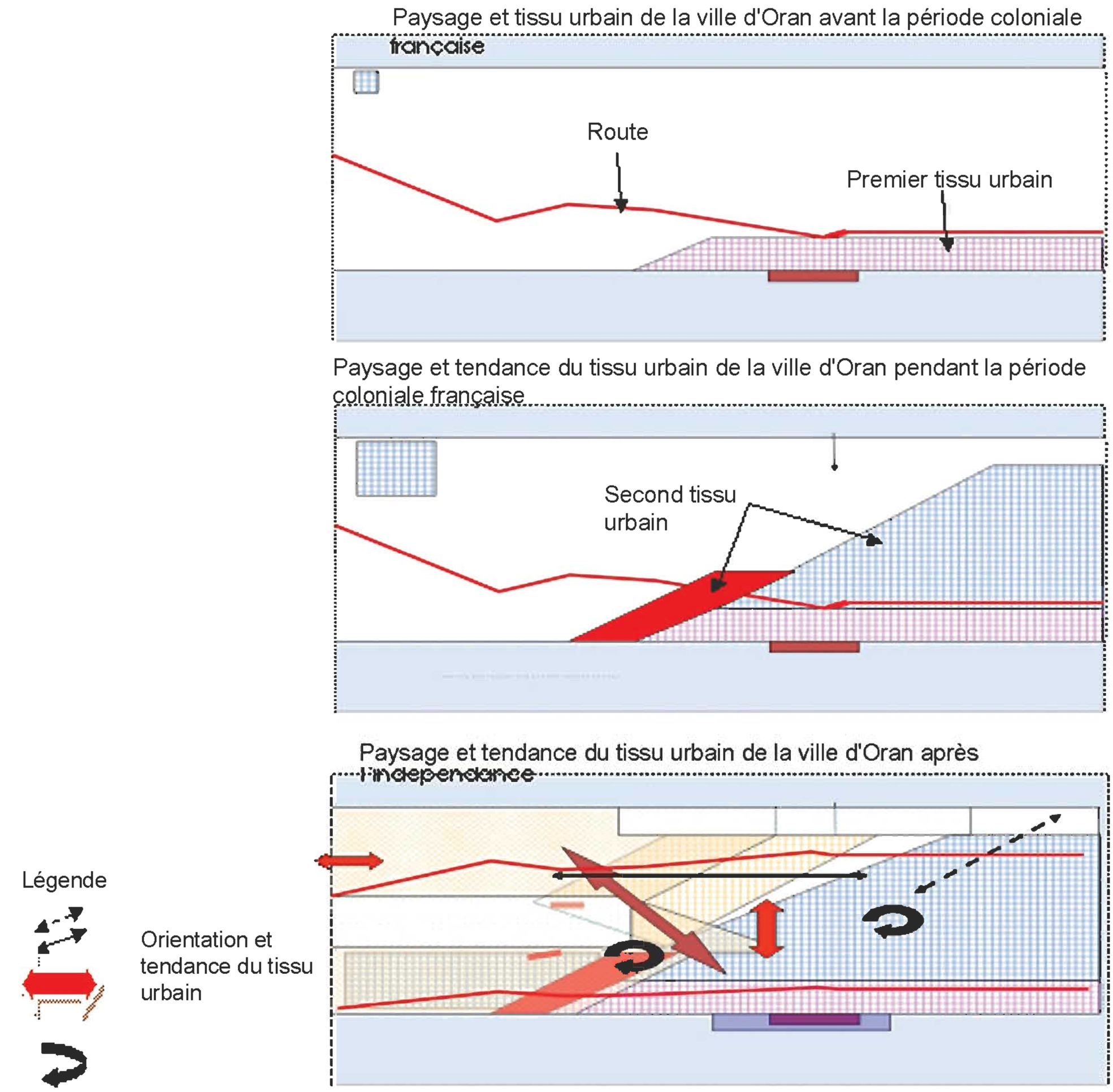

Fig. 1 Evolution paysagère et configuration urbaine de la ville d'Oran.

Une telle situation n'a rien de singulier, car on ne pense qu'à la rentabilité immédiate, alors qu'il faut penser aux conséquences de ce développement qui est entrain d'épuiser et d'anéantir toutes les ressources renouvelables en particulier littorales. Notons la disparition de gigantesques espaces forestiers le long des côtes (Kristel, Madagh), la déstabilisation des reliefs côtiers et littoraux (Marsa El Hadjadj, Ain El Turk, Terga, Macta) et les différentes pollutions que subit l'écosystème marin et côtier. Cela veut dire une absence totale d'une économie environnementale.

4. Conclusion

A travers les époques et par leur occupation, aménagement et modification, l'homme a donné aux paysages côtiers le statut d'un patrimoine,de zone touristique ou encore de point de fréquentation et de conflit, mais y a t-il plus à acquérir dans une telle démarche qu'à user en laissant régresser l'harmonie paysagère côtière?

Cet état appuie la complexité des rapports et l'intimité des paysages et d'homme : ce patrimoine paysagé est à la fois un lieu d'échange et d'assemblage, avec une évolution continue dans les deux sens (positif et négatif). C'est ainsi, des lieux très hétérogènes et très difficiles en termes de choix de gestion et d'intégration par rapport aux activités et désagrégations produites par ces espaces. De ce fait, la problématique des animations paysagères côtières évoque deux aspects : le premier est celui des limites dans les littoraux naturels (autochtone) et humaines (allochtone) dans la gouvernance de ces systèmes. Le second, est celui des rapports des dynamiques naturelles et celles anthropiques sur le fonctionnement et le devenir des littoraux.

En définitive, le développement du paysage et villes côtières doit prendre en considération toute les possibilités de la durabilité et la propreté du tissu urbains installé (agriculture nourricière, aspect vital, déchets, …).

Réferences Bibliographiques

BOURAS 2009- Urbanisation anarchique, un phénomène au long court, Echo d'Oran journal, N° 2683, 2009.

BOURAS D., 2007 - Dynamique bioclimatique et morphologique de la zone côtière oranaise : approche éco-biologique (Algérie nord occidentale). Thèse doctorat, Univ. Es Sénia, Oran, Algérie, 200 p.

BOURAS. D. & BOUTIBA. Z 2004- Ecologie discipline d'impact. Ed 3 pommes, Oran, Algérie : 117p.

FERRARI. S. 2005- Evaluation et développement durable : compte rendu de colloque (Limoges, 27-29 octobre 2003). *Natures sciences sociétés, vol. 13, n° 1 :* 87-88.

HUSSEIN K. B., 2007- Surveillance et évaluation de la qualité de la biodiversité des milieux et des habitats côtiers (côte oranaise, Algérie nord occidentale). Mémoire de Magister, Univ. Es Sénia, Oran, Algérie, 97 p.

LACAZE. J. C. 1993- La dégradation de l'environnement côtier, conséquences écologiques. Edit. Masson. Paris. France : 149.

Avis aux Auteurs

Le **B**ulletin des **S**ciences **G**éographiques est indexé dans la **Bibliographie Géographique Internationale** à l'adresse suivante : http://prodig.univ-paris1.fr/umr/Poles_comptence/Pole_Documentation%20et%20valorisation.htm

La notice bibliographique de la publication figure dans le volume annuel **n° 112, 2007**, ainsi que dans la **base de données FRANCIS-Géographie du CNRS** interrogeable sur les serveurs internationaux Questel.Orbit, OCLC/PICA, RLG et sur CD-ROM (Service payants), et dans la **BGI** publié par l'UMR PRODIG qui parait tout les ans :
http://prodig.univ-paris1.fr/umr/publications_documentaires/bgi_papier.htm

Elle a aussi été mentionnée dans la rubrique Publications du site **Infogéo** consultable sur Internet à l'adresse suivante : http://prodig.univ-paris1.fr/infogéo/Fichiers/Ouvrages.htm. La rubrique est actualisée régulièrement.

Le **B**ulletin des **S**ciences **G**éographiques est diffusé sur Internet, sur le site portail des revues scientifiques dénommé http://www.webreview.dz conçu et administré par le Centre de Recherche sur l'Information Scientifique et Technique (CERIST).

Pour soumettre un article...

Vous souhaitez proposer un article pour le Bulletin des Sciences Géographiques.

Pour faciliter votre démarche, nous vous adressons quelques recommandations :

- Ce Bulletin est un espace scientifique, consacré aux sciences géographiques.
- **NATURE DES ARTICLES :** Les articles adressés pour publication doivent traiter des sujets se rapportant aux Sciences Géographiques.
  Les articles se repartissent en deux rubriques:
  - Recherche - développement
  - Synthèse.

  LES ARTICLES DE RECHERCHE - DÉVELOPPEMENT : portent soit sur des travaux ayant une originalité et une contribution novatrice aidant au développement des sciences géographiques, soit sur des réalisations et études concrètes qui pressentent un intérêt dans la maîtrise des concepts des sciences géographiques.

  LES ARTICLES DE SYNTHÈSES : ont pour but de faire ressortir, les théories, les méthodes, les techniques ou les procèdés liés aux sciences géographiques, avec notamment des cas précis d'application.
- **LANGUES :** Les articles paraissent principalement, en Arabe, Français et Anglais.
- **CRITÈRES DE PUBLICATION :** Toute communication presentant de l'intérêt sera diffusée, quelle que soit son origine; l'appartenance de son auteur à l'INCT n'est pas exigée.
  Les articles doivent être fournis au format WORD ou équivalent, en colonnes et dans un format A4 en double interlignes, avec une marge de 2,5 cm au maximum sur chacun des quatre côtés.
  Chaque communication doit comporter un titre, qui doit être bref et informatif.
- **LE RESUMÉ :** Chaque article doit comporter un résumé en arabe accompagné d'un autre résumé en français et un autre en anglais de 100 à 200 mots.
- **MOTS CLÉS :** Citer 5 à 6 mots clés.
- **BIBLIOGRAPHIE :** Les références doivent être complètes et présentées dans l'ordre alphabétique des noms d'auteurs. La référence doit mentionner le nom et le prénom de l'auteur suivis de l'année d'édition, du titre de l'ouvrage, de l'éditeur et du lieu d'édition. Toute référence doit être clairement mentionnée dans le texte par le nom et prénom de l'auteur suivie des deux derniers chiffres de l'année de publication.
- **MODALITÉ DE PUBLICATION :** Tout article présenté pour publication est soumis à l'évaluation de deux membres du comité de lecture, en cas d'avis contraire, il est soumis à un troisième membre. Les articles non retenus ne sont pas retournés, à moins d'une demande de la part de l'auteur.
  Un exemplaire sera fournis gratuitement à chaque auteur ; d'autres seront fournis à la demande, dans la limite du stock.
- **DATES DE PARUTION :** Le Bulletin parait deux fois par an, à la fin du mois d'octobre et du mois d'avril.
- **ENVOI DES MANUSCRITS :** les manuscrits sont envoyés par email à l'adresse suivante: **inct99@wissal.dz**

INSTITUT NATIONAL DE CARTOGRAPHIE ET DE TELEDETECTION
Crée par ordonnance 211 67 du 17/10/1967 modifiée par les ordonances 84.68 du 23/04/1968 et 73.23 du 05/06/1973 et le décret présidentiel n°98.337 du 29/10/1998.
Siège: 123, rue de Tripoli - BP430 - Hussein Dey - 16040 - Alger
Tél: 213 021 47 09 20 & 021 47 00 30 **Fax:** 213 021 47 00 29 & 021 23 43 81
e-mail: inct99@wissal.dz

Bulletin d'abonnement

Tarif d'abonnement pour une année (comprenant deux numéros):

- ☐ Etudiant: 70 DA
- ☐ Particulier: 80 DA
- ☐ Etranger: 15 Euro

Prévoir en sus pour les frais d'expédition:

- ☐ Envoi Recommandé en Algérie : 400 DA
- ☐ Pour l'étranger: 10 Euro

Mode de règlement :

Pour l'Algérie :

- ☐ Par virement CCP N° 1552.04
- ☐ Par virement bancaire : CPA N° 101 401 78505 1
  BEA N° Q 22 61 570

Pour l'étranger :

- ☐ Par virement bancaire: Banque Deutsche Bank AG Munich
  Compte Nr, 85 960 BLZ: 700 700 l0

Nom et prénom / raison sociale :.....

Fonction :.....

Adresse complète :.....

.....

N°Tél :..... N°Fax :..... Email :.....

Date Signature

Retourner ce bulletin d'abonnement accompagné du règlement à Monsieur le Directeur Général de l'Institut National de Cartographie et de Télédétection

123, rue de Tripoli- BP 430, Hussein Dey- 16040 Alger.
Tél: 213 021 47 09 20 & 021 47 00 30 Fax: 213 021 47 00 29 & 021 23 43 81
E-mail: inct99@wissal.dz,

Bulletin des Sciences Géographiques
Institut National de Cartographie et Télédétection
123, Rue de Tripoli, BP 430, Hussein Dey - 16040 Alger.
Tél: (213) 021 47 09 20 & 021 47 00 30
Fax: (213) 021 47 00 29 & 021 23 43 81
E-mail: inct99@wissal.dz